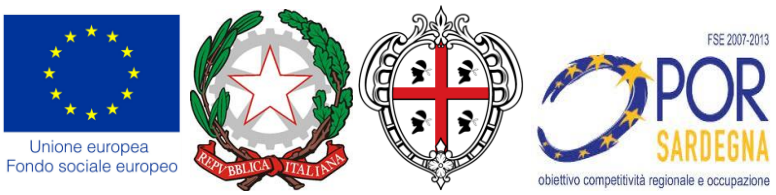

UNIVERSITÀ DEGLI STUDI DI CAGLIARI

DIPARTIMENTO DI SCIENZE BIOMEDICHE

SEZIONE DI CITOMORFOLOGIA

DOTTORATO DI RICERCA

IN

SCIENZE MORFOLOGICHE E FUNZIONALI

Coordinatore: Prof.ssa Valeria Sogos

CURRICULUM: NEUROANATOMIA E NEUROCITOLOGIA

SETTORE SCIENTIFICO-DISCIPLINARE BIO/16

NEUROCHEMICAL CHARACTERIZATION OF PRIMARY SENSORY NEURONS IN A RAT MODEL OF BORTEZOMIB-INDUCED PERIPHERAL NEUROPATHY

Tesi della Dott.ssa LAURA PODDIGHE Tutore: Prof.ssa MARINA QUARTU

ESAME FINALE ANNO ACCADEMICO 2012-2013

Acknowledgements

There are many people who have contributed toward the completion of this PhD degree.

This dissertation is the result of the work done under the expert guidance of Prof. Marina Quartu, to which I am sincerely and deeply grateful.

This work has been possible thanks to the collaboration with the research group of Prof. Guido Cavaletti of "Milan-Bicocca" University, which has provided the model and conducted the behavior experiments. In this regard, I wish to thank Prof. Cavaletti and all his staff with a special attention to the brilliant Dr Valentina Carozzi.

At beginning of my PhD I started working on translational medicine and focused my research activity on the reaction of the nervous system to injury. I had the opportunity to explore by different points of view, from animal models to humans, an extremely ample and complex theme. For that reason, I had the immense fortune to be involved in several projects and what is reported in this thesis is a part of my "journey", which involved me in a wide and deep scientific experience. Inter alia, during these three years, I have had the valuable chance to appreciate the importance of international experience, by joining the Neuroscience and Trauma group at Barts and The London School of Medicine and Dentistry, Queen Mary University of London. Therefore, I would like to sincerely warmly thank Prof. Adina Michael-Titus and Prof. John Priestley for welcoming me and giving the precious opportunity to enrol their research group. Also, last but not least in importance, my heartfelt thanks to Dr Patrick Pallier for being a great and careful guidance during my time abroad and for all his teachings.

Laura Poddighe gratefully acknowledges Sardinia Regional Government for the financial support of her PhD scholarship, P.O.R. Sardegna F.S.E. Operational Programme of the Autonomous Region of Sardinia, European Social Fund 2007-2013-Axis IV Human Resources, Objective l.3, Line of Activity l.3.1.

List of Pubblications

- Quartu M, Carozzi VA, Dorsey SG, Serra MP, **Poddighe L**, Picci C, Boi M, Melis T, Del Fiacco M, Meregalli C, Chiorazzi A, Renn CL, Cavaletti G, Marmiroli P. Bortezomib treatment produces nocifensive behavior and changes in the expression of TRPV1, CGRP and Substance P in the rat DRG, spinal cord and sciatic nerve. Bio Med Res Int, 2014, in press.
- Del Fiacco M, Quartu M, Serra MP, Boi M, Demontis R, **Poddighe L**, Picci C, Melis T. The human cuneate nucleus contains discrete subregions whose neurochemical features match those of the relay nuclei for nociceptive information. Brain Struct Funct. 2013.
- Quartu M, Serra MP, Boi M, Demontis R, Melis T, **Poddighe L**, Picci C, Del Fiacco M. Polysialylated-neural cell adhesion molecule (PSA-NCAM) in the human nervous system at prenatal, postnatal and adult ages. In: Recent Advances in Adhesion Research, Series: Human Anatomy and Physiology-Materials Science and Technologies, Nova Science Publishers, Inc., pp 27-58, 2013.
- Quartu M, Serra MP, Boi M, Pillolla G, Melis T, **Poddighe L**, Del Fiacco M, Falconieri D, Carta G, Murru E, Cordeddu L, Piras A, Collu M, Banni S. Effect of acute administration of Pistacia lentiscus L. essential oil on rat cerebral cortex following transient bilateral common carotid artery occlusion. Lipids Health Dis. 2012;11(1):8.

Congress comunications

- **Poddighe L,** Quartu M, Serra MP, Boi M, Melis T, Picci C, Del Fiacco M, Meregalli C, Canta A, Chiorazzi A, Sala B, Oggioni N, Cavaletti G, Carozzi VA. Expression of TRPV1 and CGRP in spinal primary afferent neurons in a rat model of bortezomib-induced peripheral neuropathy treated with analgesics. Abstract in Eur J Histochem, ISSN 1121-760X volume 57/supplement 3 2013.
- Boi M, Quartu M, Serra MP, **Poddighe L,** Melis T, Picci C, Del Fiacco M, Meregalli C, Canta A, Chiorazzi A, Sala B, Oggioni N, Cavaletti G, Carozzi V.A Boi M. Study of the calcitonin gene-related peptidepositive intraepidermal nerve fibers in a rat model of bortezomib-induced peripheral neuropathy. Abstract in Eur J Histochem, ISSN 1121-760X volume 57/supplement 3 2013.
- Serra M.P, Quartu M, **Poddighe L**, Picci C, Melis T, Del Fiacco M. Locus K: a novel territory of the human dorsal column nuclei. Abstract in Eur J Histochem, ISSN 1121-760X volume 57/supplement 3 2013.
- Melis T, Serra MP, Boi M, **Poddighe L**, Picci C, Del Fiacco M, Carta G, Murru E, Lisai S, Sirigu AR, Collu M. Banni S, Quartu M. Dietary essential oil components in the prevention of ischemia/reperfusion-induced tissue damage in the rat cerebral cortex. Abstract in Eur J Histochem, ISSN 1121-760X volume 57/supplement 3 2013.
- Carozzi VA, Meregalli C, Canta A, Chiorazzi A, Sala1 B, Oggioni N, Lanza M, Quartu M, Serra M.P, **Poddighe L**, Picci C, Boi M, Melis T, Del Fiacco M, Caselli G, Cavaletti G. Imidazoline receptor 2 is an effective target for neuropathic pain in a murine model of bortezomib-induced peripheral neuropathy. Abstract in Eur J Histochem, ISSN 1121-760X volume 57/supplement 3 2013.
- Pallier PN, **Poddighe L**, Choudhury R, Priestley JV and Michael-Titus AT. A new injectable form of docosahexaenoic acid improves functional outcome in rodents after spinal cord compression injury. William Harvey Day, October 2013.

- Del Fiacco M, Quartu M, Boi M, Picci C, **Poddighe L**, Serra MP., Melis T, Boccaletti R, Shevel E, Cianchetti C. Neurochemistry of scalp arteries innervation in patients suffering from chronic migraine. Abstract in Eur J Histochem, ISSN 1121-760X volume 57/supplement 1 2013.

- Boi M, Quartu M, Serra MP, **Poddighe L**, Melis T, Picci C, Del Fiacco M, Meregalli C, Chiorazzi A, Marmiroli P, Cavaletti G, Carozzi V.Calcitonin Gene-Related Peptide in dorsal root ganglia and skin of a rat model of bortezomib-induced peripheral neuropathy. Abstract in Eur J Histochem, ISSN 1121-760X volume 57/supplement 1 2013.

- Quartu M, Serra MP, Boi M, Pillolla G, Melis T, **Poddighe L**, Del Fiacco M, Falconieri D, Carta G, Murru E, Cordeddu L, Piras A, Collu M & Banni S. Attività dell'olio essenziale di Pistacia Lentiscus L. in un modello sperimentale di ipoperfusione/riperfusione nell'encefalo di ratto. Piante Medicinali, num. speciale 2013 "Scienza nella Tradizione", P16, pag. 58-59. 21° Congresso Nazionale di Fitoterapia, Abano Terme, 2013.

- Picci C, Quartu M, Serra MP, Melis T, **Poddighe L**, Boccaletti L, Shevel E, Cianchetti C, Del Fiacco M. TRPV1-, CGRP-and SP-immunoreactive innervation of scalp arteries in patiens suffering with chronic migraine. In 22th GISN national meeting, 2012.

- Quartu M, Serra MP, **Poddighe L**, Picci C, Boi M, Melis T, Del Fiacco M, Meregalli C, Chiorazzi A, Marmiroli P, Cavaletti G, Carozzi V "Expression of TRPV1, CGRP and Substance P in spinal primary afferent neurons in a rat model of bortezomib-induced peripheral neuropathy". In 22th GISN national meeting, 2012.

- Melis T, Quartu M, Serra MP, Boi M, Picci C, **Poddighe L**, Del Fiacco M. Further studies on the hystology and chemical neuroanatomy of the human cuneate nucleus. In 22th GISN national meeting, 2012.

- **Poddighe L**, Quartu M, Serra MP, Boi M, Del Fiacco M, Meregalli C, Chiorazzi A, Marmiroli P, Cavaletti G, Carozzi V. Neurochemical Characterization Of Bortezomib-Induced Peripheral Neuropathy: Expression of TRPV1, CGRP And Substance P In The Rat DRG and Spinal Cord. In: 8th FENS Forum of Neuroscience. FENS Forum abstracts, vol. 6, 2012.

- Del Fiacco M, Quartu M, Serra MP, Boi M**, Poddighe L** & Melis T. Discovery Of Novel Subregions Of The Human Cuneate Nucleus Whose Neurochemical Features Match Those Of Nociceptive Sensory Nuclei. In: 8th FENS Forum of Neuroscience. FENS Forum abstracts, vol. 6, 2012.

- Quartu M, Serra MP, **Poddighe L**, Boi M, Del Fiacco M, Meregalli C, Chiorazzi A, Marmiroli P, Cavaletti G, Carozzi V. Transient receptor potential vanilloid type 1 (TRPV1) and neuropeptides in the dorsal root ganglia and spinal cord in a rat model of Bortezomib-induced neuropathy. It. J. Anat. Embryol., 116, S151, 2011.

- Serra MP, Quartu M, Boi M, Pillolla G, Melis T, **Poddighe L**, Del Fiacco M, Falconieri D, Carta G, Piras A, Murru E, Collu M, Banni S. Effect of acute administration of dietary Pistacia lentiscus L. essential oil on the ischemia-reperfusion-induced changes in rat frontal cortex and plasma. It. J. Anat. Embryol., 116, S171, 2011.

Index

Abstract

Peripheral neuropathies, as the result of nerve damage, are characterized by pain, numbness, and tingling in the extremities and slow nerve conduction. Chemotherapy-induced peripheral neuropathy is a major dose-limiting side effect of many other commonly used chemotherapeutic agents, including platinum drugs, taxanes, epothilones and vinca alkaloids, but also newer agents such as bortezomib.

Bortezomib (VELCADE) is a boronic acid dipeptide, which causes a selective blockade of proteasome activity. Bortezomib-induced peripheral neuropathy is an important clinical complication, often difficult to manage or reverse, whose treatment usually involves dose reduction, interruption, or cessation of therapy.

Though many animal models of chemotherapy-induced peripheral neuropathy have been designed, knowledge concerning the mechanisms that may underlie neurochemical changes accompanying the onset of bortezomib-induced peripheral neuropathy is still poor. In this study, to analyze the possible neurochemical changes occurring in primary sensory neurons, the effects of a single-dose intravenous administration and a well-established "chronic" schedule (three times/week for 8 weeks) in a rat model of bortezomib-induced peripheral neuropathy have been examined.

The transient receptor potential vanilloid type 1 (TRPV1) channel and sensory neuropeptides calcitonin gene-related peptide (CGRP) and substance P (SP) were studied in L4-L5 dorsal root ganglia (DRGs), spinal cord and sciatic nerve using western blot (WB), immunohistochemistry, and reverse transcriptase-polymerase chain reaction (RT-PCR). Behavioral measures, performed at the end of the chronic bortezomib-treatment, confirmed a reduction of the mechanical nociceptive threshold, whereas no difference occurred in the thermal withdrawal latency. In the DRGs, TRPV1-, CGRP- and SP-immunoreactive neurons were mostly small- and medium-sized and the proportion of TRPV1- and CGRP-labeled neurons increased after treatment. A bortezomib-induced increase in density of TRPV1- and CGRP-immunoreactive innervation in the dorsal horn was also observed. WB analysis showed a relative increase of TRPV1 in DRG and spinal cord after both acute and chronic bortezomib-administration. Comparative RT-PCR

revealed a decrease of TRPV1 and CGRP mRNA relative levels after chronic treatment. The characterization of this animal model of peripheral neuropathy suggests that the neurochemical changes occurring in populations of DRG neurons that are likely involved in pain transmission appear to be an important component of the sensory neuropathy induced by the bortezomib-treatment and may represent the outcome of the molecular machine activated by the drug during the onset and persistence of bortezomib-induced neuropathic pain.

1. Introduction

1.1 Peripheral neuropathy

When a patient presents with symptoms of distal numbness, tingling and pain, or weakness, the first challenge to the physician is to determine whether the symptoms are the result of peripheral neuropathy (PN) or of a CNS lesion (England *et al.*, 2005). Peripheral neuropathy is a general term that indicates any disorder of the peripheral nervous system and affects both sensory and motor fibers (Hughes, 2002; Federici and Boulis, 2009). Damage to sensory nerves, in the PN early stages, can produce rapidly progressive symptoms. Among the different settings, distal symmetrical polyneuropathy is the most common one; it develops by affecting toes and soles of the feet first and often occurs in a "stocking and glove" distribution. Thus, in diabetic polyneuropathy, the prototype of motor and sensory polyneuropathy, sensory abnormalities such as numbness, pain, burning, paraesthesia, or disaesthesia in the toes or feet are among the earliest symptoms of polyneuropahty (Martyn and Hughes, 1997; England and Aubury, 2004; England *et al.*, 2005). The severity of nerve fibre impairment depends on a number of variables, among which the distance from the parent cell body appears to be a common finding: the higher the distance from the cell soma the higher the nerve fiber damage. A list of typical signs and symptoms of peripheral neuropathies (Archer *et al.*, 1983; Lindblom, 1985; Ochoa, 1996; Backonja, 2003; Marchettini *et al.*, 2006), based on a combination of clinical findings, electrophysiological tests, and laboratory investigations is given below:

- ♣ paresthesia, is a sensation of tingling, tickling, prickling, pricking, or burning of a person's skin with no apparent long-term physical effect. The manifestation of a paresthesia may be transient or chronic.The most familiar kind of paresthesia is the sensation known as "pins and needles" or of a limb "falling asleep".
- ♣ dysesthesia, is described as spontaneous or evoked burning pain, often with a superimposed lancinating component; special cases of dysesthesia include:
- hyperalgesia, an increased response to a stimulus which is normally painful;
- allodynia, pain due to a stimulus which does not normally provoke pain;

- hypoesthesia, due to a decreased sensitivity to stimulation or, reversely,
- hyperesthesia, an increased sensitivity to stimulation.

Lack of sensation (including loss of proprioception, loss of touch and temperature discrimination), areflexia and pain can cause other complications relating to recurrent injuries that may go unnoticed (e.g., unawareness of cuts or burns to the skin), and can lead to ulcers or poor wound healing. The symptoms of sensory PN can be intermittent or continuous and may significantly interfere with quality of life (Sommer, 2003; England *et al.*, 2005; Wolf *et al.*, 2012).

Damage to motor fibers results in decreased control of voluntary movements. Symptoms of damage to peripheral motor nerves usually begin as weakness or heaviness of the hands and/or feet; over time the numbness may extend proximally, and mild distal muscle weakness and atrophy may occur. Damage to motor function can also lead to abnormalities in muscle, bone, skin, and other organs (Peltier and Russell, 2002; Hay, 2002; Visovsky and Daly, 2004; Hausheer, 2006; Stillman and Cata, 2006; Ripellino *et al.*, 2014).

Diagnosis of PN requires both a complete assessment of patient conditions to determine the extent of the neurological deficit and a thorough anamnesis, and a physical examination to determine the possible aetiology (Head, 2006). In fact, a variety of causes such as diabetes, alcohol, genetic disease, thyroid dysfunction, metabolic and infectious disease, cancer and chemotherapy can be implicated in the pathogenesis of clinical syndrome (Kalet and De Angelis, 2009). Chronic polyneuropathy usually evolves in months or years and a defining branching point in its evaluation depends on whether it is demyelinating or axonal (England and Aubury, 2004). Actual origins of polyneuropathy remain a mistery in approximately 50 percent of cases; in the case of chronic polyneuropathy, even after a meticulous history, no primary cause is found in 20–25% of patients (England and Aubury, 2004). However, on the basis of the complex combination of precise anamnesis, neurological examination, and electrodiagnostic tests, specific diagnostic possibilities can be narrowed to the following few features: - the rate of development and pattern of the disease (gradually progressive or relapsing), - the relative involvement of motor and sensory fibres, - the relative involvement of large and small sensory fibres (predominantly large fibre, predominantly small fibre, or both), and - the electrophysiological findings (mainly demyelinating, mainly axonal, or both). Such a characterisation helps limiting the probable causes to a controllable degree. For example, a chronic, steadily progressive

distal symmetrical sensori–motor polyneuropathy with mainly axonal features is presumably secondary to systemic or endocrine diseases, metabolic disorders, medications or toxins. Instead, a longstanding chronic, largely motor distal symmetrical polyneuropathy with evenly demyelinating features is almost certainly an inherited polyneuropathy (eg, Charcot-Marie-Tooth disease).

Once the lesion has been localized to peripheral nerves, the next step is to diagnose the degree of nerve fiber involvement: single nerve root, multiple nerve roots, or a peripheral nerve plexus (LoMonaco *et al.*, 1992; Kannarkat, 2007; Azhary *et al.*, 2010). Infact, another very common way to classify disorders of peripheral nerves takes into account the clinico-pathological pattern of nerve damage and includes:

- ♣ FOCAL PERIPHERAL NEUROPATHY, that is a discrete lesion to a nerve, be it a spinal nerve root, a plexus, an individual major nerve trunk, or a branch from such a nerve. The neurological deficit is restricted to the motor and sensory territories supplied by the damaged nerve.
- ♣ MONONEUROPATHY MULTIPLEX, when two or more individual nerves or branches are involved. Thus, the symptoms and signs are restricted to the territories of these damaged nerves. Which of these types of peripheral neuropathies produce bladder, bowel or sexual dysfunction (Quasthoff *et al.*, 2002; England and Asbury 2004; Armstrong *et al.*, 2005; England *et al.*, 2005).
- ♣ POLYNEUROPATHY, i.e. a generalized nerve damage. The peripheral nerves are affected symmetrically and, usually, the longest nerve fibers are damaged first and maximally. Thus, the symptoms and signs involve both feet first, and as the disorder progresses, the hands are also both involved.

Taken as a whole, neuropathic pain is a debilitating condition that affects a large sector of the population, an estimated 50 million Americans, and represents a burden in terms of health care expenses and lost productivity (Pasnoor et al., 2013).

A best estimate of population prevalence of pain with neuropathic characteristics is likely to lie between 6.9% and 10% (Van Hecke *et al.*, 2013). One reason for the high prevalence rate of chronic neuropathic pain is the absence of effective treatments (Smith and Torrance, 2012). It is still unclear why neuropathies of apparently the same aetiology can be painful or painless, advances in the standardization of assessment of patients with painful neuropathies are beginning to have an impact on the design of relevant clinical treatments.

In late 2000, the US Congress passed into law a provision that declared 2001–2010 as the Decade of Pain Control and Research. Despite extensive efforts, the mainstay of analgesics for chronic pain is still morphine and its analogs, whose long term use is limited by important side effects (such as the development of tolerance, addiction, hyperalgesia, sedation, respiratory depression, and constipation) leading to premature death (Premkumar, 2010).

Overall, leading progress has been made in the understanding of cellular and molecular changes underlying the onset of peripheral neuropathy. However, both acute and chronic pain results from the engagement of highly plastic molecules and circuits, the neurochemical basis of which in the pathophysiology of a drug-induced painful sensory neuropathy are the focus of this study (Sommer, 2003; Colleoni and Sacerdote, 2010; Wolf, 2010; Ripamonti, 2012; Brix *et al.*, 2013).

1.1.1 Neuropathic pain

Neuropathic pain occurs as a result of neuronal plasticity and neuronal rewiring following traumatic, viral, surgical, metabolic, or drug-induced damage to the neurons (Premkumar, 2010). Its onset still remains an enigma. It differs from the classical senses (vision, hearing, touch, taste, and smell) because it has both a discriminative component and a graded motivational or behavioral drive (Craig, 2003).

Advances in molecular biology techniques and the subsequent discovery of specific molecules involved in pain processing have contributed to a better understanding of pain (Fürst, 1999; Scholz and Woolf, 2002; Ueda and Rashid, 2003; Ueda, 2008).

In 2011, neuropathic pain has been defined by the International Association for the Study of Pain (IASP) as "pain caused by a lesion or disease of the somatosensory system" (Jensen, 2011). Neuropathic pain is different from pain messages carried along healthy nerves from damaged tissue (eg a fall, cut, or arthritic knee) and, clinically, is treated by different drugs than pain from damaged tissue. To distinguish between nociception and pain is basic to understand sensory systems. Pain is a survival mechanism that supplies a warning sign of ongoing or impending tissue damage (Usunoff *et al.*, 2006; Basbaum *et al.*, 2009). Thus, nociception is the process by which non electrical signals (thermal, mechanical, or chemical) are converted to electrochemical ones by a subpopulation of peripheral nerve fibers, called nociceptors. By contrast, neuropathic pain involves direct

nerve stimulation. Another factor that distinguishes neuropathic pain from nociceptive pain is the different prognosis; in fact, most people with nociceptive pain (for example, after surgery) recover, whereas injury to a major nerve (for example, plexopathy or limb amputation) often generates persistent pain (Cohen and Mao, 2014).

Physiologically, pain has been broadly categorized into 3 categories (Scholz and Woolf, 2002):

- ACUTE or PHYSIOLOGICAL PAIN,
- INFLAMMATORY PAIN,
- CHRONIC PAIN.

ACUTE PAIN is experienced at the moment of an insult. It is an unpleasant sensory experience; it is part of the above mentioned rapid warning relay, evoked by stimulation of nociceptors specialized in responding only to stimuli approaching or exceeding harmful intensity responses. Lack of the ability to experience pain, as in the rare condition of congenital insensitivity to pain with anhidrosis (Ferrell, 2000; Axelrod and Hilz, 2003), can cause very serious health problems such as self-mutilation, auto-amputation, and corneal scarring.

INFLAMMATORY PAIN is associated with tissue damage and the ensuing inflammatory process, and is adaptive because it elicits physiological responses that promote healing. In inflammatory nociceptive pain, inflammation may cause damage to the neurons and produce neuropathic pain (Medzhitov, 2008).

CHRONIC PAIN is defined as pain lasting longer than 3 months, outlasting the usual healing process and generally falls into two subtypes:

- NOCICEPTIVE PAIN, caused by damage to body tissue and typically described as a sharp, aching, or throbbing pain. This kind of pain is often due to benign pathology;
- NEUROPATHIC PAIN occurs when there is an actual nerve damage. Innumerable diseases may be the culprits, examples include autoimmune disease (e.g., multiple sclerosis), metabolic diseases (e.g., diabetic neuropathy), infections (e.g., shingles and the consequent postherpetic neuralgia; HIV infections), vascular disease (stroke), trauma, cancer, and anticancer treatments such as chemotherapeutics or cytotoxic drugs (Woolf and Mannion, 1999; Bridges *et al.,* 2001; Sah *et al.,* 2003; Chen *et al.,* 2004).

The presence of neuropathic pain is often characterized by stimulus-independent persistent pain or abnormal sensory perception of pain such as allodynia, pain following a normally non-painful tactile or thermal stimulus, and hyperalgesia, exaggerated pain sensations as a result of exposure to mildly noxious stimuli (Woolf and Mannion, 1999; Bridges *et al.,* 2001).

The profound differences between acute and chronic pain emphasize the fact that pain is not generated by an immutable hardwired system, but rather implies the engagement of highly plastic molecules and circuits involving peripheral sensitization, spinal and supraspinal mechanisms, cortical reorganization (Basbaum *et al.,* 2009). Contextually, a large variety of changes at the level of components such as transduction, conduction, transmission, modulation and perception intervene in sensory processing in pain pathway (Gatchel *et al.,* 2007).

1.1.2 Chemotherapy-induced peripheral neuropathy

Beside bone marrow suppression and renal toxicity, the neurotoxic side effects of the chemotherapeutic agents are very often the reason for early cessation of anti-tumour therapy or change of the dose regimen, all of which compromise the success of cancer treatment (Quasthoff and Hartung, 2002; Mantyh, 2006). In addition, this can interfere with key aspects of quality of life including physical, social, and role functioning and emotional well being (Ostchega and Fox, 1988; Bakitas, 2007).

Chemotherapy-induced PN is a major dose-limiting side effect observed after clinical treatment with the vinca alkaloids, the taxanes, the platinum-derived compounds, suramin, thalidomide and the most recently identified proteasome inhibitors. More than 30% of patients who receive one of the above anticancer drugs will develop PN (Quasthoff *et al.,* 2002; Cata *et al.,* 2007; Dick and Flaming, 2010).

So far, the mechanisms responsible for the development of chemotherapy-induced PN are still uncovered. The mechanism of neurotoxicity is not necessarily the same as that of the anticancer effect and multiple mechanisms can contribute to the neurotoxicity. Moreover, toxicity can affect either the neuronal bodies, and generally they are represented by the primary sensory neurons in the dorsal root ganglia, or the axons or both (Krarup-Hansen *et al.,* 2007; Albers *et al.,* 2011).

Generally chemotherapy-induced PN is a group of neuromuscular symptoms that result from nerve damage, though several patterns of chemotherapy-induced PN are commonly recognized (Visovsky, 2003). Sensory symptoms, such as paresthesias and numbness, occurring usually between the first and third cycles of therapy, are the earliest. Motor weakness usually develops in a delayed fashion, and this is explained by the fact that sensory neurons and axons that transmit pain perception are unmyelinated and lightly myelinated fibers and are more susceptible than motor fibers to damage from exogenous toxins (Saif and Reardon, 2005). Many chemotherapeutics are believed to cause destruction or dysfunction of the myelin sheath that, in turn, may cause parasthesias. Loss of vibratory sense, two-point discrimination, and proprioception may also result from damage to the myelin sheath (Mantyh, 2006). It is not uncommon for symptoms to persist or even develop weeks to months after discontinuation of the chemotherapy. This phenomenon, known as “coasting”, was first recognized with the vinca alkaloid vincristine.

Vinca alkaloids, such as vincristine, and taxanes, like paclitaxel and docetaxel are microtubule stabilizing agents that exert their effects by disrupting mitosis in dividing cells (Holland *et al.,* 1973; Boyette-Davis *et al.,* 2013). Suppression of microtubule dynamics may cause activation of the mitotic checkpoint triggering apoptosit or reversion to the G-point phase of the cell cycle (Quasthoff and Hartung, 2002). Since microtubules are important for the development and maintenance of neurons, neurotoxicity appears to be one of the major side effects (Bhutani *et al.,* 2010; Jordan and Wilson, 2004). Sometimes, as after paclitaxel-tratment and on the basis of patient descriptors of pain, a peculiar syndrome of subacute aches and pains has been related to nociceptor sensitization (Loprinzi, 2011). In the case of platinum-based drug-treatment, the coasting effect has been related to their ability to bind to deoxyribonucleic acid (DNA) and form Pt-DNA adducts that, in turn, inhibit transcription and induce apoptosis through DNA damage recognition pathways (Jung and Lippard, 2007; McWhinney *et al.,* 2007). Oxaliplatin, instead, affects voltage-gated sodium-channel kinetics, leading to consequent hyperexitability of sensory neurons (Lehky *et al.,* 2004; Binder *et al.,* 2007; Park *et al.,* 2009; Cavaletti and Marmiroli, 2010; Pachman*et al.,* 2011). Thus, oxaliplatin-induced acute neuropathy is characterized by two electrophysiological hallmarks of peripheral nerve hyperexcitability, namely cold-induced paresthesias and jaw tightness. Although, from a neurochemical point of view, these symptoms have led to hypothesize that the sensitization of the Transient Receptor Potential (TRP) channels type M8 and/or A1 receptors in primary afferent neurons underlies the acute oxaliplatin-induced pain (Binder *et al.,* 2007; Stengel and Baron, 2009), interestingly mouse model of cisplatin and oxaliplatin-induced painful neuropathy using knock-down TRP type V1 mice, suggests that TRPV1 also participates in development of mechanical hyperalgesia in platinum drug-induced pain (Ta *et al.,* 2010).

1.1.3 Bortezomib-induced peripheral neuropathy

Bortezomib (VELCADE; formerly PS-341, LDP-341, MLN341) is a boronic acid dipeptide (cfr Fig. 1a). It is a novel first-in-class proteasome inhibitor, which specifically blocks the chymotryptic site of the 26S proteasome and therefore acts by disrupting various cell signaling pathways, thereby leading to cell cycle arrest, apoptosis, and inhibition of angiogenesis (Delcros *et al.,* 2003; Wu and Shi, 2013). Since numerous proteins are target of the proteasome-mediated degradation, multiple cellular processes are affected by proteasome inhibition (Ciechanover, 1998). Therefore, the effectiveness of bortezomib in arresting cell growth in different cancers probably involves a variety of molecular mechanisms. Extensive preclinical research has contributed to elucidate the bortezomib mechanism of action and to examine its activity, both as a single agent and in combination with other anticancer drugs, in a wide variety of solid and hematologic tumors and cancer models (Adams, 2004).

In cell cultures, bortezomib has been shown to induce apoptosis in both hematologic and solid tumor malignancies, including myeloma (Hideshima *et al.,* 2001), mantle cell lymphoma (Pham *et al.,* 2003), and non-small cell lung (Ling *et al.,* 2003), ovarian (Frankel *et al.,* 2000), pancreatic (Shah *et al.,* 2001; Bold *et al.,* 2001), prostate (Frankel *et al.,* 2000; Adams *et al.,* 2002), and head and neck cancer (Sunwoo *et al.,* 2001).

As a whole, proteasome inhibition appears to induce apoptosis or to increase cell sensitivity to apoptosis by shifting the balance between pro- and antiapoptotic signals (Adams, 2003). Though the mechanisms by which bortezomib induces apoptosis are not yet fully unveiled, it has been shown that proteasome inhibition is associated with the stabilization of pro- and antiapoptotic proteins (cfr Fig. 1b), including cyclin-dependent kinase inhibitors (e.g., p21 and p27) and tumor suppressors (e.g., p53) (An *et al.,* 1998; MacLaren *et al.,* 2001; Shah *et al.,* 2001). Proteasome inhibition also interferes with the unfolded protein response, thereby causing endoplasmatic reticulum stress (ER-stress) and increased apoptosis (Lee *et al.,* 2003). The involvement of regulatory proteins in apoptosis differs according to cell type. Certainly, the transcriptional activator NF-κB has been recognized a central role in mediating many of the effects of proteasome inhibition. Beside its involvement in inflammation and immune responses, NF-κB and its signaling pathways were also recently implicated in tumor development (Karin *et al.,* 2002). Under normal

conditions, NF-κB is bound to its inhibitor IκB, and transcriptional activation of genes by NF-κB is suppressed. In response to cellular stresses, IκB is degraded by the proteasome and NF-κB is released, activating transcription of genes for growth factors, stress response enzymes, cell adhesion molecules, and apoptosis inhibitors (Karin *et al.,* 2002). By contrast, bortezomib inhibits NF-κB activation through proteasome inhibition though inhibition of NF-κB activation does not completely explain its anticancer activity (Cusack *et al.*, 2001; Hideshima *et al.*, 2001; Hideshima *et al.*, 2002).

Bortezomib monotherapy, approved by the U.S. FDA in 2003 for the treatment of refractory multiple myeloma (MM), is effective in the treatment of recurrent and newly diagnosed multiple myeloma (Richardson *et al.,* 2003; San Miguel *et al.,* 2008), and of recurrent mantle cell lymphoma (Kane *et al.,* 2007).

However, as already stated above, bortezomib-treatment shows a significant dose-limiting toxicity by inducing a severe painful PN, typically occurring as earliest as the first cycles of drug administration and reaching a plateau at cycle 5, whose onset mechanisms appear to be multifactorial (Richardson *et al.,* 2006; Chaudhry *et al.,* 2008). Studies in animal models demonstrate that bortezomib exerts its effects by causing a significant neuronal dysfunction characterized by interfering with transcription, nuclear processing and transport, and cytoplasmic translation of mRNAs in DRG neurons (Casafont *et al.,* 2009). Neurophysiological and histopathological findings show that the bortezomib-induced neuronopathy is dose-dependent and mostly due to a reduction of large and C-fibers. Abnormal vesicular inclusion bodies appear to be a hallmark of bortezomib-affected unmyelinated axons together with mitochondrial and endoplasmic reticulum damage (Pei *et al.,* 2004; Landowski *et al.,* 2005; Ravaglia *et al.,* 2008). As for the molecular pathways actually involved in the bortezomib-induced neuronopathy they are far from being clearly defined. One of the inferring is that a potential role in the genesis of bortezomib-induced PN is played by the dysregulation of the neurotrophin machinery, triggered either by the activation of the mitochondrial-based apoptotic pathway or by the inhibition of the nerve growth factor-mediated neuron survival (via interference with the NF-κB pathway), plays (Hacker *et al.,* 2006; Miller *et al.,* 2009; Piperdi *et al.,* 2011).

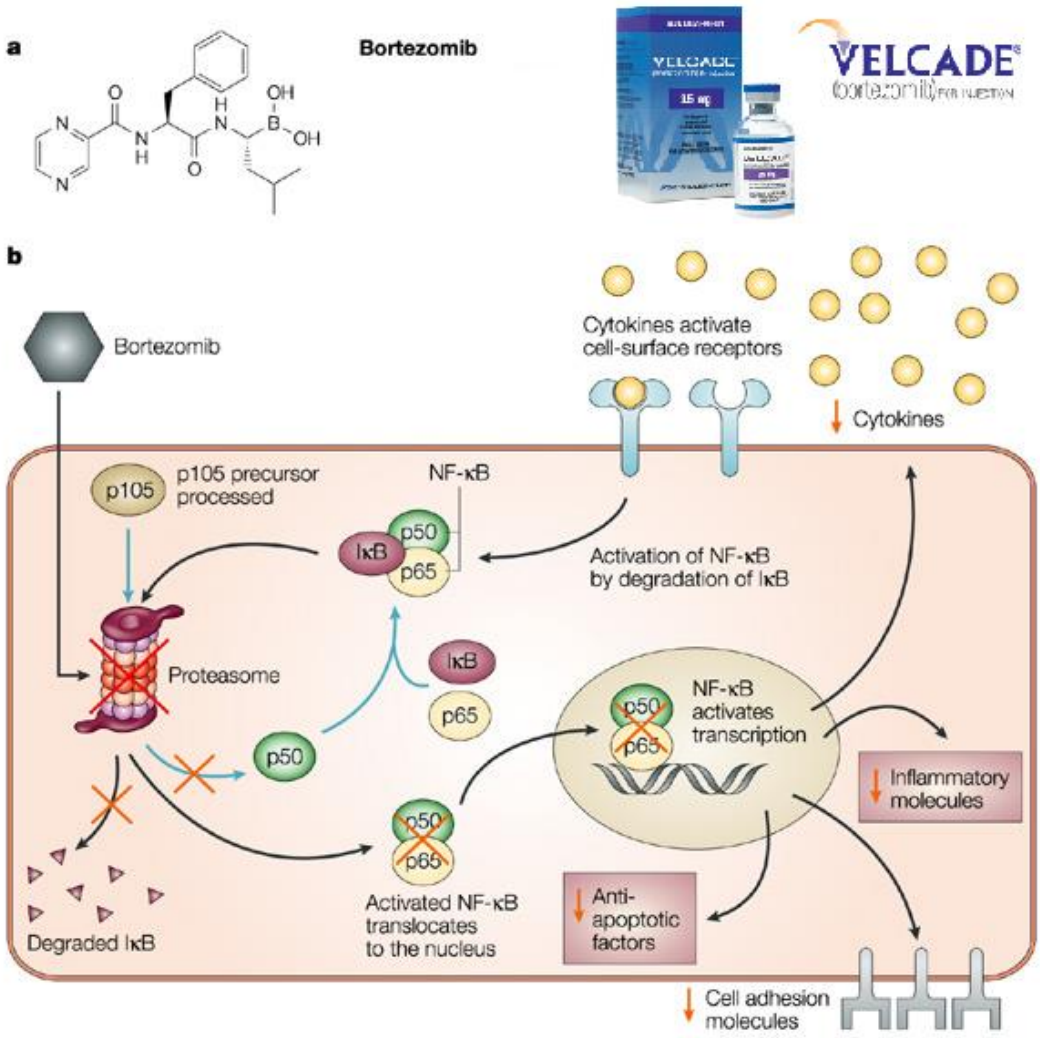

Figure 1 a, b. Mechanism of action of bortezomib

A: molecular structure of bortezomib, Velcade commercial compound.

B: schematic representation of intracellular effects of bortezomib. The activation of transcription factor nuclear factor-κB (NF-κB) is dependent on proteasome activity. NF-κB is normally sequestered in the cytoplasm and rendered inactive by its inhibitor protein IκB. However, numerous stimuli, including cell stressors, prompt the phosphorylation and subsequent proteasomal degradation of IκB, thus allowing the release of NF-κB. The transcription factor then translocates to the nucleus and initiates the transcription of a wide range of genes, including those involved in cell survival, cell adhesion, and cytokine signaling. The boron atom in bortezomib binds the catalytic site of the 26S proteasome with high affinity and specificity. In normal cells, the proteasome regulates protein expression and function by degradation of ubiquitylated proteins, and also cleanses the cell of abnormal or misfolded proteins. Proteasome inhibition may prevent degradation of pro-apoptotic factors, permitting activation of programmed cell death in neoplastic cells dependent upon suppression of pro-apoptotic pathways. Recently, it was found that bortezomib caused a rapid and dramatic change in the levels of intracellular peptides that are produced by the proteasome. Some intracellular peptides have been shown to be biologically active, and so the effect of bortezomib on the levels of intracellular peptides may contribute to the biological and side effects of the drug (original image from Sanchez-Serrano, 2009).

1.2 Dorsal Root Ganglia

Afferent sensory fibers coalesce together to enter the spinal cord via the dorsal root. Primary afferent neuronal cell bodies are grouped in a swelling along the dorsal root extension, just outside the spinal canal and lying near or within the intervertebral foramina, to form the dorsal root ganglia (DRG). Entering the spinal cord at its dorsal surface in an area known as the dorsal root entry zone (DREZ), small, medium-size, and large afferent fibers perform their various functions with glutamate serving as the primary neurotransmitter (Usunoff *et al.,* 2006). The DRG contain the primary afferent neuronal perikarya, each surrounded by the satellite glial cells, nerve fibers and Schwann cells (Lieberman, 1976; Hanani, 2005). DRG neurons are pseudo-unipolar, i.e. they emit a single axon that, a few tens or hundreds μm from the soma, divides in two branches that act as a single axon, often referred to as the distal process and the proximal process. The action potential in DRG neurons may initiate in the distal process in the periphery, bypass the cell body, and continue to propagate along the proximal process until enters the dorsal root and reaches the synaptic terminal in the dorsal horn of the spinal cord (Lawson *et al.,* 1987; Lawson, 1992; Devor, 1999). A capsule composed of connective tissue and a perineurium, similar to that of peripheral nerves, surrounds the entire DRG and keeps the microenvironment separate from surrounding extracellular fluid (Olsson, 1990).

DRG neurons can be classified into various subpopulations based on their anatomy, neurochemistry and physiology (Lawson, 1992; Snider and McMahon, 1998; Hunt and Mantyh, 2001). The Nissl staining allows to distinguish the DRG neurons into large-light and small-dark cells. Large cells show a rather pale and unevenly stained cytoplasm, due to aggregations of Nissl substance interspersed with lightly stained regions, contain microtubules and a large amount of neurofilaments; they comprise approximately 40% of lumbar DRG cells (Usunoff *et al.,* 2006). Large DRG neurons have mostly myelinated axons that conduct in the Aα/β range and receive input from peripheral mechanoreceptors (Harper and Lawson, 1985; Sommer *et al.,* 1985; LaMotte *et al.,* 1991; Lawson and Waddell, 1991; Willis and Coggeshall 1991; LaMotte *et al.,* 1992; Truong *et al.,* 2004). The small-dark cells represent the second major group of DRG neurons; they can be further subdivided into neuropeptidergic and non neuropeptidergic neurons. The former

constitutively express neuropeptides and the calcitonin gene related peptide (CGRP) represents the best marker for them.They emit unmyelinated axons, namely C fibres, and innervate mainly polymodal nociceptors (McCarthy and Lawson, 1990; Lawson *et al.,* 1997). The latter, identifiable by using a variety of histochemical markers, have been especially characterized by their binding of the lectin Griffonia simplicifolia IB4 (Streit *et al.,* 1986) or by their expression of a nonlysosomal fluoride-resistant acid phosphatase (FRAP) (Silverman and Kruger, 1988). This group of small-diameter cells (which will be referred to as IB4+) also emits unmyelinated axons (C fibres) that are likely to mediate nociception (Silverman and Kruger, 1990; Alvarez *et al.,* 1991).

While these categories are largely histochemically distinct, at the same time there is also some degree of overlap among them. Thus, a group that is intermediate in size between the large-sized and the small-sized neuropeptidergic ones is represented by CGRP- and substance P (SP) -containing cells that are medium-sized and emit finely myelinated, Aδ axons. Most of these cells are nociceptors of the high-threshold mechanoreceptor type (McCarthy and Lawson, 1990; Lawson *et al.,* 1996, 1997). Further overlap occurs between the IB4 binding and CGRP-containing populations (Bennett *et al.,* 1996).

An additional characterization allows to differentiate DRG neurons on the basis of their responsiveness to selective target-derived neurotrophic proteins. Availability of neurotrophic proteins, such as nerve growth factor (NGF) and glial cell line-derived neurotrophic factor (GDNF), has been directly related to the maintenance of mature neuronal phenotype and neuronal ability to react to injury. In this context, non-peptidergic cells appear to be regulated by GDNF since they bear ret, the high affinity GDNF receptor, whereas peptidergic neurons and large-sized ones, bearing the high affinity trkA receptor, are regulated by NGF (Priestley *et al.,* 2002).

Subsets of both types of small-sized neurons show a range of expression levels of TRPV1 capsaicin receptor, most likely making them responsive to similar types of noxious stimuli (Bennett *et al.,* 1996; Priestley *et al.,* 2002).

1.2.1 Nociceptors and nerve fiber classification

The term nociception indicates the reception of input delivered to the central nervous system by sensory receptors known as nociceptors, i.e. the peripheral endings of primary afferent neurons whose cell bodies are located in the DRG and cranial sensory ganglia. Nociceptors provide information about tissue injury, though not all information delivered through this system will be perceived as painful (Usunoff *et al.*, 2006; Julius and Basbaum, 2001).

Afferent fibers involved in pain transmission can be classified in three types (cfr Table 1), according to their structure, degree of myelination, and function:

- A-beta fibers, or mechanoreceptors, transmit sensory information regarding touch, vibration and hair deflection; they are myelinated large-diameter low-threshold fibers; they transmit with a conduction velocity of 40-70 m/sec and may contribute to the development of pathological pain sensation (Ren, 1996) (cfr Table 1);
- A-delta fibers respond to noxious mechanical stimulation. They are small-diameter, myelinated fibers with slower conduction velocity (5-15 m/sec) compared to A-beta fibers; among them are the temperature-sensitive nociceptors which are sensitive to intense heat and cold (Cook *et al.*, 1987; Ren, 1996) (cfr Table 1).
- C-type polymodal nociceptors originate in the epidermis and deep receptors located in ligaments, muscles, and connective tissues. They respond to specific chemical compounds such as histamine, bradykinin, serotonin, prostaglandins, proteolytic enzymes, potassium and acids. These fibers are the smallest and slowest of the nociceptors, conducting impulses at approximately 0,5 m/s: C fibers are unmyelinated and require intense mechanical, thermal, or chemical stimulation to transmit pain impulses. Physiologically, the C-nociceptor responds directly to increasing intensity of noxious stimulation -the greater the stimulus strength, the more vigorous the response (Besson and Chaouch, 1987). Repeated stimulation, however, enhances C-nociceptor responsivity to a given stimulus strength (LaMotte, 1984; reviewed by Campbell *et al.*, 1989) (cfr Table 1).

Table 1. General classification of nerve fibers.				
Type	**Diameter, µm**	**Conduction velocity, m/sec**	**General Function**	**Myelination**
A-alpha	13-22	70-120	alpha-motoneurons, muscle spindle primary endings, Golgi tendon organs, touch	Y
A-beta	8-13	40-70	touch, kinaesthesia, muscle spindle secondary endings	Y
A-gamma	4-8	15-40	touch, pressure, gamma-motoneurons	Y
A-delta	1-4	5-15	pain, crude touch, pressure, temperature	Y
B	1-3	3-14	preganglionic autonomic	Y
C	0.1-1	0.2-2	pain, touch, pressure, temperature, postganglionic autonomic	N

1.2.2 Cytoarchitecture of the spinal cord dorsal horn

Dorsal horn neurons receive sensory information from primary afferents that innervate the skin and deeper tissues of the body and respond to specific types of noxious and non-noxious stimuli (Todd, 2010). Primary afferents terminate in the dorsal horn with a distribution pattern that is determined by the sensory modality they are conveying and the body region of innervation, according to a very specific spatial organization (cfr Fig 2). The incoming information is processed by complex circuits involving excitatory and inhibitory interneurons, and is transmitted to projection neurons for relay to several brain areas (cfr Fig 3).

According to the original description of Rexed (1952; 1964), the spinal gray matter can be subdivided into 10 nuclei or laminae. In this setting, the dorsal horn comprises laminae I–VI, the intermediate zone comprises lamina VII, the ventral horn harbors laminae VIII and IX and the periependimal region corresponds to lamina X (cfr Fig 2).

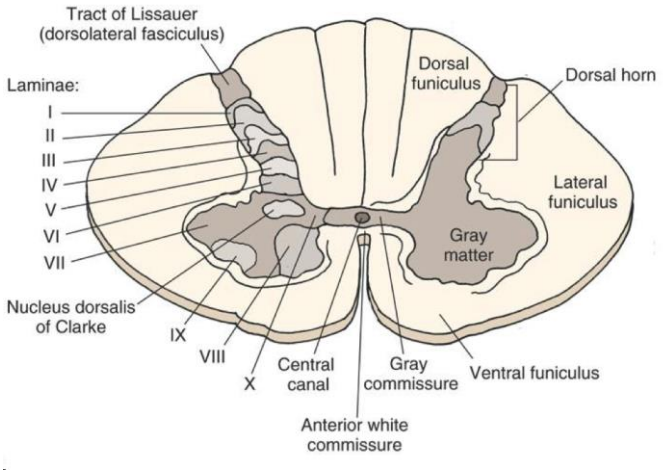

Figure 2. Spinal cord trasversal section

The axons enter the spinal cord by Lissauer's tract, they immediately divide and travel a short distance of one or two segments upward and downward in the spinal cord.before terminating in the external part of the dorsal horn The gray matter of the spinal cord is divided into laminae according to Rexed, indicated by roman numerals, the most involved in pain sensory pathways ranging from lamina I to VI (Image from http://www.studyblue.com)

Laminae I-VI

- ♣ The **dorsomarginal nucleus** - **Lamina I**, capping the dorsal horn, receives many afferent fibers carrying pain, temperature, and light touch sensations. Many intersegmental pathways arise from this layer that also contributes fibers for the lateral and ventral spinothalamic tracts (Patestas and Gartner, 2006; Gaudio, 2012)
- ♣ The **substantia gelatinosa** of Rolando - **Lamina II,** constitute the superficial dorsal horn and is characterized by the presence of numerous small neurons. Lamina II can be further divided into outer (IIo) and inner (IIi) parts, with IIi having a somewhat lower density of neurons. This nucleus extends the entire length of the cord and is most prominent in the cervical and lumbar levels. C fibers delivering pain, temperature, and light touch information terminate on neurons in dorsal horn lamina II. Cells in this lamina also form intersegmental connections. Descending fibers from higher centers (such as the cerebral cortex) form excitatory and inhibitory synapses with the cells of the substantia gelatinosa, thus modifying the incoming pain and temperature sensations (Ralston, 1979; Usunoff *et al.*, 2006; Todd, 2010)
- ♣ The **nucleus proprius - Laminae III and IV**, extends the entire length of the spinal cord. It is composed of densely clustered large nerve cell bodies, located just ventral to the substantia gelatinosa, and receives the central processes of the majority of the DRG neurons. The nucleus proprius receives pain, light touch, and temperature sensations and provides input to the lateral and ventral spinothalamic tracts (Beal and Cooper, 1978; Usunoff *et al.*, 2006)
- ♣ **Lamina V** extends across the neck of the dorsal horn and in all but the thoracic region is divided into medial and lateral portions. The lateral portion consists of the reticular nucleus that is most conspicuous in the cervical neuromeres. The C and Aβ nociceptive fibers terminate in this layer. Morevoer, corticospinal synapses have been identified in this lamina.
- ♣ **Lamina VI** is a wide zone most prominent in the cervical and lumbar enlargements. At these levels, it is divided into medial and lateral zones. Terminals from the posterior roots end in the medial region whereas descending fiber tracts project to the lateral zone.

Intermediate Region: Lamina VII

- **Lamina VII** includes most of the intermediate region of the gray matter in the spinal cord. In this lamina are found the intermediolateral and intermediomedial nuclei. The **nucleus dorsalis**, also known as **Clarke's column** is located at the base of the dorsal gray column and houses relatively large cell bodies that receive synapses from proprioceptive fibers, which bring information from Golgi tendon organs and muscle spindles. Some of the axons of these large nerve cell bodies travel in the dorsal spinocerebellar tracts. Cells in lamina VII form tracts that project to higher levels, including the cerebellum and thalamus. In the thoracic and sacral regions, this lamina also hosts visceral motor neurons whose axons leave this lamina to form preganglionic autonomic connections (Barr and Kiernan, 1983; Wall, 1987; Graham *et al.*, 2007).

To sum up, the A-delta and C fibers enter the spinal cord as the lateral bundle of the dorsal root, they bifurcate into branches that ascend and descend one or two spinal levels as constituents of the dorsolateral fasciculus of Lissauer, from where they enter and terminate on projection neurons in the dorsal horn (Grant, 1995; Jessell and Kelly, 1997) (cfr Fig 3).
In the gray matter, spatial organization of incoming primary afferent fibers provides that myelinated low-threshold mechanoreceptive afferents arborize in an area extending from lamina IIi–V, whereas nociceptive and thermoreceptive Aδ and C afferents innervate lamina I and much of lamina II, except for its most ventral part. Recent studies have identified a group of cooling-specific C afferents that terminate in lamina I, as well as two possible candidates for low-threshold mechanoreceptive C fibres that project to lamina II. In the gate control theory, small-diameter and large-diameter primary afferents converge on "pain transmission neurons" of the "action system". In particular, all somatic afferents, including nociceptors, activate second order "convergent" neurons, namely wide-dynamic-range (WDR) cells, located in the deep dorsal horn that, travelling in the spino-thalamic tract (STT), project to the main somatosensory thalamus and then to the primary somatosensory cortex (Wall 1973, Price and Dubner 1977; Price, 1988; Willis, 1985; Willis and Westlund 1997)(cfr Fig. 4). The activity of the WDR cells is viewed as necessary and sufficient for pain sensation and is characterized as graded throughout the range of tactile sensitivity, so that WDR neurons respond with progressively greater levels

of discharge to brushing hair, light touch, pressure, pinch, and squeeze (Craig, 2003) (cfr Fig 3).

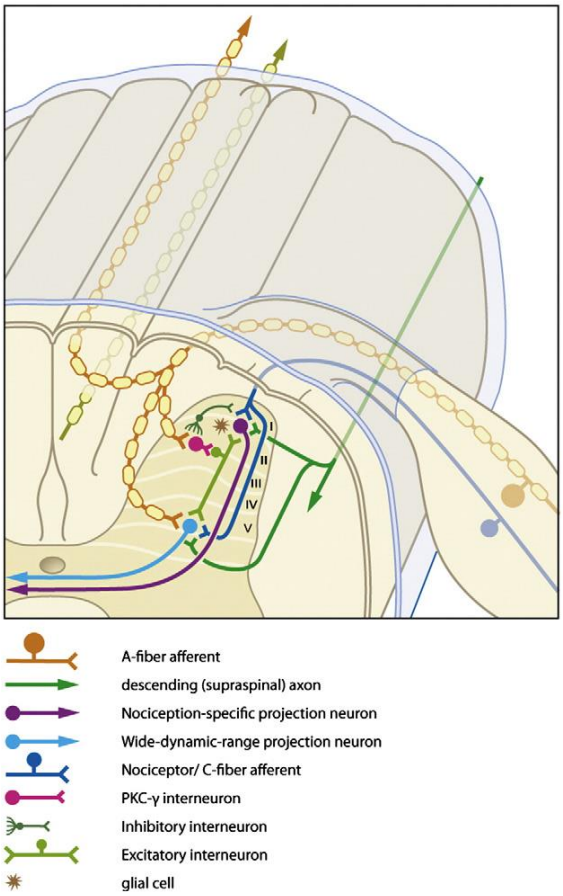

Figure 3. Neuronal architecture of the dorsal horn
Laminae (represented by numerals I-VI) are morphologically and functionally distinct layers within the gray matter of the spinal cord. Lamina I primarily contains large projection neurons that send processes up the spinal cord towards higher brain regions. Lamina II, in contrast, is more heavily populated with interneurons, many of which supply inhibitory signals to lamina I projection neurons. Lamina V con-tains wide dynamic range neurons that receive primary input from multiple sensory odalities. Peripheral afferents project to distinct laminae. While Aδ and C fibers are associated with superficial laminae, Aβ fibers project more medially (original image from Berger *et al.*, 2011).

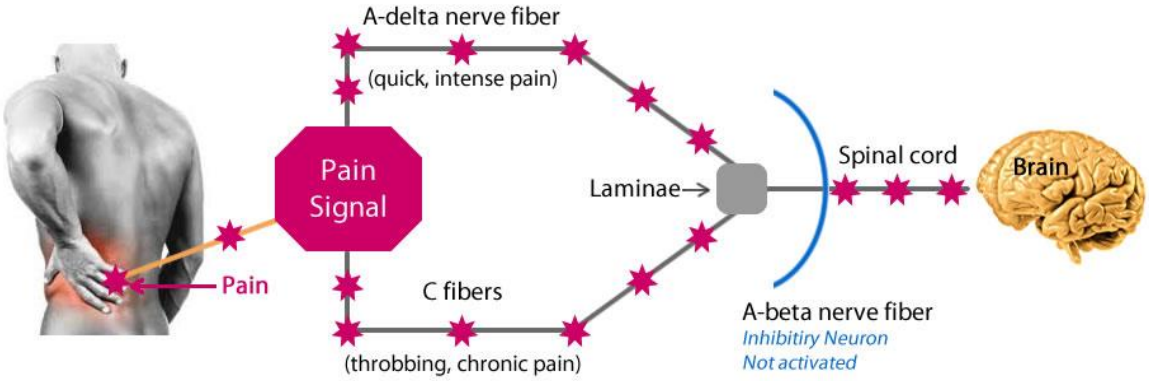

Figure 4. Gate control theory

The theory is based on the understanding that pain is transmitted by two kinds of afferent nerve fibers. One is the larger myelinated A-delta fiber, which carries quick, intense-pain messages. The other is the smaller, unmyelinated "C" fiber, which transmits throbbing, chronic pain. A third type of nerve fiber, called A-beta, is "nonnociceptive," meaning it does not transmit pain stimuli. In this concept, pain can be modulated by the balance of the interactions among the nociceptive C fibers and non-nociceptive A-alpha (proprioception) and A-beta afferent (touch) fibers of the peripheral nerves, and the interneurons and projection neurons of the dorsal horn. The interneuron, which normally inhibits the projection neuron, is spontaneously active and, thus, reduces (inhibits) the intensity of the noxious input from the C fibers. The influences exerted by the spontaneous activity of the interneuron on the projection neuron are modulated by excitation from the non-nociceptive A fibers and inhibition from the nociceptive.

C fibers. In essence, nociceptive C fibers tend to keep the gate open (enhancing perception of pain) by inhibiting the inhibitory interneuron and exciting the projection neuron. The non-nociceptive A fibers tend to keep the gate closed (suppression of pain) by exciting the inhibitory interneuron. In addition, the reflected feedback descending influences from the brain can modulate the excitability of these neurons (original image from http://www.positivehealth.com).

1.3. Pain sensory pathways

Transmission of pain through the chain of primary afferent neurons and dorsal horn cells is influenced by many factors, some of which originating within the segment, some from higher centers. The anterolateral system (ALS) has long been known to be a major pathway for the transmission of general somatic protopathic information to the cerebral cortex. ALS comprises the spinothalamic tract (STT), the spinomesencephalic tract and the spinoreticular tract. Fibers carrying pain and temperature ascend in the contralateral spinothalamic tract. Compression, intrinsic disease, or deliberate section of STT result in anesthesia of the contralateral body beginning 3 segments below the level of disruption. STT shows both somatotopic and functional arrangement, as pain fibers are located anteriorly, temperature ones are located posteriorly. Ascending spinothalamic fibers terminate in the ventral posterior lateral nucleus and in the intralaminar nuclei (Willis, 1985, Willis and Westlund, 1997; Craig, 2003; Jacobson and Marcus, 2011) (cfr Fig. 5). Only when nociceptive information reaches the thalamus and cerebral cortex, should we talk about pain. Pain perception by these higher centers triggers affective responses and suffering behaviours. The pain experience depends on the circumstances that may alter the response and varies so much from person to person that it has be also defined as "a subjective perception with a psychological dimension" (Collins *et al.*, 1960; Hunt and Mantyh 2001; Scholz and Woolf 2002; Trafton and Basbaum, 2000).

At thalamic level, sensory information from the body, limb and back of the head is collected by neurons of several thalamic nuclei including the ventral posterolateral (VPL), posterior (PTh) and intralaminar nuclei, whereas somatosensory information from the head reaches the ventral posteromedial nucleus (VPM).

As regards the processing of nociceptive information, it seems that the thalamus tells us about the quality of information (the "what" component) and the somatosensory cortex tells us about the spatial localition of the sensation (the "where" component). The (lateral) spinothalamic tract originates from projection neurons of laminae I, V, VI, and VII. That terminate primarily in VP and PTh thalamic nuclei. Some collateral branches terminate in the brainstem reticular formation. This tract conveys information perceived with an overlay of the discriminative aspects associated with various subtleties associated with the

sensation of sharp pain and, in addition, with thermal sense. At levels successively higher than the spinal cord, new fibers join the tract on its medial aspect; producing a laminated somatotopically organized tract where, in the upper spinal cord, pain and temperature fibers from the sacral region are located posterolaterally and those from the sacral region are located anteromedially. Thalamic neurons then project to somesthesic primary area in the telencephalic cortex and this projection provides the discriminative capacity of the nociceptive stimulus (Willis, 1985). VP and PTh nuclei receive input from laminae I and V via the spinothalamic pathway, conveying signals primarily from nociceptive-specific and wide dynamic range neurons (Craig *et al.,* 1999; Dubner and Gold, 1999; Casey and Morrow 1983; Gingold *et al.,* 1991; Craig, 2004; Noback *et al.,* 2005).

Collaterals of the spino-thalamic fibers originating from spinal laminae VI, VII, and VIII, activate intralaminar nuclei via the spinoreticulothalamic pathway; conveying information from large complex nociceptive fields. The intralaminar thalamic nuclei send information to the limbic system, to the somesthesic secondary area and to insula and these connections are responsible for the affective and emotional component of pain. The spinoreticular tract and the spinomesenchephalic tract carry nociceptive information to midbrain and reticular formation.

The spinomesencephalic tract is composed of the fibers of projection neurons in laminae I and Vand terminates in the periaqueductal gray (PAG) of the midbrain; this tract is involved in the modulation of pain and in the functioning of the reticular system (Reynolds, 1969, Mayer *et al.,* 1971).

The spinoreticular tract is integrated into the spinoreticulothalamic pathway terminating in the intralaminar thalamic nuclei. It originate from neurons in laminae VII and VIII, which receive inputs from large, complex, receptive fields in the periphery.

From the spinal cord, there are also direct projections to the amygdala and hypothalamus. This slowly conducting multisynaptic pathway conveys diffuse poorly localized pain from both somatic and visceral sources (Noback *et al.,* 2005; Garcia, 2012).

Finally, the thalamus also receives pain and temperature pathways from receptors in the rest of head and scalp via the trigeminothalamic and trigeminoreticulothalamic tracts. These fibers convey impulses via the three divisions of the trigeminal nerve (ophthalmic, maxillary, and mandibular) and cranial nerves VII, IX, and X. The trigeminothalamic tract

is included in the lateral pain system (Patestas and Gartner, 2006; Gaudio, 2012; Noback *et al.*, 2005) (cfr Fig. 5).

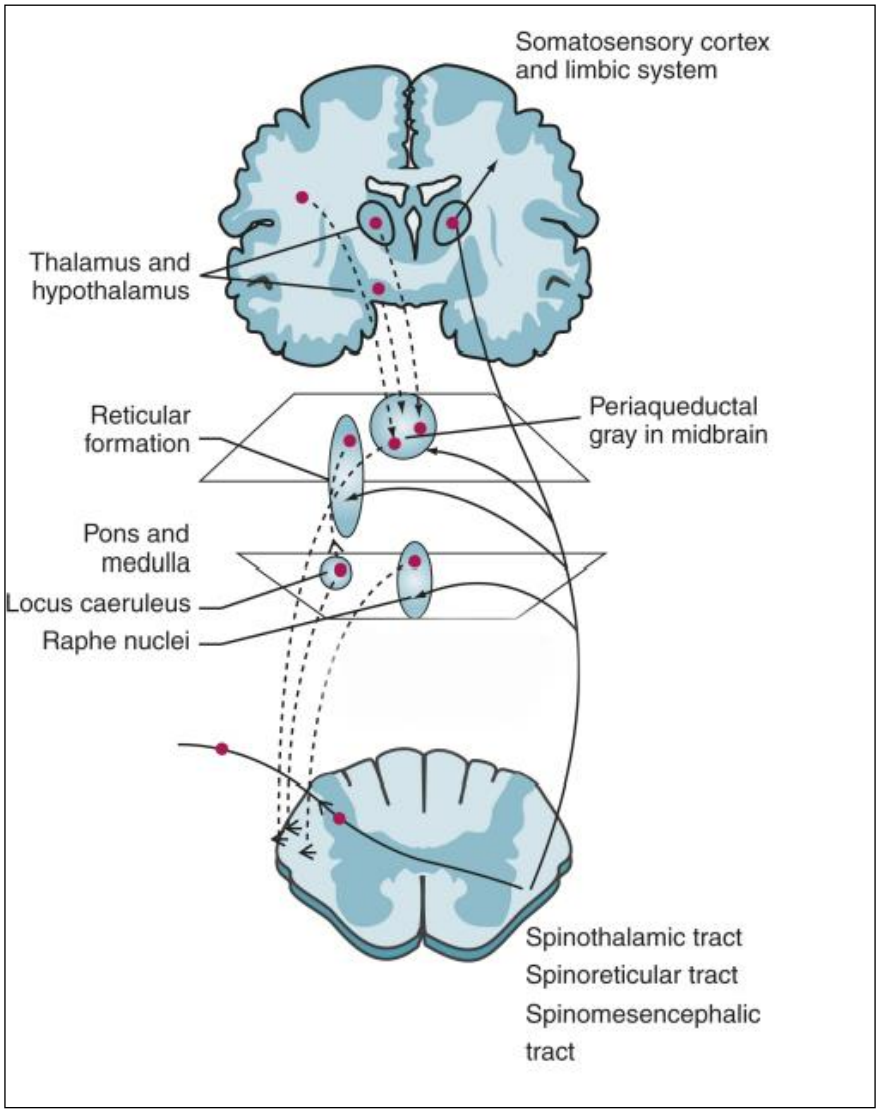

Figure 5. Schematic representation of the anterolateral system
First order neurons reside in the DRG and collect sensory information by means of their centrifugal branches reaching the periphery. Their centripetal branches enter the spinal cord, ascend 1-2 levels, and terminate in the substantia gelatinosa; second order neurones carry the sensory information from there to the thalamus. Fibers arising from second order neurons, before entering the spinothalamic tract, decussate and split: those carrying crude touch and pressure enter the lateral spinothalamic tract, those carrying pain and temperature enter the anterior spinothalamic tract. Although functionally distinct, these tracts run alongside each other, and they can be considered as a single pathway. The fibres travel in their respective pathways, synapsing in the thalamus. Third order thalamic neurones transfer the sensory signals to the primary sensory cortex. The descending pathway is represented by the dashed lines (original image from Firestein, Kelley's Textbook of Rheumatology, 8th ed.).

1.3.1 Central and peripheral mechanisms of nociceptive processing

The spinal cord actively amplifies the spinal nociceptive processing because nociceptive spinal cord neurons change their excitability to inputs from the periphery under painful conditions. On the other hand, it has to be reminded that the spinal cord is under the influence of descending influences (Schaible, 2007).

Under normal conditions, the release of excitatory amino acids by afferent fibers induces a depolarization of dorsal horn neurons. Glutamate, released during tonic activation of C fibers, is the principal excitatory transmitter acting at the synapse between primary afferent nociceptors and dorsal horn cells (Alvarez *et al.,* 2010). Glutamatergic receptors on the second order sensory neurons are mainly ionotropic, i.e. directly coupled to cation channels, which can be further subdivided into AMPA (amino 3-hydroxy-5-methyl-4-isoxazolepropionic acid)/kainate and NMDA receptors. Glutamate initially binds to AMPA receptor that produces a rapid depolarization followed by activation of the NMDA receptor (Lovinger, 2008; Latremoliere and Woolf, 2009).

Excitatory neuropeptides are co-localized with glutamate. Neuropeptide-mediated excitatory postsynaptic potentials usually occur after a latency of seconds and are long-lasting. They may not be sufficient to evoke action potential generation but act synergistically with glutamate (Urban *et al.*, 1994) Substance P (SP) is released mainly in the superficial dorsal horn by electrical stimulation of unmyelinated fibres and during noxious mechanical, thermal or chemical stimulation of the skin and deep tissue (Afrah *et al.*, 2002; Khasabov *et al.*, 2002; Ma and Woolf, 1995; Mantyh *et al.*, 1997). Neurokinin-1 (NK-1) receptors for SP are mainly located on dendrites and cell bodies of dorsal horn neurons in laminae I, IV–VI and X (Gauriau and Bernard 2002). Upon strong activation by SP, NK-1 receptors are internalized. In addition, neurokinin A (NKA) is found in small DRG cells and in the dorsal horn and spinally released upon noxious stimulation. CGRP, which is often colocalized with SP in DRG neurons, is released in the spinal cord upon electrical stimulation of thin fibres and upon noxious mechanical and thermal stimulation, potentiates the effects of SP (by inhibiting its enzymatic degradation and potentiating its release). It participates in the phenomenon of central sensitization, i.e. the changes in synaptic efficacy between afferent neurons and central neurons that increase the perception of pain. Once released by primary afferent terminals, it acts through postsynaptic CGRP

receptors, which activate PKA and PKC (Woolf and Wiesenfeld-Hallin, 1976). CGRP binding sites are located in lamina I and in the deep dorsal horn. Blockade of CGRP effects reduces nociceptive responses (Schaible, 2006).

Under pathological conditions, the second and third order neurons undergo widespread neuronal plasticity and neuronal rewiring to become hyperactive. The result of these processes may lead to the transformation of an initially adaptive reactivity in a series of counterproductive, often maladaptive responses. Observed changes include modulation of synaptic transmission and induction of LTP (Ueda, 2006; Premkumar, 2010). Peripheral sensitization involves an increase in the responsiveness of nociceptive ion channels and a reduction in activation threshold of nociceptive neurons (Julius and Basbaum, 2009; Woolf and Salter, 2008). Sensitization of nociceptive ion channels can result in ectopic or spontaneous discharges, alteration in ion channel expression, and increased neuronal sprouting (Nordin *et al.*, 1997; Premkumar, 2010).

- ♣ *Prolonged activation of C fibers by noxious stimuli depolarizes dorsal horn neurons and induces direct activation of NMDA receptors. Activation of NMDA receptors subsequently allows a massive influx of calcium within the cell, which provokes a cascade of intracellular events leading to the long-lasting modification of the properties of dorsal horn neurons. These events, including the activation of the calcium-dependent protein kinase C (PKC) and of the nitrous oxide (NO) synthase, may in turn lead to phosphorylation of the NMDA receptor and thereby enhance the calcium current generated by a given glutamate release (Kampa et al., 2004; Van Dongen, 2009; Premkumar, 2010)(cfr Fig. 6).*

•

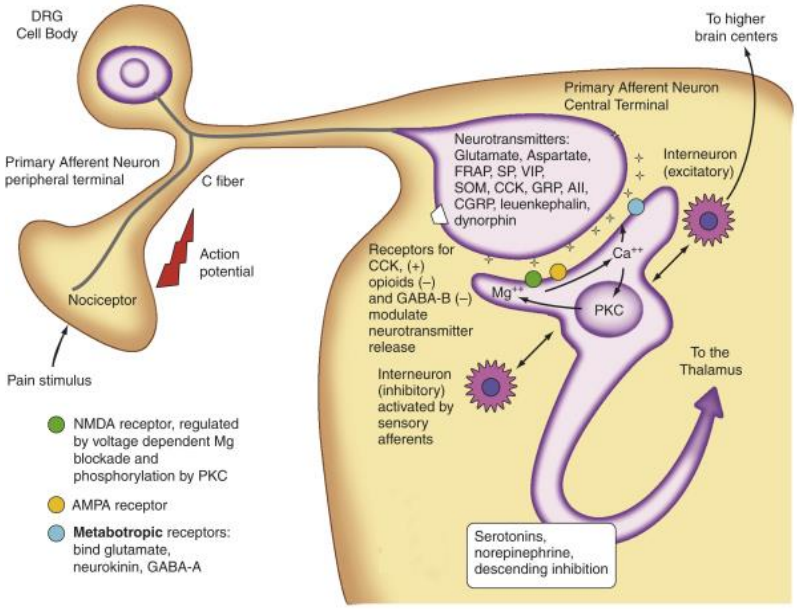

Figure 6. Nociceptive processing in the spinal cord dorsal horn

Nociceptive neurons synapse with interneurons, they stimulate nociceptive projection neurons to signal the higher centers in the brain.The interneurons that cross the anterior commissure and ascend in the contralateral spinothalamic tract transmit pain signals to the lateral thalamus, where they synapse with third-order neurons that project to the somatosensory and cingulate cortices to produce consciousness of the type and location of the tissue injury. Interneurons that inhibit the nociceptive projection neurons are activated by incoming sensory afferents and descending tracts that reduce nociceptive processing at the spinal level. These pathways originate from the brainstem (periaqueductal gray, nucleus raphe magnus) and descend through the dorsolateral funiculus of the spinal cord (original image from www.mdconsult.com).

According to the hypothesis of central sensitization, a large amount of various neurotransmitters and neuromodulators are released into the spinal cord by injury discharges (cfr Fig. 6), which have been implicated in the initiation of spinal cord circuit changes that are responsible for the neuropathic pain (Lee and Kim, 2007). Upon the repetitive C-fiber stimulation, the spinal dorsal horn neurons are in a depolarized state as a result of prolonged and amplified neuronal responses, which is dependent on NMDA receptor activation (Suzuki and Dickenson, 2005; Woolf and Salter, 2000; Premkumar, 2010). The spinal cord neurons increase their receptor expression and neurotransmitter/neuropeptide release. Central sensitization also involves descending projections from supraspinal sites that facilitate nociceptive transmission (Urban and Gebhart, 1999). In certain conditions, loss of inputs from the periphery may reorganize both spinal and supraspinal circuitry, which include glutamatergic, GABAergic, glycinergic and neuropeptidergic systems. Among the latter, substance P and CGRP as pain-transmitting or pain-modulating peptides are released into the spinal cord from the

central terminals of thinly myelinated and unmyelinated primary sensory neurons and are involved in central sensitization (Dubin and Patapoutian, 2010).

In addition, nociceptive ion channels contribute to the specificity of primary afferent fibers carrying a selective modality of pain. Among these, the identification of the transient receptor potential type 1 receptor -TRPV1- was the major catalyst that launched the fields of somatosensory and pain transduction research to the molecular level (Stucky *et al.,* 2009).

TRPV1 is a non selective cation channel which likely consists of four subunits, with each containing 6 transmembrane domains (Voets *et al.,* 2005), it is mainly expressed in peptidergic neurons, and to a lesser extent in the non-peptidergic nociceptors, the expression also occurs in various other brain regions and in several non-neuronal tissues. Particularly TRPV1 is expresed in a subset of small-sized DRG, trigeminal and nodose ganglia nociceptive neurons bearing C and Aδ fibers (Caterina et al, 1997; Tominaga *et al.,* 1998) where mediates sensory perception especially in nociception. (Caterina *et al.,* 1997)

- *Physiologically its role is essential for detecting noxious stimuli such as acidic pH (Tominaga, 1998), heat (>43 °C) (Caterina et al., 1997), and chemicals including capsaicin (Caterina et al., 1997) and anandamide (Zygmunt et al., 1999). TRPV1 exerts a pronociceptive role acting as a "molecular integrator" due to the multimodal sensory stimuli activation (Guo et al., 1999; Caterina et al., 2000) thus it is essential in modulation of pain sensation and development of thermal hypersensitivity (Caterina et al., 2000; Davis et al., 2000). Also it plays a key role in the development of the burning pain sensation associated with acute exposure to heat, and with inflammation in peripheral tissues (Valtschanoff et al., 2001) (cfr Fig. 7).*

TRPV1 activation causes neuronal depolarization and triggers sensory nerve efferent function that occurs by the release of neuropeptides, such as bradykinin, CGRP and SP, from peripheral and central nerve terminals (Maggi and Meli, 1988; Holzer, 2008). The neuropeptides, upon activation of their effector cell receptors, are able to recruit fibers that carry light touch resulting in allodynia around the injected area and enhance the

sensitization of nociceptors (Holzer, 2008; Szallasi and Blumberg, 2009). Repeated activation of the TRPV1 receptor causes the overload of intracellular Ca2+, resulting in oxidative stress and apoptotic cell injury (Shin *et al.,* 2003; Kim *et al.,* 2005). For these reasons the receptor has also been shown to play a role in certain chronic pain conditions, such as neuropathic pain, osteoarthritis, bone cancer pain, inflammatory bowel disease and migraine (O'Neill *et al.,* 2012). Chronic pain-induced sensitization also intensifies the expression of TRPV1 receptor in sensory neurons through transcriptional and translational regulation, post-translational changes and altered trafficking, contributing to the development of pathological pain states in which increased sensitivity to noxious stimuli occurs (Hucho and Levine, 2007)

Capsaicin-induced nocifensive behaviour and hyperalgesia in rodents and pain in humans are well established (Gilchrist *et al.,* 1996; Simone *et al.,* 1987; Szolcsányi, 1977).

TRPV1 antagonists have shown efficacy in animal models of both inflammatory and neuropathic pain (Patapoutian *et al.,* 2009) but systemic administration of TRPV1 antagonists commonly results in hyperthermia caused by peripheral TRPV1 blockade (Steiner *et al.,* 2007). Activation of spinal TRPV1 can generate central sensitization and mechanical allodynia (Patwardhan *et al.,* 2009) and spinal administration of TRPV1 antagonists can attenuate mechanical allodynia induced by nerve injury (Patapoutian *et al.,* 2009), but the cell types or circuits underlying these effects are unknown (Kim *et al.,* 2012).

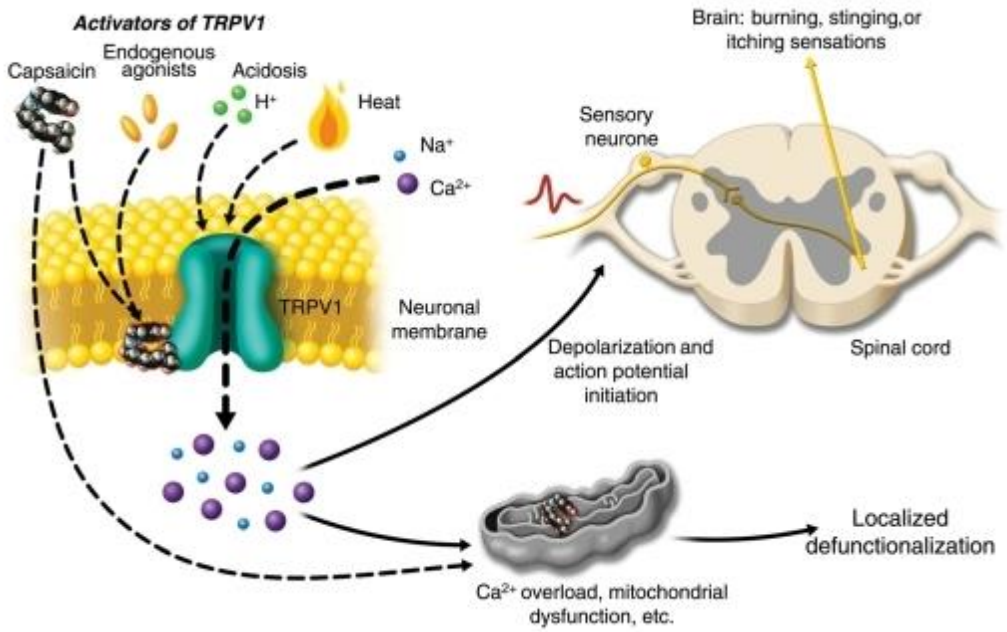

Figure 7. TRPV1 activation

The TRPV1 channel can be activated by vanilloids such as capsaicin, as well as endogenous stimulators including H^+, heat, lipoxygenase products and anandamide. TRPV1 channel function is upregulated by several endogenous mediators present in inflammatory conditions which decrease the threshold for activation of the channel. Under these conditions, TRPV1 can be activated by physiological body temperature, slight acidification or lower concentration of TRPV1 agonists. There is evidence that TRPV1 plays a role in the development of pathophysiological changes and symptoms in chronic pain sensation Activation of TRPV1 by capsaicin results in sensory neuronal depolarization, and can induce local sensitization. High concentrations of capsaicin or repeated applications can produce a persistent local effect on cutaneous nociceptors, which is best described as defunctionalization and constituted by reduced spontaneous activity and a loss of responsiveness to a wide range of sensory stimuli. When activated by a combination of heat, acidosis, or endogenous/exogenous agonists, TRPV1 may open transiently and initiate depolarization mediated by the influx of sodium and calcium ions. In the nociceptive sensory nerves which selectively express TRPV1 (mostly C- and some Aδ-fibres), depolarization results in action potentials, which propagate into the spinal cord and brain, and may be experienced as warming, burning, stinging, or itching sensations. (original Image from http://www.medscape.com).

1.4. The importance of animal models of chemotherapy-induced PN

In the past 20 years, several animal models have been published and used to further investigate mechanisms of anticancer agent-induced neuropathic pain. Most frequently experimental models have been developed in rodents (Authier *et al.,* 2009). Many models were not intended to suggest an immediate translation into clinical use, but rather to illustrate a concept and to identify a possible novel mechanism that could be exploited to avoid this important chemotherapy-induced side effect. Collectively, findings achieved by means of animal models add to the complexity and multiplicity of the mechanisms underlying the chemotherapy-induced PN.

Primary afferent nerve fibers affected by chemotherapy-induced neurotoxicity exhibit both positively and negatively regulated nociceptive thresholds (Nahman-Averbuch *et al.,* 2011). As a whole, nociceptive thresholds are increased when there occurs nerve fiber loss, whereas are reduced as a result of peripheral and central sensitization (Nahman-Averbuch *et al.,* 2011). So, thermal hypoalgesia has been associated to chemotherapy-induced PN in both humans (Dougherty *et al.,* 2004; Cata *et al.,* 2006; Attal *et al.,* 2009; Nahman-Averbuch *et al.,* 2011) and rodent models (Authier *et al.,* 2000, 2003; Fischer *et al.,* 2001; Cata *et al.,* 2006, 2008; Garcia *et al.,* 2008; Hori *et al.,* 2010; Xiao *et al.,* 2012; Zheng *et al.,* 2012). Cold allodynia, a characteristic symptom of painful chemotherapy-induced PN, also occurs in both patients (Cata *et al.,* 2006) and experimental models (Cata *et al.,* 2006; Authier *et al.,* 2009; Xiao *et al.,* 2012).

Variations in nociceptive thresholds are accompanied by neurochemical changes. For example, in the DRGs and hindpaw skin of hyperalgesic mice TRPV1 expression levels are increased, whereas they decrease in hypoalgesic animals (Pabbidi *et al.,* 2008). Conversely, thermal hypoalgesia may be underpinned by reduced TRPV1 expression and function (Pabbidi *et al.,* 2008).

Aim of the study

The present work is the result of a cooperative study on the bortezomib-induced PN, carried out on a rat model of PN induced by the drug chronic administration, that shares common neurophysiological, behavioral and pathological features with the sensory neuropathy described in humans (Cata *et al.*, 2007; Argyriou *et al.*, 2012). The rat model of bortezomib-induced PN has been developed and characterized by the reaserch team of prof. Guido Cavaletti, Department of Surgery and Translational Medicine, University of Milan-Bicocca, Italy.

The research has been designed to provide insight on an intrinsic contraddition emerging from the previous histopathological characterization of the model. In fact, though an evident axonopathy, affecting mainly Adelta and C fibers, can be easily detected, no evident changes in DRG neuronal cell body morphology could be observed (Cavaletti *et al.*, 2007; Meregalli *et al.*, 2010). Considering those findings, the aim of this study was to investigate whether the lack of morphological alterations revealed by histopathological analysis could be in line with observations of neurochemical changes likely involved in the onset and persistence of nociceptive symptoms caused by bortezomib-induced neurotoxicity occurring in DRGs and peripheral nerve fibers. For this reason, it was examined whether intravenous bortezomib administration, either as a single-dose or on a "chronic" schedule, affects the expression of neurochemical sensory markers such TRPV1, CGRP and SP in lumbar DRGs, spinal cord and sciatic nerve by means of immunohistochemical, western blot (WB) and reverse transcriptase-polymerase chain reaction (RT-PCR) assays.

2.Results

2.1 General toxicity

Bortezomib administration at doses of 0.20 mg/kg was well tolerated by rats while in the chronic experiment 8 animals treated with bortezomib died within the first 4 weeks of treatment. No acute distress was observed in the rats sacrificed 1 hour after bortezomib administration. During the first week of treatment only occasionally the animals showed mild signs of discomfort such as piloerection, hypokinesia and chromodacryorrhoea; in general, animal behavior was otherwise normal and no other remarkable evidence of general toxicity was observed**.**

Furthermore a not statistically significant weight loss during the first 10 days of bortezomib treatment was observed. As shown in Figure 8, the body weight assumed the same trend of control rats during the treatment, therefore no significant difference occurs in the body weight of control and bortezomib-treated animals.

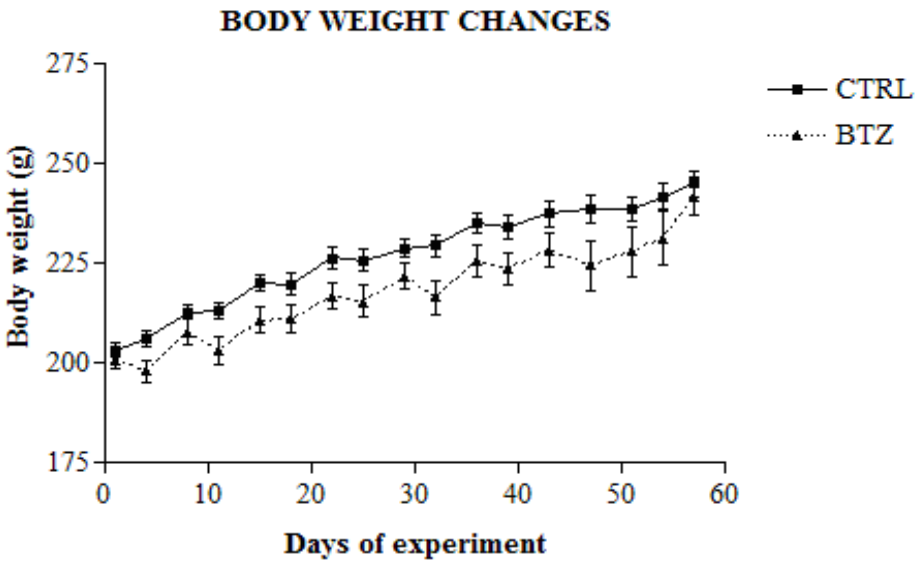

Figure 8. Body weight changes

Body weight changes throughout the chronic bortezomib-treatment. No evident differences in weight gain vs. control (CTRL) are evident during the treatment (mean values ± SD).

2.2 Neurotoxicity and pain assessment

2.2.1 Mechanical nociceptive threshold

Bortezomib-treatment induced changes in mechanical nociceptive threshold as evaluated by means of the Dynamic Aesthesiometer test. The mechanical threshold was measured before starting the pharmacological treatment (baseline value) and after 8 weeks of chronic treatment (mean values ± SD, n = 12 in each group during the treatment period). Figure 9 shows that no significant difference in the mean withdrawal response at baseline occurs. At the end of the bortezomib-treatment, the mechanical paw-withdrawal threshold significantly decreased in the treated animals compared to the control ones.

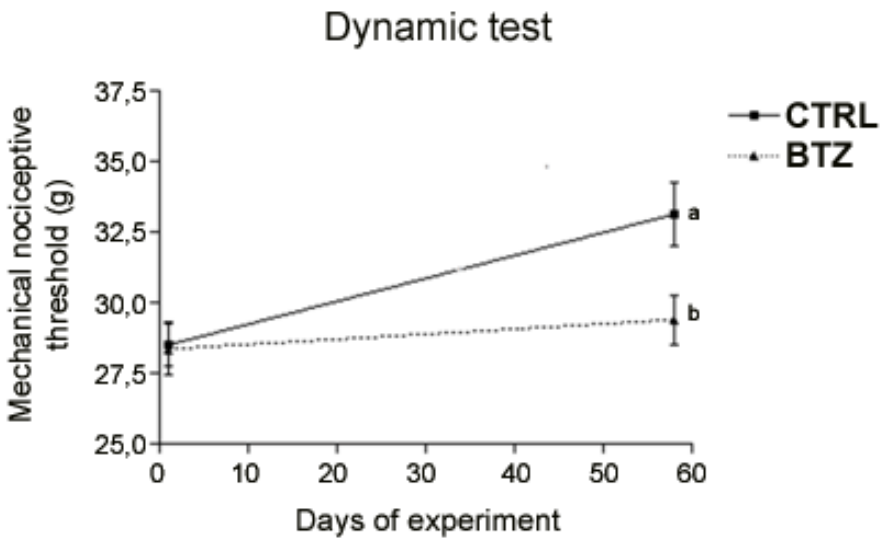

Figure 9. Dynamic Aesthesiometer test
Bortezomib-induced changes in Dynamic Aesthesiometer test.

2.3 Immunohistochemistry

Tissue sections were processed for immunohistochemistry for both ABC method and immunofluorescence to ascertain possible neurochemical changes in TRPV1 receptor and the neuropeptides SP and CGRP, likely involved in neuropathic pain transmission.

2.3.1 Dorsal Root Ganglia

The immunostaining for TRPV1-, CGRP- and SP-like protein in the DRG was intense in a subpopulation of small neurons, whereas a more moderate level of staining was observed in other small and medium neurons (cfr Fig 10, 11).

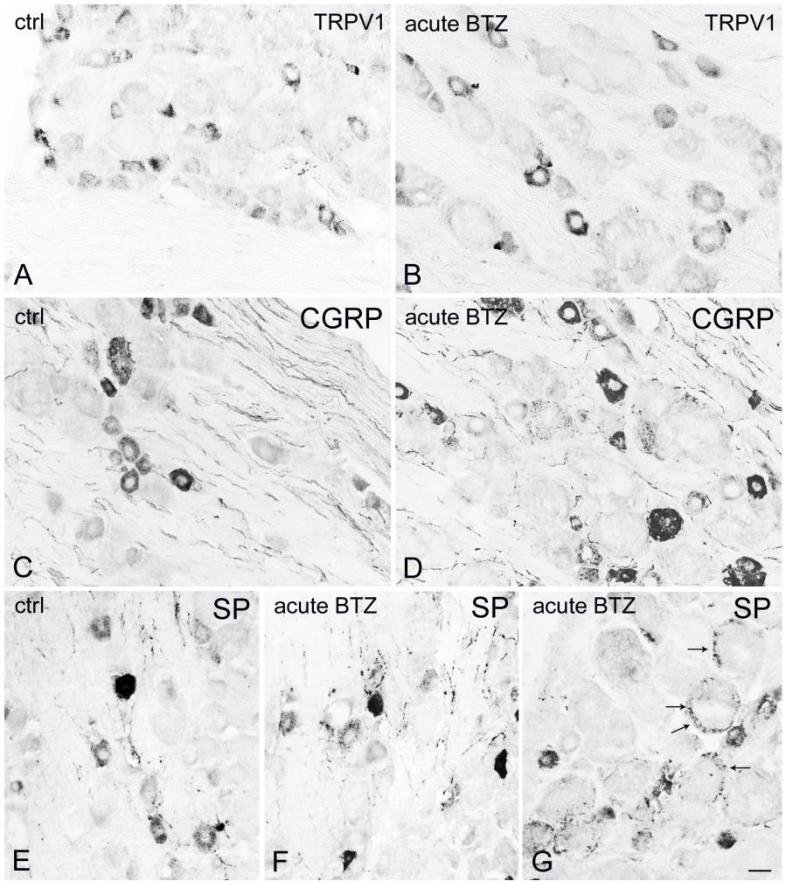

Figure 10. Bortezomib acute treatment
Immunoreactivity to TRPV1 (A, B), CGRP (C, D) and SP (E-F-G) in representative sections of lumbar DRG from control (ctrl) (A, C, E) and Acute bortezomib-treated rats (B, D, F, G). Scale bars = 25 μm.

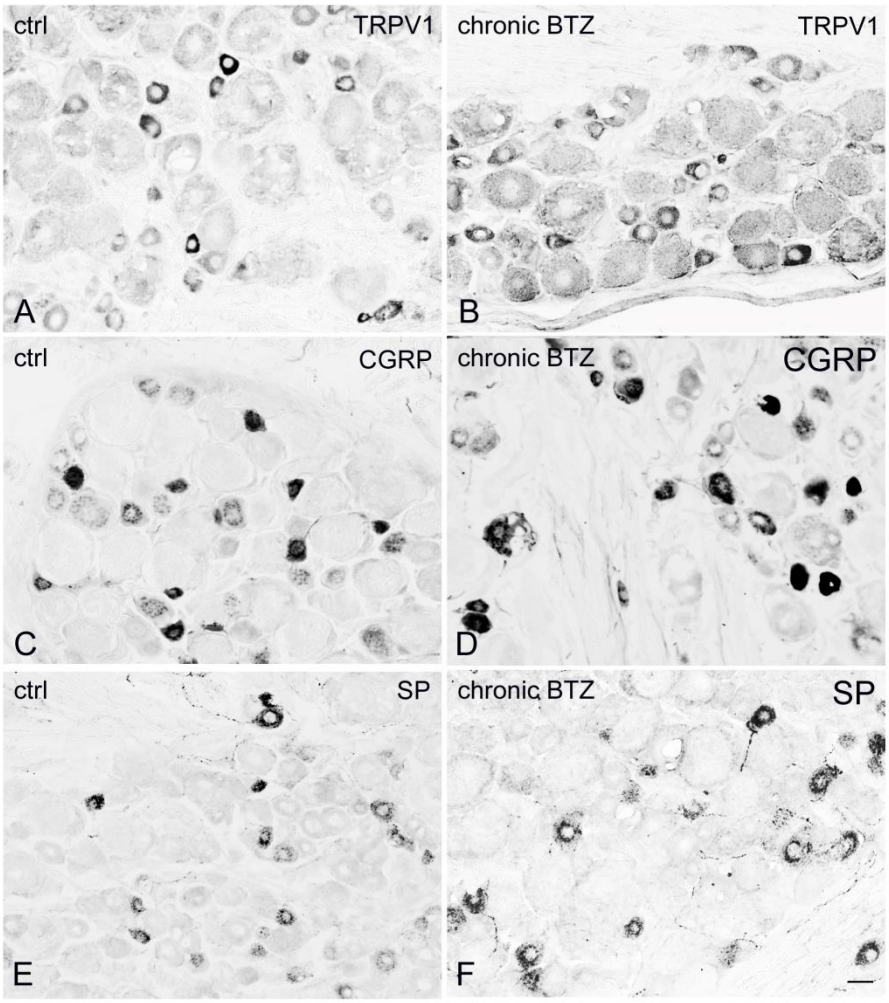

Figure 11. Bortezomib chronic treatment
Immunoreactivity to TRPV1 (A, B), CGRP (C, D) and SP (E-F) in representative sections of lumbar DRG from control (ctrl) (A, C, E) and chronically bortezomib-treated rats (B, D, F). Scale bars = 25 μm.

TRPV1-, CGRP- and SP-like immunoreactive (LI) neurons were fairly heterogeneous in both the density of reaction product and the cell size after acute (cfr Fig. 10) and chronic (cfr Fig. 11) bortezomib treatment. The immunolabeling had a granular appearance and it was distributed throughout the cytoplasm. Uneven positive staining, suggestive of a discrete localization in the Golgi apparatus and Nissl substance, could be seen in a number of immunostained neurons. TRPV1-, CGRP- and SP-LI nerve fibers were also present between neuronal cell bodies and in nerve bundles.

2.3.2 Morphometry

After acute treatment the proportion of DRG labeled neurons increased by about 3 % ($p < 0.005$) for TRPV1 and about 10% for CGRP ($p < 0.001$), whereas it did not change for SP (cfr Fig. 12, top). In some specimens, peripheral neuronal SP-like immunoreactivity suggestive of labeled satellite cells was observed (cfr Fig. 10).

After chronic bortezomib-treatment the proportion of TRPV1-LI neurons significantly increased by about 11% ($p < 0.001$) and that of CGRP-LI neurons by about 5% ($p < 0.001$), whereas it did not change for the SP-LI neuronal subpopulation (cfr Fig.12, bottom).

Size frequency histograms of labeled neurons in acutely and chronically treated rat DRGs shows the mean cell diameter of TRPV1-, CGRP- and SP-LI DRG neurons ranged from 8 to 55 μm in acutely treated rats, and from 10 to 65 μm in chronically treated animals. The majority of measured neurons were in the range of small (diameter < 25 μm) and medium (25-35 μm)-sized cells, with a mean cell diameter between 15 μm and 30 μm. Moreover, for all markers, a statistically significant rearrangement in the size distribution of positive neurons was observed in both acutely and chronically treated rats, with differential changes involving the relative frequency of small- and medium-sized immunoreactive neurons. In particular, after acute treatment, the TRPV1-, CGRP- and SP-LI neurons with a mean diameter of 5-20 μm decreased, whereas those with a mean diameter > 25 μm increased in number. After chronic treatment, TRPV1-LI small (15-25 μm) and medium-large neurons (35-60 μm) slightly increased; whereas, the number of stained neurons with a mean cell diameter of 25-30 μm decreased. CGRP-LI neurons with a mean cell diameter of 10-25 μm decreased, while those between 25 and 55 μm increased.A slight, but non-significant increase occurred in the SP-LI neurons with a mean cell diameter of 10-20 μm ($p = 0.058$).

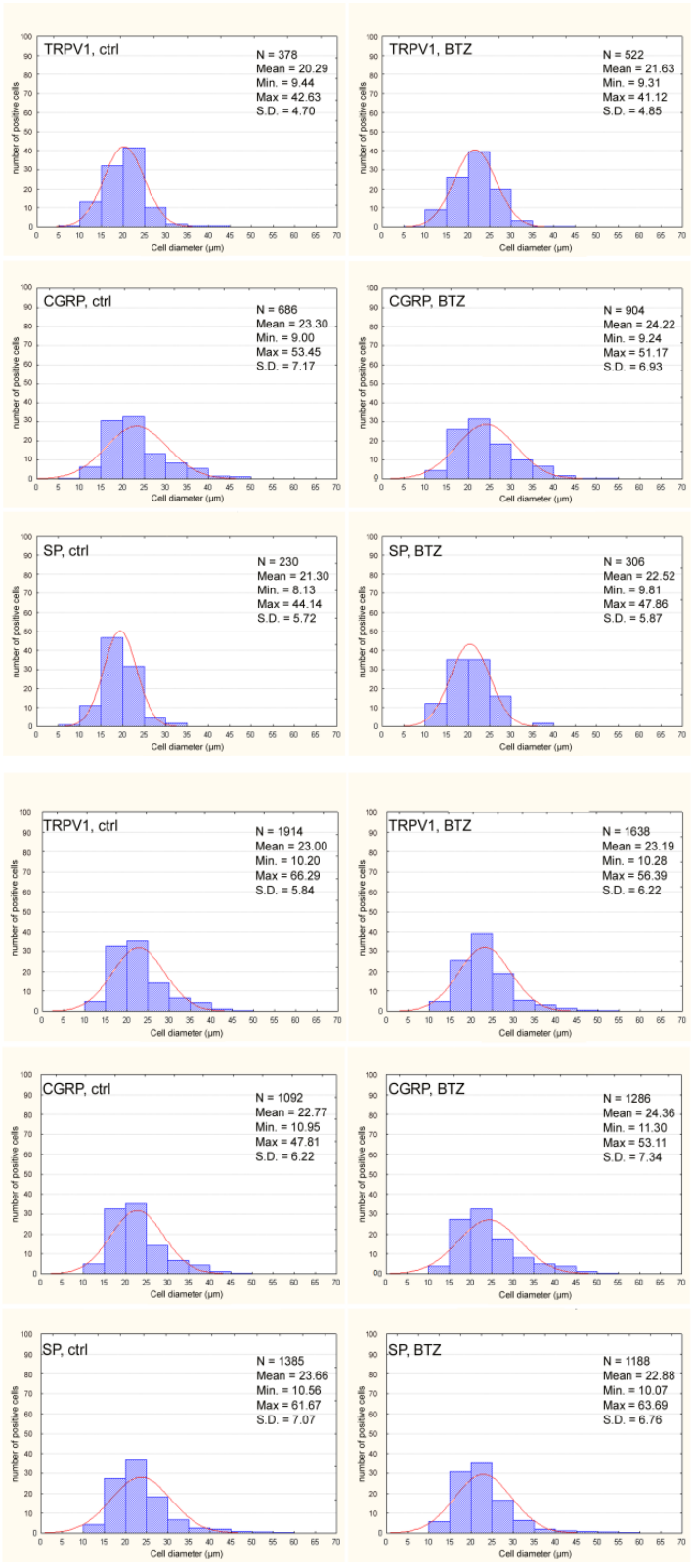

Figure 12. Percentage relative frequency

Size frequency histogram of TRPV1-, CGRP-, and SP-LI DRG eurons from control (ctrl) and acute bortezomib-treated rats (on top) and from control (ctrl) and chronic bortezomib-treated rats (on bottom)**.** Cells present in at least 6 sections were measured. X-axis values represent the mean cell diameters expressed in µm; y-axis reports values of relative percent

frequency. Curve superimposed on the histogram represents the theoretical normal distribution. N = total number of sized positive neurons; S.D. = standard deviation.

Table 2. Percentage (± confidence limits) of TRPV1-, CGRP- and SP-LI DRG neurons in BTZ-treated rats

	Acute BTZ-treatment	
	ctrl	**BTZ**
TRPV1	26.86 ± 0.01%	29.55 ± 0.01%
CGRP	25.32 ± 0.01%	34.89 ± 0.01%
SP	15.86 ± 0.04%	14.73 ± 0.03%
	Chronic BTZ-treatment	
	ctrl	**BTZ**
TRPV1	28.65± 0.02%	39.93 ± 0.03%
CGRP	28.59± 0.02%	34.87± 0.02%
SP	20.60± 0.01%	19.85± 0.01%

2.3.3 Immuno-colocalization

The analysis of double immunofluorescence-stained tissue for TRPV1 and either neuropeptide revealed that the neuronal co-expression of TRPV1/SP and TRPV1/CGRP is partial, occurring in approximately 45% of TRPV1-LI neurons in control animals. An estimation of changes in TRPV1/either neuropeptide co-expressing neurons suggested that, in the acute treated group (cfr Fig. 13), the TRPV1/CGRP subpopulation did not show any statistically significant change, whereas the TRPV1/SP one decreased significantly (-12%, $p < 0.05$; Table 1). In the chronic treated group (cfr Fig. 14), both TRPV1/CGRP- (-7%; $p < 0.05$) and TRPV1/SP-coexpressing neurons (-8%, $p < 0.005$) showed a statistically significant decrease (Table 3).

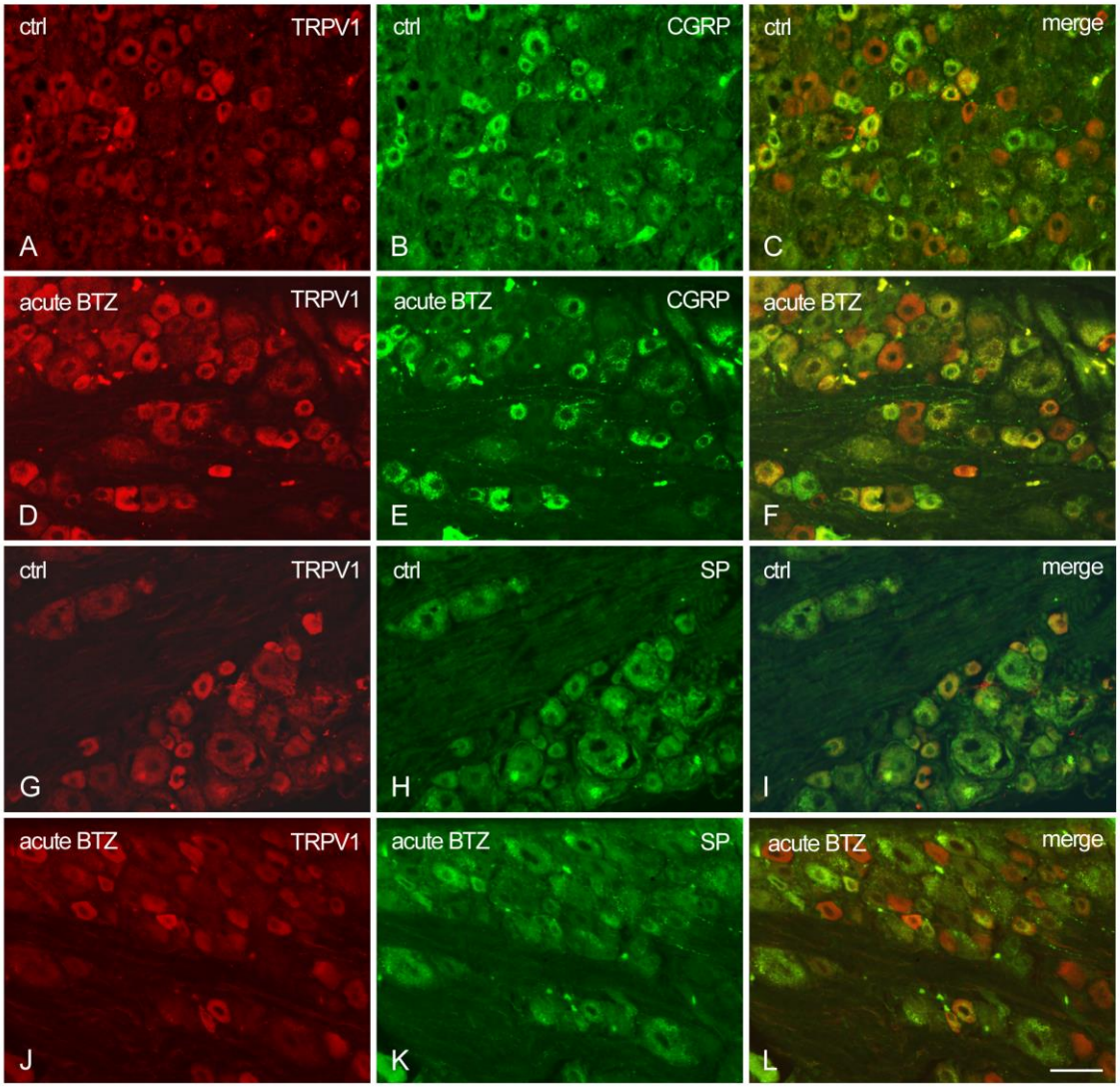

Figure 13 Bortezomib acute treatment

Double labeling immunofluorescence for TRPV1/CGRP (A-C, D-F) and TRPV1/SP (G-I, J-L) in DRG neurons from control (ctrl) (A-C, G-I) and acutely bortezomib-treated rats (D-F, J-L) C, F, I, L represent the composite images obtained by overlay of A-B, D-F, G-I and J-L, respectively. Scale bar = 25 μm.

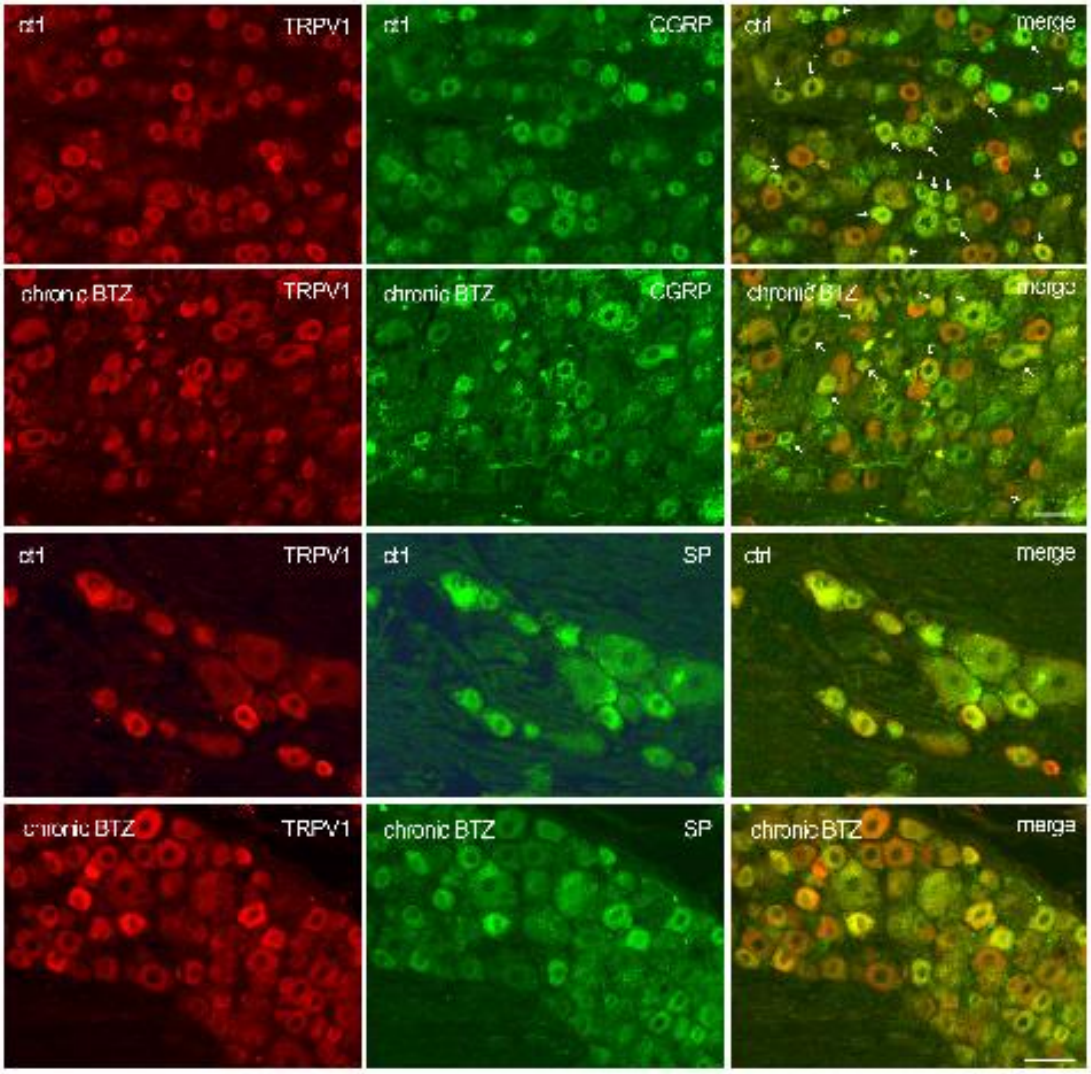

Figure 14. Bortezomib chronic treatment.

Double labeling immunofluorescence for TRPV1/CGRP (A-C, D-F) and TRPV1/SP (G-I, J-L) in DRG neurons from control (ctrl) (A, D, G, J) and chronically bortezomib-treated rats (B, E, H, K)**.** C, F, I, L represent the composite images obtained by overlay of A-B, D-E, G-H and J-K, respectively. Scale bar = 25 μm.

Acute bortezomib-treatment	
Ctrl	**Bortezomib**
TRPV1/CGRP 43.68 ± 0.06% (58 colocalized/87 TRPV1)	**TRPV1/CGRP** 49.43 ± 0.11% (43 colocalized/87 TRPV1)
CGRP/TRPV1 39.58 ± 0,10% (58 colocalized/96 CGRP)	**CGRP/TRPV1** 41.35 ± 0.01% (38 colocalized/104 CGRP)
TRPV1/SP 43.53 ± 0.11% (37 colocalized/85 TRPV1)	**TRPV1/SP** 32.33 ± 0.06 %* (86 colocalized/266 TRPV1)
SP/TRPV1 35.92 ± 0.1% (37 colocalized/103 SP)	**SP/TRPV1** 44.10 ± 0.07%** (86 cocalized/195 SP)

Table 3
Percentage (± confidence limits) of TRPV1/neuropeptide DRG neurons in bortezomib-treated rats.P value of ctrl rat vs bortezomib-treated rat colocalization degree: * p 0.05, ** p = 0.090.

Chronic bortezomib-treatment	
ctrl	bortezomib
TRPV1/CGRP 43.86 ± 0.092% (50 colocalized/114 TRPV1)	**TRPV1/CGRP** 36.84 ± 0.11% (28 colocalized/76 TRPV1)
CGRP/TRPV1 36.76 ± 0.003% (50 colocalized/136 CGRP)	**CGRP/TRPV1** 27.72 ± 0.09% * (28 colocalized/101 CGRP)
TRPV1/SP 43.33 ± 0.1% (39 colocalized/90 TRPV1)	**TRPV1/SP** 24.81 ± 0.07% ** (33 colocalized/133 TRPV1)
SP/TRPV1 50.00 ± 0.006% (39 colocalized/78 SP)	**SP/TRPV1** 61.11 ± 0.13% (33 cocalized/54 SP)

Table 4
Percentage (± confidence limits) of TRPV1/neuropeptide DRG neurons in bortezomib-treated rats. p value of ctrl rat vs bortezomib-treated rat colocalization degree: *p=0.072; ** p=0.0016

2.3.4 Spinal cord

The majority of immunoreactivity to TRPV1, CGRP and SP was found in the dorsal horn both in acute (cfr Fig. 15) and chronic (cfr Fig. 16) bortezomib treated rats.

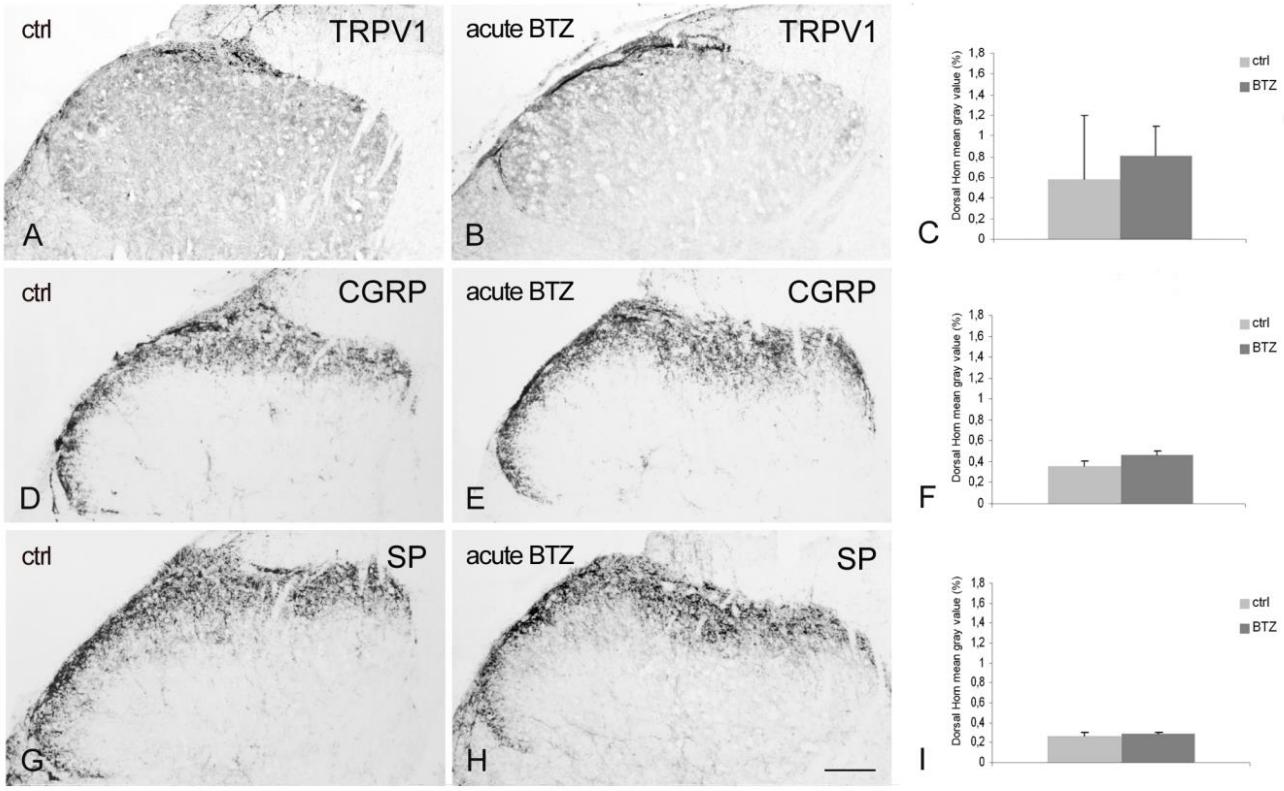

Figure 15. Bortezomib acute treatment
Immunoreactivity to TRPV1 (A, B, C), CGRP (D, E, F) and SP (G, H, I) in representative sections of lumbar spinal cord dorsal horn from control (ctrl) (A, D, G) and chronically bortezomib-treated rats (B, E, H). Scale bar = 100 μm.

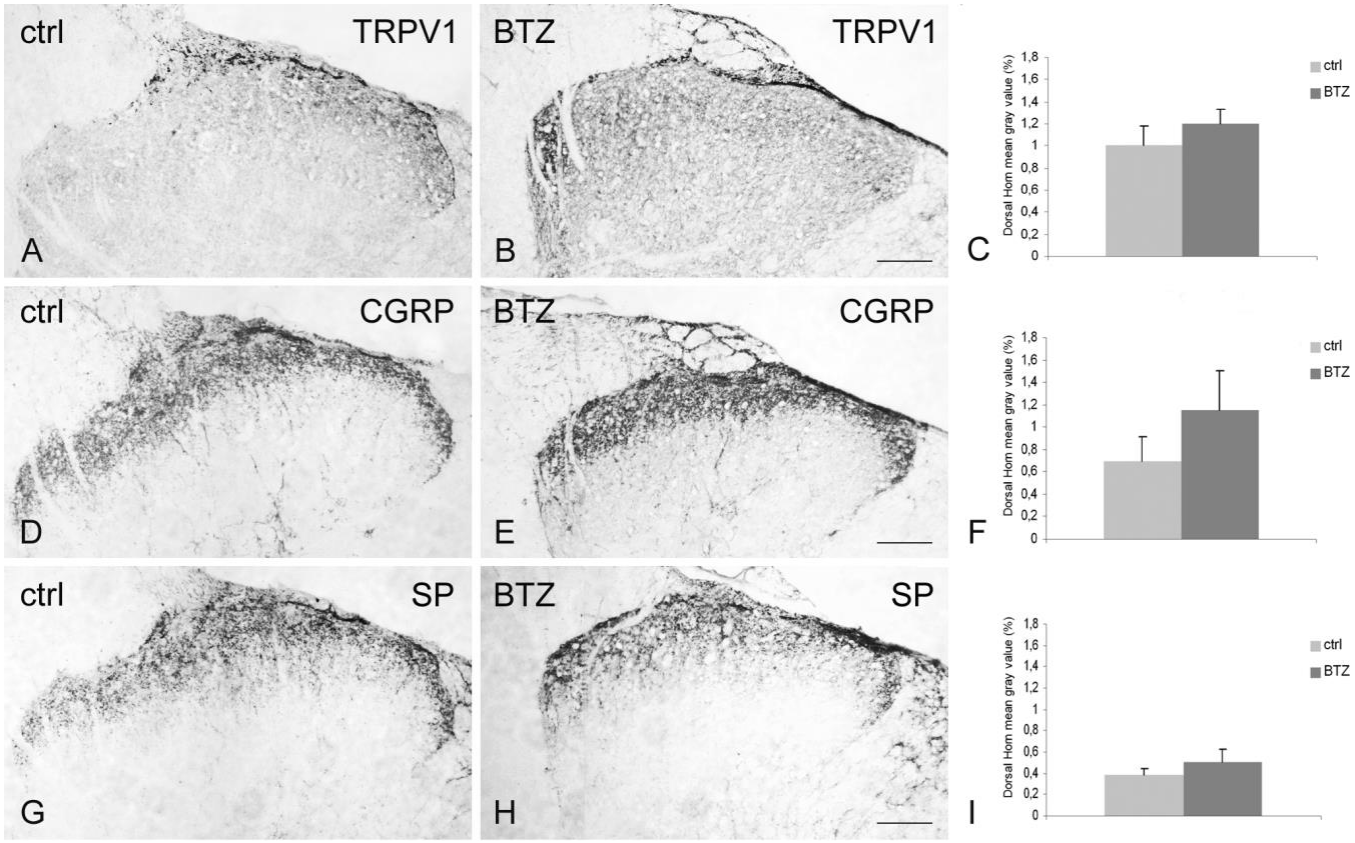

Figure 16. Bortezomib chronic treatment
Immunoreactivity to TRPV1 (A, B, C), CGRP (D, E, F) and SP (G, H, I) in representative sections of lumbar spinal cord dorsal horn from control (ctrl) (A, D, G) and chronically bortezomib-treated rats (B, E, H). Scale bar = 100 μm.

As can be appreciate from the figures 15 and 16 TRPV1-LI structures were prominent in Lissauer's tract and lamina I and occurred with a lighter labeling in inner lamina II. CGRP- and SP-LI structures showed a wider distribution, being present in Lissauer's tract, laminae I-III and lamina V. No changes were found in the ventral horn, where CGRP immunolabeled motoneurons were detectable.

2.3.5 Image densitometry

Image densitometric analysis of dorsal horn labeling showed a statistically significant increase in CGRP immunostaining in the acutely treated animals ($p < 0.05$) (cfr Fig. 15 F) and a trend to increase in chronically treated ones ($p = 0.057$) (cfr Fig. 16 C, F, I).

2.3.6 Sciatic nerve

TRPV1-, CGRP and SP-LI nerve fibers were easily detectable in longitudinal sections of sciatic nerves. The results show in the pictures releaved apparent differences between treated and control animals were found in both acute (cfr Fig.17) and chronic (cfr Fig 18) treated rats.

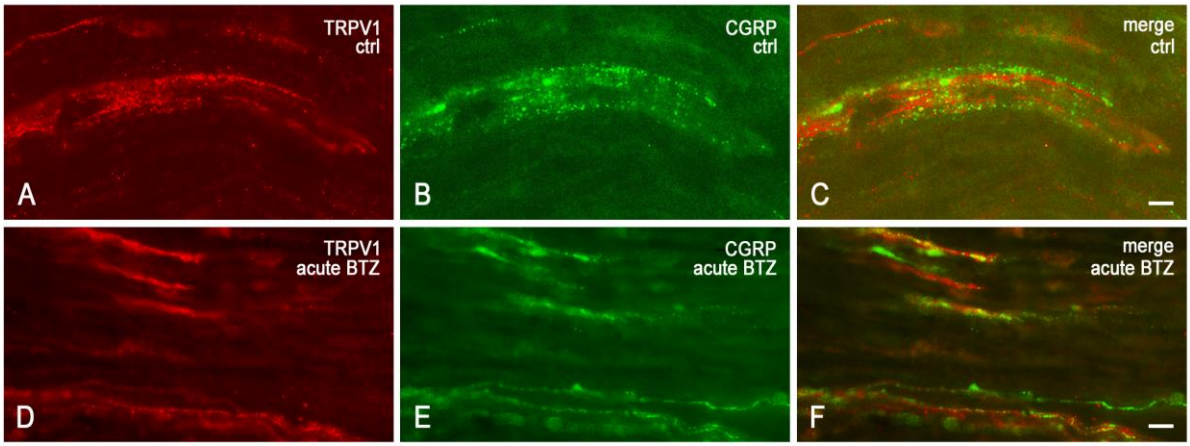

Figure 17. Longitudinal sections of sciatic nerves of acute bortezomib treated rats
Double labeling immunofluorescence for TRPV1/CGRP in sciatic nerve from control (ctrl) (A-C) and acute bortezomib-treated rats (D-F). C, F represent the composite images obtained by overlay of A-B and D-E, respectively. Scale bar = 10 μm.

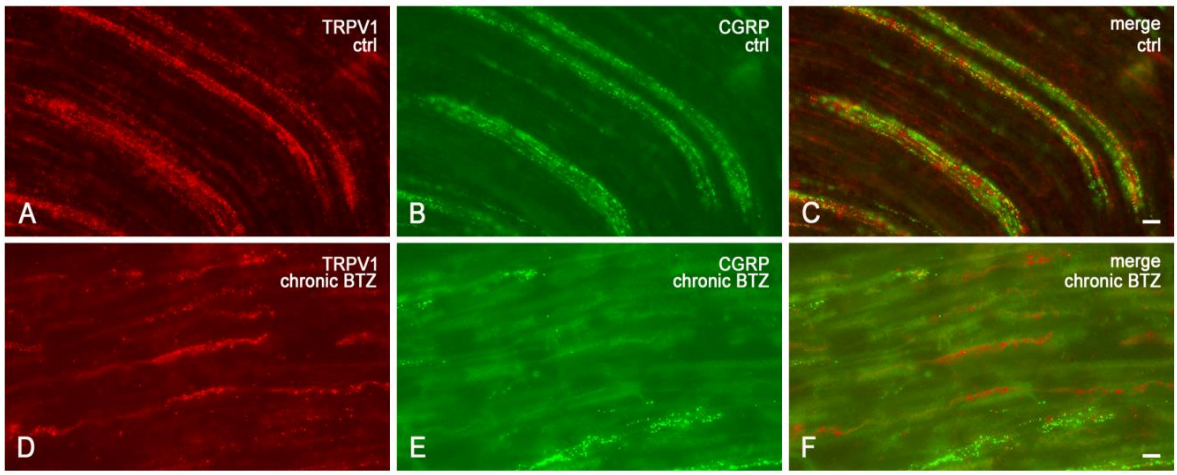

Figure 18. Longitudinal sections of sciatic nerves of chronic bortezomib treated rats.
Double labeling immunofluorescence for TRPV1/CGRP in sciatic nerve from control (ctrl) (A-C) and chronically bortezomib-treated rats (D-F). C, F represent the composite images obtained by overlay of A-B and D-E, respectively. Scale bar = 10 μm.

Analysis of colocalization performed on double immunofluorescence preparations for TRPV1 and CGRP revealed that, in both acutely (cfr Fig. 17) and chronically treated animals (cfr Fig. 18), TRPV1-like immunoreactivity occurred mainly in fibers that did not show CGRP labeling. Due to the paucity of double-labeled structures, no quantitative evaluation was performed.

2.4 Western blot

The western blot was performed only for TRPV1 on homogenate of total protein, we did not have suitable equipment to recognize CGRP and SP due to their low molecular weight.

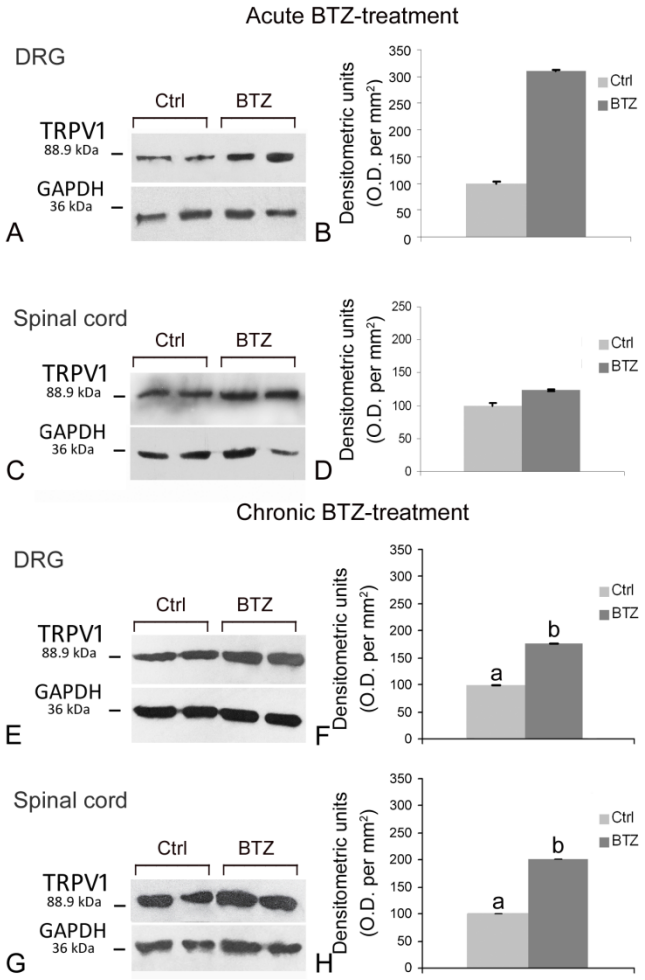

Figure 19. Western blot analysis for acute and chronic bortezomib treated rats
Western blot analysis of TRPV1 in DRG (A, E) and spinal cord (C, G) of acutely and chronically bortezomib-treated rats. B, D, F, H: Relative levels of TRPV1 expression in DRG and spinal cord with densitometric analysis of the grey levels expressed as a percentage of the optical density (O.D.) ratio of the TRPV1-positive bands to the GAPDH-positive ones. Ctrl = control rats. Error bars represent standard deviation. Letters "a" and "b" denote significant differences ($p < 0.05$).

The antibody against TRPV1 labeled a single protein band at the expected mw of 88.9 kDa (cfr Fig. 19) in DRGs and spinal cord tissue homogenates. In both acute and chronic bortezomib treated rats, TRPV1 protein levels were higher than in control animals. After acute treatment, relative optical density (O.D.) of TRPV1 protein bands increased threefold in DRG homogenates (cfr Fig. 19 A, B) ($p < 0.05$) and a mild but not significant increase

of TRPV1 protein was also evident in the spinal cord (cfr Fig. 19 C, D). Chronic bortezomib-treatment produced a statistically significant increase in the relative O.D. of the TRPV1 protein band in both DRGs (cfr Fig. 19 E, F) and spinal cord (cfr Fig. 19 G, H), amounting to 75% ($p < 0.05$) and 100% ($p < 0.05$), respectively, in bortezomib-treated versus control animals.

2.5 TRPV1- and CGRP mRNAs

Comparative RT-PCR was performed amplifying the mRNA by means of specific primers for TRPV1 and CGRP in acute and chronic bortezomib treated rats.

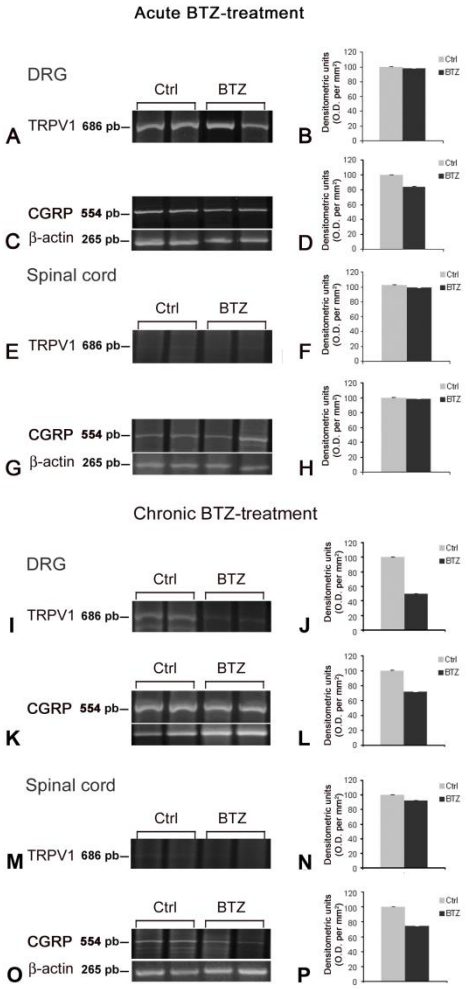

Figure 20. Comparative PCR analysis for acute and chronic bortezomib treated rats
RT-PCR analysis of TRPV1 and CGRP mRNAs in DRG (A, C, I, K) and spinal cord (E, G, M, O) of acutely and chronically bortezomib-treated rats. B, D, F, H, J, L, N, P: Relative levels of TRPV1 and CGRP expression with densitometric analysis of the grey levels expressed as a percentage of the optical density (O.D.) ratio of the TRPV1- and CGRP-positive bands to the relevant GAPDH-positive ones. Ctrl = control rats. Error bars represent standard deviation. Letters "a" and "b" denote significant differences between relative mRNA levels in ctrl versus bortezomib-treated rats (B: $p < 0.001$; DH: $p < 0.05$), while letter "a" alone denotes non-significant differences.

After acute bortezomib-treatment, no significant changes in the relative O.D. of TRPV1 mRNA bands occurred in the DRGs (cfr Fig. 20 A, B) and spinal cord (cfr Fig. 20 E, F). In addition, relative O.D. of CGRP mRNA bands were unaltered in the DRGs (cfr Fig. 20 C, D) and spinal cord (cfr Fig. 20 G, H). After chronic bortezomib-treatment, a significant

decrease of the relative O.D. of TRPV1 mRNA band occurred in the DRGs (-50%, $p < 0.001$; cfr Fig. 20 I, J), but not in the spinal cord (cfr Fig. 20 M, N), while a significant decrease of the relative O.D. of CGRP mRNA band occurred in the DRGs (- 28%, $p < 0.05$; cfr Fig. 20 K, L) as well as in the spinal cord (-26%; $p < 0.05$; cfr Fig. 20 O, P).

3. Discussion

The identification of the key effectors of the bortezomib cytotoxicity as well as of the molecular factors able to contrast or inhibit its action has been hampered, so far, by the fact that the proteasome controls the half-life of the vast majority of cellular proteins (Jesenberger and Jentsch, 2004; Adams, 2004). Morevoer, it has been suggested that the bortezomib molecule per se, compared to other proteasome inhibitors, could be responsible of a neurotoxic effect, because it induces an hyperaccumulation of not degraded ubiquitinated proteins (Fernandez *et al.*,2006). It has been inferred that bortezomib acts downstream of proteasome inhibition by interfering with stress kinases, survival signals and/or apoptotic factors (Mitsiades *et al.*, 2002). The dysregulation of mitochondrial functions and release of reactive oxygen species (ROS) are also common processes induced by bortezomib (Liu *et al.*, 2003; Jesenberger and Jentsch, 2004; Adams, 2004). Thus, as early as 3–4 h after bortezomib treatment, epithelial tumor cells show a dysregulated mitochondrial membrane potential and accumulate ROS, that subsequently lead to caspase activation (Ling *et al.*, 2003; Fribley *et al.*, 2004).

In this scenario, the present study investigated the effects of bortezomib-treatment given either as a single acute or a chronic schedule on the neurochemical features of DRG primary afferent neurons and their relevant peripheral and central processes. Our results, in agreement with previous observations (Meregalli, 2010), show that prolonged bortezomib administration induces a PN without appreciable adverse effects on the general condition of the animals.

As expected based on previous observations (Meregalli *et al.*, 2010; 2012), the histopathological analysis carried out by colleagues at the University of Milan-Bicocca revealed that acute bortezomib-treatment did not induce morphological alterations neither in the sciatic nerve nor in the DRG neuronal perikarya. Histopathological analyssi further confirmed that, in chronically treated animals, the sciatic nerve showed a mild axonopathy, affecting mostly the small myelinated and unmyelinated fibers. Similarly, clear cytoplasmic vacuolization was detected in some DRG satellite cells. No obvious changes were observed in the dorsal horn of the spinal cord (data not shown).

3.1 Neurophysiological evaluation

Neurophysiological and neuropathological assessments were consistent with measures at baseline and end of treatment time points previously observed (Meregalli *et al.*, 2010; 2012). As regards the modification of nocifensive behavior, the chronic model of bortezomib-induced PN was associated with the onset of mechanical allodynia as assessed after the 8-week treatment. Interestingly, data concerning the weekly outcome of bortezomib-treatment showed a significant reduction in withdrawal latency after 4 weeks of treatment; however, at the later time point of 8-weeks (end of treatment period) and the follow-up 4-week period, the difference was no longer significant (Meregalli *et al.*, 2010).

Although the bortezomib schedule used in this study differs from that used in clinical practice with respect to the duration of administration and dosage, calculations to translate drug doses from animal to human studies (Reagan-Shaw *et al.*, 2008) indicate that our model of bortezomib-induced neurotoxicity is highly relevant. In fact, it closely mimics the sensory neuropathy described in human patients by sharing with it common neurophysiological, behavioral and pathological features, occurring often within the first cycle of treatment (Cata *et al.*, 2007; Argyriou *et al.*, 2008).

3.2 Bortezomib-induced effects on expression of TRPV1 and CGRP mRNAs and proteins

Our results provide novel evidence that bortezomib-induced nocifensive behavior is accompanied by increased TRPV1 protein levels in DRGs and spinal cord and down-regulated levels of TRPV1 mRNA. Decreased levels of CGRP mRNA were also observed in both DRGs and spinal cord.

We do not have a clear-cut explanation of the mismatch between levels of TRPV1 mRNA and protein and details about neuronal mechanisms underlying protein/mRNA reciprocal changes in this context remain to be elucidated. However, the ubiquitin-proteasome system has a role in receptor protein catabolism; as an example, NMDA receptor subunits have

been shown to be degraded by the proteasome following ubiquitination initiated by several ligases (Kato *et al.,* 2005). Interestingly, novel evidence has been provided that also TRPV1 receptor is susceptible to proteasomal degradation, unless it translocates to the plasma membrane; in fact, blocking TRPV1 trafficking to the plasma membrane markedly decreases total TRPV1 expression due to proteasomal degradation (Shimizu *et al.,* 2012). Proteasome-regulated TRPV1turnover appears to be dynamic and has been suggested to be related to the fine-tuning of nociception (Kato *et al.,* 2005). In bortezomib-induced NP models, the occurrence of axonal degeneration and Schwann cell endosomal membrane dilations likely accounts for impaired protein membrane trafficking (Cavaletti *et al.,* 1992; Shin *et al.,* 2012; Bruna *et al.,* 2010). In our specimens, the enduring bortezomib-induced proteasome inhibition might have well caused a TRPV1 accumulation in the cytoplasm which therefore can account for the increased levels of TRPV1 in DRGs.

As for the observed decrease of TRPV1 and CGRP mRNA relative levels, it has to be highlighted that proteasome blockade causes reduction of transcriptional activity and nuclear retention of poly(A)RNAs (Voorhees *et al.,* 2003; Cata *et al.,* 2007; Casafont *et al.,* 2010), though the increase in protein expression itself may act as a retrograde signal to modulate transcription. Yet, NF-κB proteasome-independent activation pathways have also been reported (Mühlen *et al.,* 2001; Pearson *et al.,* 2011) and, depending on the targeted cell type, bortezomib may activate rather than inhibit the NF-κB canonic pathway

Plasticity of TRPV1 expression in chronic pain conditions is considered to represent one of the mechanisms involved in hyperalgesia (Hideshima *et al.,* 2009). The functional characterization of TRPV1-labeled neurons goes beyond the aim of this study. However, available experimental studies on the systemic administration of different TRPV1 antagonists demonstrate a reduction of mechanical allodynia and hyperalgesia in animal models of neuropathic, inflammatory and postoperative pain and suggest a role of TRPV1 in the modulation of mechanical hyperalgesia (Pomonis *et al.,* 2003; McGaraughty *et al.,* 2008; Yu *et al.,* 2008)

Regarding the specific time profile and turnover of TRPV1 protein after the acute bortezomib delivery, we were not able to find literature data with which to compare our results, since experimental studies on the effect of a bortezomib single dose, both in rats

(Casafont *et al.*, 2010) and mice (Trevisan *et al.*, 2013) were not designed to investigate the immediate neurotoxicity of its administration. However, pharmacokinetics of bortezomib are well known because the drug has been shown to be rapidly distributed into tissues after administration of a single dose, with an initial plasma distribution half-life of less than 10 minutes. Maximum proteasome inhibition occurs within 1 hour and recovers close to baseline within 72 to 96 hours after administration (Schwartz and Davidson, 2004). Recently, in the same rat model of bortezomib-induced PN as ours and with the same dose used in this study, Meregalli *et al.* (2014) found that a maximal time-dependent proteasome inhibition can be observed in peripheral blood mononuclear cells and sciatic nerve specimens asearly as 1 hour after a single dose bortezomib delivery, thus supporting the possibility of a quick cytoplasmic accumulation of TRPV1 protein, as also suggested by the low but significant increase of the proportion of TRPV1-LI neurons in the DRG (present data).

3.3 Bortezomib-induced effects on primary afferent neuron histochemical features

Bortezomib-treatment also induced an augmented immunoreactivity to TRPV1 and CGRP in the DRG neurons and spinal dorsal horn, and caused a decrease of TRPV1/neuropeptide colocalization in DRG neurons. No bortezomib-dependent changes were observed for SP immunohistochemical detectability. In some specimens, peripheral neuronal SP-like immunoreactivity suggestive of labeled satellite cells was observed giving a neurochemical support to our histopathological assessment (see above). They further suggest that the histological alterations, already visible after a single acute dose of bortezomib and previously reported also for paclitaxel (Authier *et al.*, 2000), are an early trait of chemotherapy-induced PN. In addition the preponderance of experimental evidence and theoretical considerations, support the notion that changes in satellite glial cells, alone or in concert with changes in neuronal function, do affect nociception (Ohara *et al.*, 2009).

3.4 Percent frequency of labeled DRG neurons

To our knowledge this is the first study reporting that bortezomib treatment in a rat model causes a general increase in the percent frequency of TRPV1- and CGRP-LI DRG neurons after both acute and chronic administration. Our immunohistochemical data are in keeping with those on CGRP-LI neuronal frequency in mouse DRGs after chronic bortezomib-treatment (Bruna *et al.,* 2010). The increase in TRPV1- and CGRP-LI in the DRGs occurs with a parallel increase in the spinal cord dorsal horn. Interestingly, increased immunoreactivity for TRPV1 (Yu *et al.,* 2008; Hudson *et al.,* 2005; Kim *et al.,* 2008) and CGRP (Zheng *et al.,* 2008) has been previously shown in uninjured primary afferent neuronal perikarya in different models of nerve lesion. Moreover, CGRP expression may increase in several pathological conditions, including partial nerve injury, where pain hypersensitivity occurs (Menard *et al.,* 1996.). In comparison, cisplatin has been previously reported not alter the DRG expression of SP (Apfel *et al.,* 1992)

3.5 Relative size frequency of labeled DRG neurons

In our model, bortezomib administration induced a rearrangement in the relative size frequency of TRPV1-, CGRP- and SP-LI neuronal subgroups, suggesting the possibility of a drug-induced neuronal phenotype switch that may go with the onset of bortezomib-induced mechanical hyperalgesia. These observations are in agreement with those obtained in the mouse model of bortezomib neurotoxicity where medium-sized neurons slightly decrease, small neurons increase and the relative number of large CGRP-LI neurons increases (Bruna *et al.,* 2010). Taken together, these data suggest that the phenotypic switch secondary to bortezomib-treatment may partly represent the neuronal response to treatment, as also suggested by Bruna *et al.* (Bruna *et al.,* 2010).

3.6 TRPV1/neuropeptide colocalization

Overall, the colocalization data support that a portion of the TRPV1-LI DRG neurons are neuropeptidergic. The analysis of changes in neuronal colocalization of TRPV1 with neuropeptides provides a morphological basis to suggest a role for TRPV1 in the release of these molecules and thus in nociceptor sensitization, and supports the possible implication of TRPV1-, CGRP- and SP-positive neurons in the persistence of painful neuropathic symptoms (Holzer, 2007). The fact that the TRPV1/neuropeptide colocalization seen in the DRGs did not parallel that observed in both central and peripheral nerve processes of primary afferent neurons is in keeping with previous observations by Guo *et al.*(1999), who suggested alternative mechanisms of neuropeptide release in response to capsaicin application. Future studies will examine how these neurochemical changes affect neurophysiological function in DRG neurons and the spinal dorsal horn.

3.7 Bortezomib-induced effects on spinal cord histochemical features

The neuronal response to bortezomib neurotoxicity involves not only the DRGs but extends to the spinal cord dorsal horn, where neurochemical alterations parallel those observed in the periphery. In particular, following bortezomib treatment, densities of dorsal horn immunolabelling for TRPV1 and CGRP were increased. Importantly, this response is larger in the chronically bortezomib-treated animals.

The basal expression of TRPV1 mRNA in the spinal cord is in keeping with previous RT-PCR studies (Sanchez *et al.,* 2001; Kim *et al*, 2012) and with the recent demonstration that TRPV1 expression occurs in GABAergic interneurons of the rat dorsal horn, where it mediates neuropathic mechanical allodynia and disinhibits nociceptive circuits in the spinal cord (Doly *et al.,* 2004). Interestingly, TRPV1 expression by glial cells has also been described (Chen *et al.,* 2010) and TRPV1 has been reported to be involved in activating spinal glia in mice with nociceptive and pathological pain. Moreover, since bidirectional axonal transport of TRPV1 mRNA along primary afferents has been demonstrated in some pathological conditions such as experimental acute inflammation (Barajon *et al.,* 1996), it cannot be excluded that part

of the TRPV1 mRNA detected in our specimens has a primary afferent origin. If this was the case, the reduction of TRPV1 mRNA secondary to bortezomib administration might be explained by the reduction of its production, and hence by the reduction of centripetal transport, by DRG neurons.

Consistent with changes in TRPV1 transcript and protein levels, CGRP mRNA also showed a decrease that may be correlated to the increase in density of CGRP-immunoreactive structures in the bortezomib-treated versus control rats.

3.8 Comparison with neurochemical phenotype changes observed in other chemotherapy-induced PN

While experimental evidence regarding the effects of bortezomib on the neurochemical phenotype is limited to data on CGRP and TRP receptors in mouse models, after acute (Trevisan *et al.,* 2013) and chronic administration (Bruna *et al.*, 2010; Trevisan *et al.,* 2013), several studies of sensory neuropeptides (Verdú, *et al.,* 1999; Alessandri-Haber *et al.,* 2008) and TRP receptors in the spinal cord and DRG (Ta *et al.,* 2010; Hudson *et al.,* 2005) following treatment with different classes of antineoplastic drugs are available in rodents. It has been demonstrated for instance that platinum-based compounds, taxanes and vinca alkaloids modulate the expression of TRPV1, as well as other TRP receptors, in DRG neurons *in vitro* and *in vivo* (Zhao *et al.,* 2012; Hudson *et al.,* 2005). Cisplatin and oxaliplatin affect the expression of TRPV1 and TRPA1 mRNA by causing a 3 fold mRNA increase as early as 6 hours after treatment in cultured DRG neurons (Zhao *et al.,* 2012). Similarly, trigeminal ganglia (TG) of cisplatin-treated mice had significant increases in TRPV1 mRNA expression (Zhao *et al.,* 2012). However, mRNA changes are not mirrored by immunohistochemistry studies, showing that no change occurred in the proportion of the TRPV1 immunopositive TG neurons in cisplatin- and oxaliplatin-treated mice compared to naïve animals (Zhao *et al.,* 2012). In the same way, TRP receptors have been shown to have a role in the pathogenesis of paclitaxel-associated pain symptoms that were related to increased TRPV1 mRNA and protein expression in rat DRG neurons (Hudson *et al.,* 2005). A single injection of paclitaxel is

sufficient to increase the expression of TRPV1 mRNA and protein in rat DRG (as seen in both homogenates and tissue sections by RT-PCR, in situ hybridization and immunochemistry), and to enhance TRPV1 expression in the paw skin at day 14 after treatment (Hudson *et al.,* 2005). By contrast, the development of sensory disorders following vincristine treatment has been related to changes in the expression of TRPV4 (Zhao *et al.,* 2012).

Conclusions

- Our data support the notion that bortezomib treatment selectively affects primary sensory neurons that for their anatomical and neurochemical characteristics are likely involved in the processing of painful sensory stimuli.
- In DRG neurons and the spinal cord, the bortezomib-induced neurochemical changes appeared after a single dose of the drug and were enhanced after chronic treatment.
- Taken together, these findings increase our understanding of the nociceptive symptoms associated with bortezomib-induced sensory neuropathy and may contribute to the development of new targeted therapies.

4.Materials and methods

4.1 Animals and animal care

Animals. A total of 80 adult female Wistar rats (Harlan Italy, Correzzana, Italy), weighing 175–200 g at the beginning of the experiment, were used for the study. Animals were housed in a limited access animal facility with controlled room temperature (22 ± 2°C) and relative humidity (55 ± 10%) and under an artificial 12h light/dark cycle (light 7 a.m.–7 p.m.). The care and husbandry of the animals were in conformity with the institutional guidelines in compliance with national (D.L. n.116, Gazzetta Ufficiale della Repubblica Italiana, Additional40, Feb 18, 1992 and subsequent modifications) and international laws and policies (EEC Council Directive 86/609, OJ L 358, 1, Dec.12, 1987; Guide for the Care and Use of Laboratory Animals, US National Research Council, 8th ed., 2011). The experimental plan was examined and approved by the Ethics Committee of the University of Milan Bicocca.

4.1.1 Drug administration

Bortezomib (LC Laboratories, Woburn, MA) was dissolved in 5% Tween 80, 5% ethanol, 90% sterile saline. Animals were divided into two experimental groups. One group of 40 rats was treated with bortezomib by tail vein injection. Eighteen animals received 0.20 mg/kg of bortezomib as single dose for “acute” schedule and 22 animals underwent an 8-week period of bortezomib administration for “chronic” schedule, 0.20 mg/kg/day three times per week. The remaining 40 animals were left untreated and used as controls for the 2 time points of examination. Euthanasia for tissue harvesting was done under deep xylazine/ketamine anesthesia 1 hour after the single bortezomib dose in the “acute” experimental schedule and one day after the last bortezomib administration in the “chronic” experimental schedule.

4.1.2 General toxicity

The general condition of treated animals was assessed daily and body weight of the chronically treated rats was measured twice/week to monitor drug toxicity and for drug dose calculation. Animals with evident distress or remarkable weight loss were carefully examined by a certified veterinarian experienced with *in vivo* studies for possible withdrawal from the study for humane reasons.

4.2 Neurotoxicity and pain assessment

4.2.1 Mechanical nociceptive threshold

The mechanical nociceptive threshold was assessed using a Dynamic Aesthesiometer Test (model 37450, Ugo Basile Biological Instruments, Comerio, Italy), which generated a linearly increasing mechanical force. Rats were habituated to the full procedure for 30 min/day on two consecutive days and testing was conducted on the third day. On each day of testing, animals were placed in a Plexiglas chamber (28 x 40 x 35-cm, wire mesh floor) in the dynamic aesthesiometer for a 15 min acclimatization period followed by testing. At each time point, after the acclimatization period, a servo-controlled mechanical stimulus (a pointed metallic filament, 0.5mm diameter) was applied to the plantar surface of the hind paw, which exerted a progressively increasing punctuate pressure, reaching up to 50g within 20 sec. The pressure evoking a clear voluntary hind-paw withdrawal response was recorded automatically and taken as representing the mechanical nociceptive threshold index. The mechanical threshold was always assessed alternatively on each side every 2 min on 3 occasions to yield a mean value. The results represent the maximal pressure (expressed in grams) tolerated by the animals. There was an upper limit cut-off of 30 sec after which the mechanical stimulus was automatically terminated. If paw movement subsequent to stimulus initiation appeared to be related to grooming or locomotion, that trial was repeated after a lapse of 1 min.

4.3 Sampling

Immediately after sacrifice, the L4-L6 DRGs with the corresponding spinal cord segments and the sciatic nerves were rapidly dissected out and either frozen at -80°C for western blot and RT-PCR analyses or fixed by immersion in freshly prepared 4% phosphate-buffered paraformaldehyde, pH 7.3, for 4–6 h at 4°C, and then rinsed overnight in 0.1 M phosphate buffer (PB), pH 7.3, containing 20% sucrose for immunohistochemistry. After sucrose infiltration, samples were embedded in Optimal Cutting Temperature (OCT) medium for cryostat sectioning.

4.4 Immunohistochemistry

A total of 36 DRGs and lumbar spinal cord segments were processed: 16 from the acutely treated group (8 bortezomib-treated, 8 controls) and 20 from the chronically treated ones (10 bortezomib-treated, 10 controls). Sixteen sciatic nerve segments, 8 from the acutely treated group (4 bortezomib-treated, 4 controls) and 8 from the chronically treated ones (4 bortezomib-treated, 4 controls), were examined. Cryostat semiconsecutive sections (12 μm thick) were collected on chrome alum-gelatin (USB Corporation, Cleveland, OH, USA) coated slides and processed either by the avidin–biotin–peroxidase complex (ABC) immunohistochemical technique or by immunofluorescence double labeling.

4.4.1. ABC Immunohistochemical technique

For ABC processing, endogenous peroxidase activity was blocked with 0.1% phenylhydrazine in phosphate buffered saline (PBS) containing 0.2% Triton X-100 (PBS/T) followed by incubation with 20% of either normal goat (NGS) or normal horse serum (Vector, Burlingame, CA, USA) for 1h at RT and then incubated with primary antiserum (cfr Table 5).

Biotin-conjugated goat anti-rabbit, donkey anti-goat, and goat anti-guinea-pig serum (Vector, Burlingame, CA, USA), diluted 1:400, were used as secondary antiserum. The reaction product was revealed by the ABC complex (BioSpa Div. Milan, Italy), diluted

1:250, and followed by incubation with a solution of 0.1 M PB, pH 7.3, containing 0.05% 3-3′-diaminobenzidine (Sigma, Milan, Italy), 0.04% nickel ammonium sulfate and 0.01% hydrogen peroxide.

4.4.2 Indirect immunofluorescence

For IF the slides were incubated with either 20% normal goat (NGS) or normal horse serum (Vector, Burlingame, CA, USA) for 1 h at RT then incubated with primary antiserum overnight at 4°C (cfr Table 5).

For double labeling, after a pre-incubation with 20% NGS, sections were double stained for TRPV1/CGRP, TRPV1/SP by means of subsequent incubations with primary antiserum, diluted as reported in Table 3. Sections were then incubated with Alexa Fluor 488- or Alexa Fluor 594-conjugated secondary antibodies (Invitrogen, Eugene, OR, USA), diluted 1:500 and 1:600, respectively. Control immunostaining was obtained substituting the primary antiserum with normal serum. Slides were examined with an Olympus BX61 microscope, equipped with epifluorescence illumination, and digital images were captured with a Leica DF 450C camera

4.4.3 Morphometry

Morphometric analysis, carried out by the same examiner blinded to animals' treatment, was performed on DRG neuronal cell profiles in digital images captured with a 20x objective magnification from 10 to 12 animals out of the acutely and chronically treated groups, respectively. The tissue sections were separated by at least 108 μm and only cells that obviously showed the nuclear profile were considered. Neuronal mean diameters were automatically measured by ImageProPlus software. Statistical parameters (mean, minimum, maximum, S.D.) and histograms of the neuron sizes, processed as a pool, were obtained by Statistica 6 software. The percentage of DRG immunostained perikarya, processed as a pool, was calculated as the ratio of the total number of labeled cells found in four to eight sections to the total number of cells found in the same sections after a modified Mayer's hematoxylin [certified hematoxylin (1.0 g/l), sodium iodate (0.2 g/l),

aluminum ammonium sulfate·12 H2O (50 g/l), chloral hydrate (50 g/l) and citric acid (1 g/l) counterstaining.

4.4.4 Image densitometry

For the quantitative evaluation of SP, CGRP and TRPV1 immunohistochemical labeling in the dorsal horn of the spinal cord, 6 representative 10x magnification microscopic fields for each marker (three bortezomib-treated animals and three controls) were blindly analyzed with ImageJ (http://rsb.info.nih.gov/ij/). Mean gray values from negative controls were subtracted from the gray values of the immunostained sections to exclude background staining. Histograms were obtained by calculating the ratio of bortezomib-treated values to control values.

4.5 Protein and RNA extraction

A total of 32 DRGs and spinal cord segments were analyzed: 12 from the acutely treated group (6 bortezomib-treated, 6 controls) and 20 from the chronically treated group (10 bortezomib-treated, 10 controls). Total protein and RNA from DRGs and spinal cord tissue were isolated by the TRIzol® method (Invitrogen, Carlsbad, CA) (1 ml/100 mg of tissue), the samples were homogenated with TRIzol® using.polytron and followed by addition of chloroform (200 µl/ml of TRIzol®), the tubes were inverted vigorously by handin then incubeted for 5 min at room temperature (RT). After centrifugation at 12000*g for 15 min at 4°C protein and RNA were separated into a lower organic phase and an upper aqueous phase, respectively.

4.5.1 Protein extraction

The organic phase was incubated in absolute ethanol (EtOH) (300 µl/ml of TRIzol® used for the initial homogenization) for 2-3 min at RT followed by centrifugation at no more than 2000 * g for 5 min at 4°C. The supernatant was then combined with isopropyl alcohol (1.5 ml/ml of TRIzol® used for the initial homogenization), incubated for 10 min at RT, and then centrifuged at 12000 * g for 10 min at 4°C. The supernatant was withdrawn

and the protein pellet was washed 3 times in a solution containing 0.3 M guanidine hydrocloride (IBI scientific, Kapp Court, Peosta, IA, USA) in 95 % EtOH (2 ml/ml of TRIzol® used for the initial homogenization) then after 20 min incubation centrifuged at 7500 * g for for 5 min at 4°C, this procedure was repeated for ech wash cycle.
After the final wash the protein pellet was vortexed in asbolute EtOH (2ml) and stored for 20 min at RT, finally was centrifuged at 7500 * g a for 5 min at 4°C. Samples were then resuspended in distilled water containing 2% sodium dodecilsulfate (SDS) (300 µl/100 mg of initial tissue). Protein concentrations were determined using the Lowry protein assay with bovine serum albumin as the standard.

4.5.2 RNA extraction

The aqueous phase was transferred into a fresh tube, the organic phase was saved for protein extraction. In the fresh tube was added isopropyl alcohol (0,5 ml/ml of TRIzol® used for the initial homogenization) and incubated for 10 min at RT, then centrifuged at no more than 12000*g at 4°C for 10 min to allow RNA precipitation. The RNA precipitate form a gel like pellet on the side and bottom of the vial.
The supernatant was removed and RNA-pellet was washed once with 75% of Ethanol in RNase-free (RF) diethyl pyrocarbonate (DEPC) water (1ml/ml of TRIzol®used for the initial homogenization), the mix was vortexed and centrifuged at no more then 7500*g for 5 min. at 4°C.
At the end of the procedure the RNA-pellet was briefly dryed (air dry) for 5-10 min then was risuspended in DEPC RF water.
The quantity and purity of the RNA was assessed using both nano-volume spectrophotometer (Nanophotometer P-360 Implen GmbH, München, Germany) and electrophoresis technique in 2% agarose gel in TAE.

TAE preparation
For 1 liter of 50x TAE buffer use:
242 g Tris base (2-amino-2-hydroxymethyl-propane-1,3-diol) (= 2 moles)
57.1 mL glacial acetic acid (= 100% acetic acid) (57.19 mL = 1 mole)
100 mL 0.5 M Na2 EDTA (pH 8.0)
Pour H_2O to reach a total volume of 1 L.
To prepare 0.5 M Na_2EDTA (pH 8.0) add 186.1 g of disodium ethylene diamino tetraacetate in ddH_2O up to 800 ml of H_2O. Adjust the pH to 8.0 with NaOH (20 g approx. NaOH). Solution must be sterilized by autoclaving.

4.6 Western blot

Total proteins (40 μg) were separated by SDS-polyacrilamide gel electrophoresis (SDS-PAGE) using a 10% (w/v) polyacrilamide resolving gel. Internal molecular weight (mw) standards (Kaleidoscope Prestained Standards, Bio-Rad, Hercules, CA, USA) were run in parallel. Two gels were run simultaneously for Coomassie staining and immunoblotting. Proteins for immunoblotting were electrophoretically transferred to a polyvinylidene fluoride membrane (Bio-Rad, Hercules, CA, USA) using the Mini Trans Blot Cell (Bio-Rad, Hercules, CA, USA). Blots were blocked by immersion in 20mM Tris base and 137mM sodium chloride (TBS) containing 5% milk powder and 0.1% Tween 20 (TBS-T), for 60 min at room temperature and incubated overnight at 4 °C with a rabbit polyclonal primary antibody against TRPV1 (cfr Table 5) (Abcam, Cambridge, UK), diluted 1:1000 in TBS containing 5% milk powder and 0.2% NaN_3 (Sigma, Milan, Italy). After a TBS-T rinse, blots were incubated for 60 min, at room temperature, with peroxidase-conjugated goat anti-rabbit serum (Sigma Aldrich, St Luis, MO, USA), diluted 1:10000 in TBS/T. Loading controls were obtained by stripping and immunostaining the membranes as above, using a monoclonal mouse antibody against glyceraldehyde-3-phosphate dehydrogenase (GAPDH) (Chemicon, Temecula, CA, USA), diluted 1:1000, as the primary antiserum, and a peroxidase-conjugated goat anti-mouse serum (Chemicon, Temecula, CA, USA), diluted 1:5000, as the secondary antiserum. To control for non specific staining, the blots were stripped and incubated with the relevant secondary antiserum. After a TBS-T rinse, protein bands were visualized on an autoradiograph (Kodak X-Omat LS, Kodak, Rochester, NY) using the ECL™ Prime reagents (GE Healthcare, Buckinghamshire, UK). The approximate mw of immunolabelled protein bands was determined by means of Molecular Analyst© Software (Version 1.4, Bio-Rad Hercules, CA, USA) by comparing the position of relevant bands on the autoradiograph film with that of nearby prestained mw standards. Relative optical density (O.D.) was quantified by means of the GS800™ Calibrated Densitometer and the Quantity One 1 (Bio-Rad, Hercules, CA, USA) software.

4.7 RT-PCR

For each sample: the total RNA was treated with RNase-free DNase I (RQ1, Promega Corporation, Madison, WI, USA) for 20 min at 37°C. cDNA was then synthesized following a two-step RT-PCR proctol from Enhanced Avian HS RT-PCR Kit (Sigma-Aldrich® , St. Luis, MO, USA)

1) optional step (this step may denature RNA secondary structure, which will allow for more efficent reverse transcription): in a fresh RNase-free tube the following reagents were added

Volume	**Reagent**	**Final concetration**
1 µl	Deoxynucleotide mix	500 µM each dNTP
1 µl	Anchored oligo $(dT)_{23}$	3.5 µM
100 ng	RNA template	0.005-0.250µg/µl total RNA
q.s	Water, PCR reagent	- - - - - - - - - - -- - -
10 µl final volume		

- The reaction mix was mixed gently and briegly centrifuged to collect all components at the bottom of the tube than incubated in thermocycler for 10 min at 70°C. The tube was removed and placed on ice.

  2) Reverse transcription: the tube was centrifuged and added the following components:

Volume	**Reagent**	**Final concetration**
6 µl	Water, PCR reagent	
2 µl	10X buffer for AMV-RT	1X
1 µl	RNase inhibitor	1 U/ µl
1 µl	Enchenced Avian RT	1 U/ µl

20 µl final volume

The tube was incubated in thermocycler for 50 min at a temperature between 42-50°C. The first strand of cDNA is now ready for subsequent PCR amplification.

4.7.1 PCR amplification

Hot start PCR was performed using 2X Taq DNA Polymerase Master Mix (VWR International, Geldenaaksebaan, Belgium), containing

- 150 mM Tris-HCl pH 8.5, 40 mM(NH4)2SO4, 3 mM $MgCl_2$, 0.2% Tween 20®
- 0.4 mM dNTP
- 0.05 U/µl Ampliqon Taq DNA-polymerase Stabilizer

For PCR amplification, specific primers for TRPV1, CGRP and Beta-actin mRNAs were designed using the http://www.premierbiosoft.com/netprimer/ open source software. Each cDNA was amplified twice. Amplification of the β-actin housekeeping gene and mw DNA Ladder (VWR international, Geldenaaksebaan, Belgium) were run in parallel.

Primer sequences for RT-PCR

mRNA	**Primer sequences**	**Amplification product**
TRPV1	Forward: 5'-gcactcctccctttatgac-3' Reverse: 5'-gccgatggtgaacttgaac-3'	686 bp fragment (NCBI Ref. sequence: NM_031982.1)
CGRP	Forward: 5'-ctctcagcagcatgtgggt-3' Reverse: 5'-taactcatttatacttggtttca-3'	554 bp fragment (NCBI Ref. sequence: NM_138513.1)
β-actin	Forward: 5'-ccagagcaagagaggcatc-3' Reverse: 5'-gtccctgtat gcctctggt-3'	265 bp fragment (NCBI Ref. Sequence: NM_031144.2)

After setting the parameters and the optimum conditions for the different primers,in clean vials were prepared mix PCR reaction with the following reagents:

Volume	Reagent	Final concetration
10 µl	2X Taq Master Mix	1X
1 µl	Forward Primer	0.25 µM
1 µl	Reverse Primer	0.25 µM
7 µl	Distilled Water	----------
1 µl	cDNA template	100 ng
20 µl Final Volume		

The PCR was performed according to the following procedure: 95°C for 3 min, 30-40 cycles 95°C for 30 sec, 54/56°C for 1 min, 72°C for 30 sec, final elongation at 72°C for 10 min. PCR products were then separated by electrophoresis in a 1.5% agarose gel in TAE buffer containing GelRed (Biotium, Hayward, CA, USA). cDNA bands were visualized by means of an ultraviolet transilluminator (UVP PhotoDoc-It^{TM} Imaging System) and digital images of the gel were acquired with a Canon PowerShot A480 camera. The approximate mw of amplification products and relative O.D. was determined on digital images using ImageJ Software (http://rsb.info.nih.gov/ij/) by comparing the position of relevant bands to that of nearby mw standards.

4.8 Statistical analysis

The differences in body weight and behavioral data were statistically evaluated using the unpaired Student's t test (significance level set at $p < 0.05$). Paired Student's t-test was used for comparing differences between percent frequencies of DRG labelled neurons, relative frequencies of neuronal size groups and grey levels. One-way ANOVA and the Fisher's test for post hoc analyses were applied to evaluate statistical differences among groups in the western blot and RT-PCR analysis.

TRPV1	Synthetic peptide, RASLDSEESESPPQENSC corresponding to aa 4-21 of rat	1:6000(ABC), 1:1000 (IF),	Neuromics Rabbit Polyclonal
TRPV1	Synthetic peptide, CGSLKPEDAEVFKDSMVPGEK corresponding to C-terminal residues 816-838 of rat VR1	1:600 (ABC), 1:100 (IF), 1:1000 (WB	AbCam Rabbit Polyclonal
TRPV1	Epitope mapping near N-terminus of VR1 of rat origin in human	1:800 (ABC), 1:100 (IF)	SantaCruz Biotechnology Goat Polyclonal

CGRP	Synthetic CGRP from rat	1:1200 (ABC), 1:600 (IF)	Chemicon Int. Rabbit Polyclonal
CGRP	Synthetic rat alpha-CGRP conjugated to bovine serum albumin using glutaraldehyde	1:5000 (ABC), 1:2000 (IF)	Enzo Life Sciences Rabbit Polyclonal
CGRP	Rat alpha-CGRP peptide	1:500 (ABC), 1:100 (IF)	SantaCruz Biotechnology Goat Polyclonal

SP	Synthetic peptide: CRPKPQQFFGLM, corresponding to amino acids 1-11 of Rat Substance P	AbCam Guinea pig Polyclonal	1:1500 (ABC), 1:500 (IF)

GAPDH	GAPDH from rabbit muscle	Millipore Chemicon

Table 5. List of antibodies used for immuhistochemistry and western blot

5. REFERENCES

1. Adams J. The development of proteasome inhibitors as anticancer drugs. Cancer Cell. 2004; 5(5):417-421.
2. Adams J. The proteasome: a suitable antineoplastic target. Nat Rev Cancer.2004 May;4(5):349-360.
3. Adams J. The proteasome: structure, function, and role in the cell. Cancer Treat Rev. 2003; 29 Suppl 1:3-9.
4. Afrah AW, Fiskå A, Gjerstad J, Gustafsson H, Tjølsen A, Olgart L, Stiller CO, Hole K, Brodin E. Spinal substance P release in vivo during the induction of long-term potentiation in dorsal horn neurons. Pain. 2002; 96(1-2):49-55.
5. Albers JW, Chaudhry V, Cavaletti G, Donehower RC. Interventions for preventing neuropathy caused by cisplatin and related compounds. Cochrane Database Syst Rev; (2):CD005228.
6. Alessandri-Haber N, Dina OA, Joseph EK, Reichling DB, Levine JD. Interaction of transient receptor potential vanilloid 4, integrin, and SRC tyrosine kinase in mechanical hyperalgesia. J Neurosci. 2008; 28(5):1046-1057.
7. Alvarez FJ, Morris HR, Priestley JV. Sub-populations of smaller diameter trigeminal primary afferent neurons defined by expression of calcitonin gene-related peptide and the cell surface oligosaccharide recognized by monoclonal antibody LA4. J Neurocytol. 1991; 20(9):716-731.
8. Alvarez FJ, Priestley JV. Anatomy of somatostatin-immunoreactive fibres and cell bodies in the rat trigeminal subnucleus caudalis. Neuroscience. 1990; 38(2):343-357.
9. Alvarez FJ, Villalba RM, Carr PA, Grandes P, Somohano PM. Differential distribution of metabotropic glutamate receptors 1a, 1b, and 5 in the rat spinal cord. J Comp Neurol. 2000; 422(3):464-487.
10. An B, Goldfarb RH, Siman R, Dou QP. Novel dipeptidyl proteasome inhibitors overcome Bcl-2 protective function and selectively accumulate the cyclin-dependent kinase inhibitor p27 and induce apoptosis in transformed, but not normal, human fibroblasts. Cell Death Differ. 1998; 5(12):1062-1075.

11. Apkarian AV, Bushnell MC, Treede RD, Zubieta JK. Human brain mechanisms of pain perception and regulation in health and disease. Eur J Pain. 2005; 9(4):463-484.
12. Archer AG, Watkins PJ, Thomas PK, Sharma AK, Payan J. The natural history of acute painful neuropathy in diabetes mellitus. J Neurol Neurosurg Psychiatry. 1983; 46(6):491-499.
13. Armstrong T, Almadrones L, Gilbert MR. Chemotherapy-induced peripheral neuropathy. Oncol Nurs Forum. 2005; 32(2):305-311.
14. Attal N, Bouhassira D, Gautron M, Vaillant JN, Mitry E, Lepère C, Rougier P, Guirimand F. Thermal hyperalgesia as a marker of oxaliplatin neurotoxicity: a prospective quantified sensory assessment study. Pain. 2009; 144(3):245-252.
15. Attal N, Bouhassira D, Gautron M, Vaillant JN, Mitry E, Lepère C, Rougier P,Guirimand F. Thermal hyperalgesia as a marker of oxaliplatin neurotoxicity: a prospective quantified sensory assessment study. Pain. 2009 ;144(3):245-252.
16. Authier N, Balayssac D, Marchand F, Ling B, Zangarelli A, Descoeur J, Coudore F, Bourinet E, Eschalier A. Animal models of chemotherapy-evoked painful peripheral neuropathies. Neurotherapeutics. 2009; 6(4):620-629.
17. Authier N, Fialip J, Eschalier A, Coudoré F. Assessment of allodynia and hyperalgesia after cisplatin administration to rats. Neurosci Lett. 2000; 291(2):73-6.
18. Authier N, Gillet JP, Fialip J, Eschalier A, Coudore F. An animal model of nociceptive peripheral neuropathy following repeated cisplatin injections. Exp Neurol. 2003; 182(1):12-20.
19. Averill S, McMahon SB, Clary DO, Reichardt LF, Priestley JV. Immunocytochemical localization of trkA receptors in chemically identified subgroups of adult rat sensory neurons. Eur J Neurosci. 1995; 7(7):1484-1494.
20. Awada A, Albanell J, Canney PA, Dirix LY, Gil T, Cardoso F, Gascon P, Piccart MJ, Baselga J. Bortezomib/docetaxel combination therapy in patients with anthracycline-pretreated advanced/metastatic breast cancer: a phase I/II doseescalation study. Br. J. Cancer. 2008; 98, 1500–1507.
21. Axelrod FB, Hilz MJ. Inherited autonomic neuropathies. Semin Neurol. 2003; 23(4):381-390.
22. Azhary H, Farooq MU, Bhanushali M, Majid A, Kassab MY. Peripheral

neuropathy: differential diagnosis and management. Am Fam Physician. 2010; 81(7):887-892.

23. Backonja MM. Defining neuropathic pain. Anesth Analg. 2003; 97(3):785-90. Review. Erratum in: Anesth Analg. 2004; 98(1):67.
24. Bakitas MA. Background noise: the experience of chemotherapy-induced peripheral neuropathy. Nurs Res. 2007; 56(5):323-331.
25. Bandell M, Story GM, Hwang SW, Viswanath V, Eid SR, Petrus MJ, Earley TJ, Patapoutian A. Noxious cold ion channel TRPA1 is activated by pungent compounds and bradykinin. Neuron 2004; 41:849–857.
26. Barajon I, Bersani M, Quartu M, Del Fiacco M, Cavaletti G, Holst JJ, Tredici G. Neuropeptides and morphological changes in cisplatin-induced dorsal root ganglion neuronopathy. Exp Neurol. 1996; 138(1):93-104.
27. Barr ML & Kiernan JA. The human nervous system (4th ed). 1983 Philadelphia: Harper and Row.
28. Basbaum AI, Bautista DM, Scherrer G, Julius D. Cellular and molecular mechanisms of pain. Cell. 2009; 139(2):267-284.
29. Bautista DM, Jordt SE, Nikai T, Tsuruda PR, Read AJ, Poblete J, Yamoah EN,Basbaum AI, Julius D. TRPA1 mediates the inflammatory actions of environmental irritants and proalgesic agents. Cell. 2006; 124(6):1269-1282.
30. Bautista DM, Siemens J, Glazer JM, Tsuruda PR, Basbaum AI, Stucky CL, Jordt SE, Julius D. The menthol receptor TRPM8 is the principal detector of environmental cold. Nature. 2007; 448(7150):204-208.
31. Beal JA, Cooper MH. The neurons in the gelatinosal complex (Laminae II and III) of the monkey (Macaca mulatta): a Golgi study. J Comp Neurol. 1978; 179(1):89-121.
32. Bennett DL, Dmietrieva N, Priestley JV, Clary D, McMahon SB. trkA, CGRP and IB4 expression in retrogradely labelled cutaneous and visceral primary sensory neurones in the rat. Neurosci Lett. 1996; 206:33–36.
33. Bennett GJ. Does a neuroimmune interaction contribute to the genesis of painful peripheral neuropathies? Proc Natl Acad Sci U S A. 1999; 96(14):7737-7738.
34. Bennett GJ. Pathophysiology and animal models of cancer-related painful peripheral neuropathy. Oncologist. 2010; 15 Suppl 2:9-12.

35. Besson JM, Chaouch A. Peripheral and spinal mechanisms of nociception. Physiol Rev. 1987; 67(1):67-186.
36. Bhave G, Zhu W, Wang H, Brasier DJ, Oxford GS, Gereau RW 4th. cAMP-dependent protein kinase regulates desensitization of the capsaicin receptor (VR1) by direct phosphorylation. Neuron. 2002; 35(4):721-731.
37. Binder A, Stengel M, Maag R, Wasner G, Schoch R, Moosig F, Schommer B, Baron R. Pain in oxaliplatin-induced neuropathy--sensitisation in the peripheral and central nociceptive system. Eur J Cancer. 2007; 43(18):2658-2663.
38. Bold RJ, Virudachalam S, McConkey DJ. Chemosensitization of pancreatic cancer by inhibition of the 26S proteasome. J Surg Res. 2001; 100(1):11-7.
39. Boyette-Davis JA, Cata JP, Driver LC, Novy DM, Bruel BM, Mooring DL, Wendelschafer-Crabb G, Kennedy WR, Dougherty PM. Persistent chemoneuropathy in patients receiving the plant alkaloids paclitaxel and vincristine. Cancer Chemother Pharmacol. 2013; 71(3):619-626.
40. Bridges D, Thompson SW, Rice AS. Mechanisms of neuropathic pain. Br J Anaesth. 2001; 87(1):12-26.
41. Brix Finnerup N, Hein Sindrup S, Staehelin Jensen T. Management of painful neuropathies. Handb Clin Neurol. 2013; 115:279-290.
42. Campbell IN, Raja SN, Cohen RH, Manning DC, Khan AA and Mayer RA Peripheral neural mechanisms of nociception. In: Textbook of Pain, 2nd Ed. Eds. Wall, P.D. and Melzack, R, Churchill Livingstone, Edinburgh. 1989. 22-45.
43. Campbell JN, Meyer RA. Mechanisms of neuropathic pain. Neuron. 2006; 52(1):77-92.
44. Caponigro F, Lacombe D, Twelves C, Bauer J, Govaerts AS, Marréaud S, Milano A, Anthoney A. An EORTC phase I study of Bortezomib in combination with oxaliplatin, leucovorin and 5-fluorouracil in patients with advanced colorectal cancer. Eur J Cancer. 2009; 45(1):48-55.
45. Casafont I, Berciano MT, Lafarga M. Bortezomib induces the formation of nuclear poly(A) RNA granules enriched in Sam68 and PABPN1 in sensory ganglia neurons. Neurotox Res. 2010; 17(2):167-178.
46. Casey KL, Morrow TJ. Ventral posterior thalamic neurons differentially responsive to noxious stimulation of the awake monkey. Science 1983; 221: 675-677.

47. Cata JP, Weng HR, Burton AW, Villareal H, Giralt S, Dougherty PM. Quantitative sensory findings in patients with bortezomib-induced pain. J Pain. 2007; 8(4):296-306.
48. Cata JP, Weng HR, Burton AW, Villareal H, Giralt S, Dougherty PM. Quantitative sensory findings in patients with bortezomib-induced pain. J Pain. 2007; 8(4):296-306.
49. Caterina MJ, Leffler A, Malmberg AB, Martin WJ, Trafton J, Petersen-Zeitz KR, Koltzenburg M, Basbaum AI, Julius D. Impaired nociception and pain sensation in mice lacking the capsaicin receptor. Science. 2000; 288(5464):306-313.
50. Caterina MJ, Schumacher MA, Tominaga M, Rosen TA, Levine JD, Julius D. The capsaicin receptor: a heat-activated ion channel in the pain pathway.Nature.1997; 389:816–824.
51. Cavaletti G, Marmiroli P. Chemotherapy-induced peripheral neurotoxicity. Nat Rev Neurol. 2010; 6(12):657-666.
52. Cavaletti G, Tredici G, Marmiroli P, Petruccioli MG, Barajon I, Fabbrica D. Morphometric study of the sensory neuron and peripheral nerve changes induced by chronic cisplatin (DDP) administration in rats. Acta Neuropathol. 1992;84(4):364-371.
53. Chaudhry V, Cornblath DR, Polydefkis M, Ferguson A, Borrello I. Characteristics of bortezomib- and thalidomide-induced peripheral neuropathy. J Peripher Nerv Syst. 2008; 13(4):275-282.
54. Chen H, Lamer TJ, Rho RH, Marshall KA, Sitzman BT, Ghazi SM, Brewer RP. Contemporary management of neuropathic pain for the primary care physician. Mayo Clin Proc. 2004; 79(12):1533-1545.
55. Chen Y, Willcockson HH, Valtschanoff JG. Influence of the vanilloid receptor TRPV1 on the activation of spinal cord glia in mouse models of pain. Exp Neurol. 2009; 220(2):383-390.
56. Ciechanover A. The ubiquitin-proteasome pathway: on protein death and cell life. EMBO J. 1998; 17(24):7151-7160.
57. Cohen SP, Mao J. Neuropathic pain: mechanisms and their clinical implications. BMJ. 2014; 348:f7656.
58. Colburn RW, Lubin ML, Stone DJ Jr, Wang Y, Lawrence D, D'Andrea MR,

Brandt MR, Liu Y, Flores CM, Qin N. Attenuated cold sensitivity in TRPM8 null mice. Neuron 2007; 54:379–386.

59. Collins WR Jr, Nulsen FE, Randt CT. Relation of peripheral nerve fiber size and sensation in man. Arch Neurol. 1960; 3:381-385.
60. Conner JM, Lauterborn JC, Yan Q, Gall CM, Varon S. Distribution of brain-derived neurotrophic factor (BDNF) protein and mRNA in the normal adult rat CNS: evidence for anterograde axonal transport. J Neurosci. 1997; 17(7):2295-2313.
61. Cook AJ, Woolf CJ, Wall PD, McMahon SB. Dynamic receptive field plasticity in rat spinal cord dorsal horn following C-primary afferent input. Nature. 1987; 325(7000):151-153.
62. Coudoré-Civiale MA, Ling B, Balayssac D. Spinal Substance P and CGRP staining in vincristine, cisplatin, streptozocin or constriction injury-induced neuropathies M.A Coudoré-Civiale et al, /J. Pharm. Sci. & Res. Vol.2 (9), 2010, 590-598.
63. Craig AD. Distribution of trigeminothalamic and spinothalamic lamina I terminations in the macaque monkey. J Comp Neurol 2004a; 477:119 –148.
64. Craig AD. Lamina I, but not lamina V, spinothalamic neurons exhibit responses that correspond with burning pain. J Neurophysiol. 2004b; 92:2604-2609.
65. Craig AD. Pain mechanisms: labeled lines versus convergence in central processing. Annu Rev Neurosci. 2003; 26:1-30.
66. Csillik B, Janka Z, Boncz I, Kálmán J, Mihály A, Vécsei L, Knyihár E. Molecular plasticity of primary nociceptive neurons: relations of the NGF-c-jun system to neurotomy and chronic pain. Ann Anat. 2003, 185(4):303-314.
67. Cusack JC Jr, Liu R, Houston M, Abendroth K, Elliott PJ, Adams J, Baldwin AS Jr. Enhanced chemosensitivity to CPT-11 with proteasome inhibitor PS-341: implications for systemic nuclear factor-kappaB inhibition. Cancer Res. 2001; 61(9):3535-3540.
68. Davis JB, Gray J, Gunthorpe MJ, Hatcher JP, Davey PT, Overend P, Harries MH, Latcham J, Clapham C, Atkinson K, et al. et al.,Vanilloid receptor-1 is essential for inflammatory thermal hyperalgesia. Nature 2000; 405:183–187.
69. Decosterd I, Woolf CJ. Spared nerve injury: an animal model of persistent peripheral neuropathic pain. Pain. 2000; 87(2):149-158.

70. Delcros JG, Floc'h MB, Prigent C, Arlot-Bonnemains Y. Proteasome inhibitors as therapeutic agents: current and future strategies. Curr Med Chem. 2003; 10(6):479-503.
71. Devor M. The pathophysiology of damaged peripheral nerves. In:Wall PD,Melzack R (eds) Textbook of pain, 3rd edn. 1994. Churchill Livingstone, Edinburgh, pp 79–100.
72. Dhaka A, Murray AN, Mathur J, Earley TJ, Petrus MJ, Patapoutian A. TRPM8 is required for cold sensation in mice. Neuron. 2007; 54(3):371-378.
73. Dick LR, Fleming PE. Building on bortezomib: second-generation proteasome inhibitors as anti-cancer therapy. Drug Discov Today. 2010; 15(5-6):243-249.
74. Doly S, Fischer J, Salio C, Conrath M. The vanilloid receptor-1 is expressed in rat spinal dorsal horn astrocytes. Neurosci Lett. 2004; 357(2):123-126.
75. Dougherty PM, Cata JP, Cordella JV, Burton A, Weng HR. Taxol-induced sensory disturbance is characterized by preferential impairment of myelinated fiber function in cancer patients. Pain. 2004; 109(1-2):132-142.
76. Dubin AE, Patapoutian A. Nociceptors: the sensors of the pain pathway. J Clin Invest. 2010 Nov;120(11):3760-3772.
77. Dubner R, Gold M. The neurobiology of pain. Proc Natl Acad Sci U S A. 1999 Jul 6;96(14):7627-7630.
78. England JD, Asbury AK. Peripheral neuropathy. Lancet. 2004; 363(9427):2151-2161.
79. England JD, Gronseth GS, Franklin G, Miller RG, Asbury AK, Carter GT, Cohen JA, Fisher MA, Howard JF, Kinsella LJ, Latov N, Lewis RA, Low PA, Sumner AJ; American Academy of Neurology; American Association of Electrodiagnostic Medicine; American Academy of Physical Medicine and Rehabilitation. Distal symmetric polyneuropathy: a definition for clinical research: report of the American Academy of Neurology, the American Association of Electrodiagnostic Medicine, and the American Academy of Physical Medicine and Rehabilitation. Neurology. 2005; 64(2):199-207.
80. Erdös eg, skidgel ra. Neutral endopeptidase 24.11 (enkephalinase) and related Regulators of peptide hormones. Faseb j. 1989; 3(2):145-151.
81. Federici T, Boulis NM. Invited review: festschrift edition of neurosurgery

peripheral nervous system as a conduit for delivering therapies for diabetic neuropathy, amyotrophic lateral sclerosis, and nerve regeneration. Neurosurgery. 2009; 65 (4 Suppl).

82. Fernández-Carvajal A, Fernández-Ballester G, Devesa I, González-Ros JM, Ferrer-Montiel A. New strategies to develop novel pain therapies: addressing thermoreceptors from different points of view. Pharmaceuticals (Basel). 2011; 5(1):16-48.
83. Ferrell BA. Pain management. Clin Geriatr Med. 2000; 16(4):853-74.
84. Fischer SJ, McDonald ES, Gross L, Windebank AJ. Alterations in cell cycle regulation underlie cisplatin induced apoptosis of dorsal root ganglion neurons in vivo. Neurobiol Dis. 2001; 8(6):1027-1035.
85. Frankel A, Man S, Elliott P, Adams J, Kerbel RS. Lack of multicellular drug resistance observed in human ovarian and prostate carcinoma treated with the proteasome inhibitor PS-341. Clin Cancer Res. 2000; 6(9):3719-3728.
86. Fribley A, Zeng Q, Wang CY. Proteasome inhibitor PS-341 induces apoptosis through induction of endoplasmic reticulum stress-reactive oxygen species in head and neck squamous cell carcinoma cells. Mol Cell Biol. 2004; 24(22):9695-9704.
87. Fürst S. Transmitters involved in antinociception in the spinal cord. Brain Res Bull. 1999; 48(2):129-141.
88. Garcia JM, Cata JP, Dougherty PM, Smith RG. Ghrelin prevents cisplatin-induced mechanical hyperalgesia and cachexia. Endocrinology. 2008; 149(2):455-460.
89. Garcia-Larrea L. Insights gained into pain processing from patients with focal brain lesions. Neurosci Lett. 2012; 520(2):188-191.
90. Gatchel RJ, Peng YB, Peters ML, Fuchs PN, Turk DC. The biopsychosocial approach to chronic pain: scientific advances and future directions. Psychol Bull. 2007; 133(4):581-624.
91. Gaudio E, Il Sistema Nervoso Centrale, Piccin (nuova libreria S.p.a).2012, Padova.
92. Gauriau C, Bernard JF. Pain pathways and parabrachial circuits in the rat. Exp Physiol 2002; 87:251–258.
93. Gerke MB, Plenderleith MB. Binding sites for the plant lectin Bandeiraea simplicifolia I-isolectin B(4) are expressed by nociceptive primary sensory neurones. Brain Res. 2001; 911(1):101-104.

94. Gilchrist HD, Allard BL, Simone DA. Enhanced withdrawal responses to heat and mechanical stimuli following intraplantar injection of capsaicin in rats. Pain.1996; 67(1):179-188.
95. Giordano J. The neurobiology of nociceptive and anti-nociceptive systems. Pain Physician. 2005; 8(3):277-290.
96. Graham BA, Brichta AM, Callister RJ. Moving from an averaged to specific view of spinal cord pain processing circuits. J Neurophysiol. 2007; 98(3):1057-1063.
97. Grant G. Primary afferent projections to the spinal cord. In: "The Rat Nervous system", G. Paxinos ed. 2 vol, pp 303-309, Academic Press.1986, Orlando Florida.
98. Guo A, Vulchanova L, Wang J, Li X, Elde R. Immunocytochemical localization of the vanilloid receptor 1 (VR1): relationship to neuropeptides, the P2X3 purinoceptor and IB4 binding sites. Eur J Neurosci. 1999; 11(3):946-958.
99. Hacker H, Karin M. Regulation and function of IKK and IKK-related kinases. Sci STKE 2006; 2006:re13.
100. Hanani M. Satellite glial cells in sensory ganglia: from form to function. Brain Res Brain Res Rev. 2005; 48(3):457-476.
101. Harper AA, Lawson SN. Conduction velocity is related to morphological cell type in rat dorsal root ganglion neurones. J Physiol. 1985; 359:31-46.
102. Hausheer FH, Schilsky RL, Bain S, Berghorn EJ, Lieberman F. Diagnosis, management, and evaluation of chemotherapy-induced peripheral neuropathy. Semin Oncol. 2006; 33(1):15-49.
103. Hay JW. Quality of life effects of chemotherapy-induced neuropathy in ovarian cancer [abstr 886]. Proc Am Soc Clin Oncol 2002; 21:222a.
104. Head KA. Peripheral neuropathy: pathogenic mechanisms and alternative therapies. Altern Med Rev. 2006; 11(4):294-329.
105. Henry JL. Effects of substance P on functionally identified units in cat spinal cord. Brain Res. 1976; 114(3):439-451.
106. Hideshima T, Chauhan D, Podar K, Schlossman RL, Richardson P, Anderson KC. Novel therapies targeting the myeloma cell and its bone marrow microenvironment. Semin Oncol. 2001; 28(6):607-612.
107. Hideshima T, Chauhan D, Richardson P, Mitsiades C, Mitsiades N, Hayashi T, Munshi N, Dang L, Castro A, Palombella V, Adams J, Anderson KC. NF-kappa B

as a therapeutic target in multiple myeloma. J Biol Chem. 2002; 277(19):16639-16647.

108. Hideshima T, Ikeda H, Chauhan D, Okawa Y, Raje N, Podar K, Mitsiades C, Munshi NC, Richardson PG, Carrasco RD, Anderson KC. Bortezomib induces canonical nuclear factor-kappaB activation in multiple myeloma cells. Blood. 2009; 114(5):1046-1052.

109. Holland JF, Scharlau C, Gailani S, Krant MJ, Olson KB, Horton J, Shnider BI, Lynch JJ, Owens A, Carbone PP, Colsky J, Grob D, Miller SP, Hall TC. Vincristine treatment of advanced cancer: a cooperative study of 392 cases. Cancer Res. 1973; 33(6):1258-1264.

110. Hori K, Ozaki N, Suzuki S, Sugiura Y. Upregulations of P2X(3) and ASIC3 involve in hyperalgesia induced by cisplatin administration in rats. Pain. 2010; 149(2):393-405.

111. Hucho T, Levine JD. Signaling pathways in sensitization: toward a nociceptor cell biology. Neuron. 2007; 55(3):365-376.

112. Hudson LJ, Bevan S, Wotherspoon G, Gentry C, Fox A, Winter J. VR1 protein expression increases in undamaged DRG neurons after partial nerve injury. Eur J Neurosci. 2001 Jun;13(11):2105-2114.

113. Hughes RA. Peripheral neuropathy. BMJ. 2002; 324(7335):466-469.

114. Hunt SP, Mantyh PW and Preastley JV. The organization of biochemically characterized sensory neurons. In Sensory Neurones: Diversity, Development and Plasticity, ed. Scott, S. A., pp. 60–76. 1992. Oxford University Press, New York.

115. Hunt SP, Mantyh PW. The molecular dynamics of pain control. Nat Rev Neurosci. 2001; 2(2):83-91.

116. Jacobson S and Marcus EM. Neuroanatomy for the Neuroscientist. 2008 Springer Science, New York.

117. James SE, Burden H, Burgess R, Xie Y, Yang T, Massa SM, Longo FM, Lu Q. Anti-cancer drug induced neurotoxicity and identification of Rho pathway signaling modulators as potential neuroprotectants. Neurotoxicology. 2008; 29(4):605-612.

118. Jesenberger V, Jentsch S. Deadly encounter: ubiquitin meets apoptosis. Nat Rev Mol Cell Biol. 2002; 3(2):112-121.

119. JesseU, T.M. and Kelly, D.D. Pain and analgesia. In: Principles of Neural Science,

3rd Edition, Eds. Kandel, E.R., Schwartz, lH. and Jessell, T.M. 1997. 385-399.

120. Ji RR, Samad TA, Jin SX, Schmoll R, Woolf CJ. p38 MAPK activation by NGF in primary sensory neurons after inflammation increases TRPV1 levels and maintains heat hyperalgesia. Neuron. 2002; 36(1):57-68.

121. Jordan MA, Wilson L. Microtubules as a target for anticancer drugs. Nat Rev Cancer. 2004; 4(4):253-265.

122. Jordt SE, Bautista DM, Chuang HH, McKemy DD, Zygmunt PM, Högestätt ED, Meng ID, Julius D. Mustard oils and cannabinoids excite sensory nerve fibres through the TRP channel ANKTM1. Nature. 2004 ;427 (6971):260-265.

123. Julius D, Basbaum AI. Molecular mechanisms of nociception. Nature. 2001; 413(6852):203-210.

124. Julius D. TRP channels and pain. Annu Rev Cell Dev Biol. 2013; 29:355-84.

125. Kaley TJ, Deangelis LM. Therapy of chemotherapy-induced peripheral neuropathy.Br J Haematol. 2009; 145(1):3-14.

126. Kampa BM, Clements J, Jonas P, Stuart GJ. Kinetics of Mg2+ unblock of NMDA receptors: implications for spike-timing dependent synaptic plasticity. J Physiol. 2004; 556(Pt 2):337-345.

127. Kane RC, Dagher R, Farrell A, Ko CW, Sridhara R, Justice R, Pazdur R. Bortezomib for the treatment ofmantle cell lymphoma. Clin.Cancer Res. 2007; 13, 5291–5294.

128. Kannarkat G, Lasher EE, Schiff D. Neurologic complications of chemotherapy agents. Curr Opin Neurol. 2007; 20(6):719-725.

129. Karin M, Cao Y, Greten FR, Li ZW. NF-kappaB in cancer: from innocent bystander to major culprit. Nat Rev Cancer. 2002; 2(4):301-310.

130. Kim SR, Lee DY, Chung ES, Oh UT, Kim SU, Jin BK. Transient receptor potential vanilloid subtype 1 mediates cell death of mesencephalic dopaminergic neurons in vivo and in vitro. J Neurosci. 2005; 25(3):662-671.

131. Kim YH, Back SK, Davies AJ, Jeong H, Jo HJ, Chung G, Na HS, Bae YC, Kim SJ, Kim JS, Jung SJ, Oh SB. TRPV1 in GABAergic interneurons mediates neuropathic mechanical allodynia and disinhibition of the nociceptive circuitry in the spinal cord. Neuron. 2012; 74(4):640-647.

132. Krarup-Hansen A, Helweg-Larsen S, Schmalbruch H, Rørth M, Krarup C.

Neuronal involvement in cisplatin neuropathy: prospective clinical and neurophysiological studies. Brain. 2007; 130(Pt 4):1076-1088.

133. LaMotte RH, Lundberg LE, Torebjörk HE. Pain, hyperalgesia and activity in nociceptive C units in humans after intradermal injection of capsaicin. J Physiol. 1992; 448:749-764.

134. LaMotte RH, Shain CN, Simone DA, Tsai EF. Neurogenic hyperalgesia: psychophysical studies of underlying mechanisms. J Neurophysiol. 1991; 66(1):190-211.

135. Landowski TH, Megli CJ, Nullmeyer KD, Lynch RM, Dorr RT. Mitochondrial-mediated disregulation of Ca2+ is a critical determinant of Velcade (PS-41/bortezomib) cytotoxicity in myeloma cell lines. Cancer Res. 2005; 65(9):3828-3836.

136. Latremoliere A, Woolf CJ. Central sensitization: a generator of pain hypersensitivity by central neural plasticity. J Pain. 2009; 10(9):895-926.

137. Lawson SN, Crepps BA, Perl ER. Relationship of substance P to afferent characteristics of dorsal root ganglion neurones in guinea-pig. J Physiol. 1997; 505 (Pt 1):177-191.

138. Lawson SN, Waddell PJ, McCarthy PW. A comparison of the electrophysiological and immunocytochemical properties of rat dorsal root ganglion neurons with A and C-fibers. In: Schmidt RF, Schaible HG, Vahle-Hinz C (eds) Fine afferent nerve fibers and pain. 1987. VCH Publishers,Weinheim and New York, pp 193–203.

139. Lawson SN. Morphological and biochemical cell types of sensory neurons. In: Scott SA (ed) Sensory neurons: diversity, development and plasticity. 1992. Oxford University Press, New York, pp 27–59.

140. Lee AH, Iwakoshi NN, Anderson KC, Glimcher LH. Proteasome inhibitors disrupt the unfolded protein response in myeloma cells. Proc Natl Acad Sci U S A. 2003; 100(17):9946-9951.

141. Lee SE, Kim JH. Involvement of substance P and calcitonin gene-related peptide in development and maintenance of neuropathic pain from spinal nerve injury model of rat. Neurosci Res. 2007; 58(3):245-9.

142. Lieberman AR, Sensory ganglia, in: D.N. Landon (Ed.), The Peripheral Nerve, Chapman and Hall, London, 1976, pp. 188 – 278.

143. Lindblom, U. Assessment of abnormal evoked pain in neurological pain patients and its relation to spontaneous pain: a descriptive and conceptual model with some analytical results. In: Fields, H.L., Dubner, R., Cervero, F. Eds, Proceeding of the Fourth World congress on Pain. Advances in Pain Research and Therapy. 1985; New York, Raven Press. Vol. 9, pp. 409-423.
144. Ling YH, Liebes L, Jiang JD, Holland JF, Elliott PJ, Adams J, Muggia FM, Perez-Soler R. Mechanisms of proteasome inhibitor PS-341-induced G(2)-M-phase arrest and apoptosis in human non-small cell lung cancer cell lines. Clin Cancer Res. 2003; 9(3):1145-1154.
145. Ling YH, Liebes L, Zou Y, Perez-Soler R. Reactive oxygen species generation and mitochondrial dysfunction in the apoptotic response to Bortezomib, a novel proteasome inhibitor, in human H460 non-small cell lung cancer cells. J Biol Chem. 2003; 278(36):33714-33723.
146. Liu CW, Corboy MJ, DeMartino GN, Thomas PJ. Endoproteolytic activity of theproteasome. Science. 2003; 299(5605):408-411.
147. LoMonaco M, Milone M, Batocchi AP, Padua L, Restuccia D, Tonali P. Cisplatin neuropathy: clinical course and neurophysiological findings. J Neurol. 1992; 239(4):199-204.
148. Lovinger DM. Communication networks in the brain: neurons, receptors,neurotransmitters, and alcohol. Alcohol Res Health. 2008; 31(3):196-214.
149. Lukacs V, Thyagarajan B, Varnai P, Balla A, Balla T, Rohacs T. Dual regulation
150. Lukacs V, Thyagarajan B, Varnai P, Balla A, Balla T, Rohacs T. Dual regulation of TRPV1 by phosphoinositides. J Neurosci. 2007; 27(26):7070-7080.
151. Ma QP, Woolf CJ. Involvement of neurokinin receptors in the induction but not the maintenance of mechanical allodynia in rat flexor motoneurones. J Physiol. 1995 Aug 1; 486 (Pt 3):769-777.
152. Ma QP, Woolf CJ. Noxious stimuli induce an N-methyl-D-aspartate receptor-dependent hypersensitivity of the flexion withdrawal reflex to touch: implications for the treatment of mechanical allodynia. Pain. 1995; 61(3):383-390.
153. Maag R, Baron R. Neuropathic pain: translational research and impact for patient care. Curr Pain Headache Rep. 2006; 10(3):191-198.
154. MacLaren AP, Chapman RS, Wyllie AH, Watson CJ. p53-dependent apoptosis

induced by proteasome inhibition in mammary epithelial cells. Cell Death Differ. 2001; 8(3):210-218.

155. Macpherson LJ, Geierstanger BH, Viswanath V, Bandell M, Eid SR, Hwang S, Patapoutian A. The pungency of garlic: activation of TRPA1 and TRPV1 in response to allicin. Curr Biol. 2005; 15(10):929-934.

156. Mantyh PW, Rogers SD, Honore P, Allen BJ, Ghilardi JR, Li J, Daughters RS, Lappi DA, Wiley RG, Simone DA. Inhibition of hyperalgesia by ablation of lamina I spinal neurons expressing the substance P receptor. Science. 1997; 278(5336):275-279.

157. Mantyh PW. Cancer pain and its impact on diagnosis, survival and quality of life. Nat Rev Neurosci. 2006; 7(10):797-809.

158. Marchettini P, Lacerenza M, Mauri E, Marangoni C. Painful peripheral neuropathies. Curr Neuropharmacol. 2006; 4(3):175-181.

159. Martyn CN, Hughes RA. Epidemiology of peripheral neuropathy. J Neurol Neurosurg Psychiatry. 1997; 62(4):310-318.

160. McCarthy PW, Lawson SN. Cell type and conduction velocity of rat primary sensory neurons with calcitonin gene-related peptide-like immunoreactivity. Neuroscience. 1990; 34(3):623-632.

161. McGaraughty S, Chu KL, Brown BS, Zhu CZ, Zhong C, Joshi SK, Honore P, Faltynek CR, Jarvis MF. Contributions of central and peripheral TRPV1 receptors to mechanically evoked and spontaneous firing of spinal neurons in inflamed rats. J Neurophysiol. 2008; 100(6):3158-3166.

162. McKemy DD, Neuhausser WM, Julius D. Identification of a cold receptor reveals a general role for TRP channels in thermosensation. Nature 2002; 416:52–58.

163. McNamara CR, Mandel-Brehm J, Bautista DM, Siemens J, Deranian KL, Zhao M, Hayward NJ, Chong JA, Julius D, Moran MM, Fanger CM. TRPA1 mediates formalin-induced pain. Proc Natl Acad Sci U S A 2007; 104:13525–13530.

164. McWhinney SR, Goldberg RM, McLeod HL. Platinum neurotoxicity pharmacogenetics. Mol Cancer Ther. 2009 Jan;8(1):10-6.

165. Medzhitov R. Origin and physiological roles of inflammation. Nature. 2008 24; 454(7203):428-435.

166. Menard DP, van Rossum D, Kar S, St Pierre S, Sutak M, Jhamandas K, Quirion R.

A calcitonin gene-related peptide receptor antagonist prevents the development of tolerance to spinal morphine analgesia. J Neurosci. 1996; 16(7):2342-2351.

167. Meregalli C, Canta A, Carozzi VA, Chiorazzi A, Oggioni N, Gilardini A, Ceresa C, Avezza F, Crippa L, Marmiroli P, Cavaletti G. Bortezomib-induced painful neuropathy in rats: a behavioral, neurophysiological and pathological study in rats. Eur J Pain. 2010; 14(4):343-350.

168. Meregalli C, Ceresa C, Canta A, Carozzi VA, Chiorazzi A, Sala B, Oggioni N, Lanza M, Letari O, Ferrari F, Avezza F, Marmiroli P, Caselli G, Cavaletti G. CR4056, a new analgesic I2 ligand, is highly effective against bortezomib-induced painful neuropathy in rats. J Pain Res. 2012; 5:151-167.

169. Michael GJ, Averill S, Nitkunan A, Rattray M, Bennett DL, Yan Q, Priestley JV. Nerve growth factor treatment increases brain-derived neurotrophic factor selectively in TrkA-expressing dorsal root ganglion cells and in their central terminations within the spinal cord. J Neurosci. 1997; 17(21):8476-8490.

170. Millan MJ. The induction of pain: an integrative review. Prog Neurobiol. 1999; 57(1):1-164.

171. Miller SC, Huang R, Sakamuru S, Shukla SJ, Attene-Ramos MS, Shinn P, Van Leer D, Leister W, Austin CP, Xia M. Identification of known drugs that act as inhibitors of NF-kappaB signaling and their mechanism of action. Biochem Pharmacol. 2010; 79(9):1272-1280.

172. Mitsiades N, Mitsiades CS, Poulaki V, Chauhan D, Richardson PG, Hideshima T,Munshi N, Treon SP, Anderson KC. Biologic sequelae of nuclear factor-kappaB blockade in multiple myeloma: therapeutic applications. Blood. 2002; 99(11):4079-4086.

173. Miyano K, Tang HB, Nakamura Y, Morioka N, Inoue A, Nakata Y. Paclitaxel and vinorelbine, evoked the release of substance P from cultured rat dorsal root ganglion cells through different PKC isoform-sensitive ion channels. Neuropharmacology. 2009; 57(1):25-32.

174. Mogil JS, Yu L, Basbaum AI. Pain genes?: natural variation and transgenic mutants. Annu Rev Neurosci. 2000; 23:777-811.

175. Mühlen S, Ruchaud-Sparagano MH, Kenny B. Proteasome-independent degradation of canonical NFkappaB complex components by the NleC protein of

pathogenic Escherichia coli. J Biol Chem. 2011 Feb 18; 286(7):5100-5107.

176. Nahman-Averbuch H, Yarnitsky D, Granovsky Y, Sprecher E, Steiner M, Tzuk-ShinaT, Pud D. Pronociceptive pain modulation in patients with painful chemotherapy-induced polyneuropathy. J Pain Symptom Manage. 2011; 42(2):229-38.

177. Nakatsuka K, Gupta R, Saito S, Banzawa N, Takahashi K, Tominaga M, Ohta T. Identification of molecular determinants for a potent mammalian TRPA1 antagonist by utilizing species differences. J Mol Neurosci. 2013; 51(3):754-762.

178. Ocean AJ, Vahdat LT. Chemotherapy-induced peripheral neuropathy: pathogenesis and emerging therapies. Support Care Cancer. 2004; 12(9):619-625.

179. Ochoa, J. Management of neuropathic pain patients. In: Current therapy of Neurologic diseases, eds. RT Johnson, JW Griffin, 5th ed. 1996; New York: Mosby.

180. Ohara PT, Vit JP, Bhargava A, Romero M, Sundberg C, Charles AC, Jasmin L.Gliopathic pain: when satellite glial cells go bad. Neuroscientist. 2009; 15(5):450-463.

181. Olsson Y. Microenvironment of the peripheral nervous system under normal and pathological conditions. Crit Rev Neurobiol. 1990;5 (3):265-311.

182. O'Neill J, Brock C, Olesen AE, Andresen T, Nilsson M, Dickenson AH. Unravelling the mystery of capsaicin: a tool to understand and treat pain. Pharmacol Rev. 2012; 64(4):939-971.

183. Ostchega Y, Donohue M, Fox N. High-dose cisplatin-related peripheral neuropathy. Cancer Nurs. 1988; 11(1):23-32.

184. Pabbidi RM, Yu SQ, Peng S, Khardori R, Pauza ME, Premkumar LS. Influence of TRPV1 on diabetes-induced alterations in thermal pain sensitivity. Mol Pain. 2008;4:9.

185. Pasnoor M, Dimachkie MM, Barohn RJ. Cryptogenic sensory polyneuropathy. Neurol Clin. 2013; 31(2):463-476.

186. Patapoutian A. TRP channels and thermosensation. Chem Senses. 2005; 30 Suppl 1:i193-194.

187. Patestas M and Gartner L, A Textbook of Neuroanatomy. 2006, Wiley-Blackwell.

188. Pearson JS, Riedmaier P, Marchès O, Frankel G, Hartland EL. A type III effector

protease NleC from enteropathogenic Escherichia coli targets NF-κB for degradation. Mol Microbiol. 2011; 80(1):219-230.

189. Pei XY, Dai Y, Grant S. Synergistic induction of oxidative injury and apoptosis in human multiple myeloma cells by the proteasome inhibitor bortezomib and histone deacetylase inhibitors. Clin Cancer Res. 2004; 10(11):3839-3852.

190. Peier AM, Moqrich A, Hergarden AC, Reeve AJ, Andersson DA, Story GM, Earley TJ, Dragoni I, McIntyre P, Bevan S, Patapoutian A. A TRP channel that senses cold stimuli and menthol. Cell. 2002; 108(5):705-715.

191. Peltier AC, Russell JW. Recent advances in drug-induced neuropathies. Curr Opin Neurol. 2002; 15(5):633-638.

192. Pham LV, Tamayo AT, Yoshimura LC, Lo P, Ford RJ. Inhibition of constitutive NF-kappa B activation in mantle cell lymphoma B cells leads to induction of cell cycle arrest and apoptosis. J Immunol. 2003; 171(1):88-95.

193. Piperdi B, Ling YH, Liebes L, Muggia F, Perez-Soler R. Bortezomib: understanding the mechanism of action. Mol Cancer Ther. 2011; 10(11):2029-2030.

194. Pomonis JD, Harrison JE, Mark L, Bristol DR, Valenzano KJ, Walker K. N-(4-Tertiarybutylphenyl)-4-(3-cholorphyridin-2-yl)tetrahydropyrazine -1(2H)-carbox-amide (BCTC), a novel, orally effective vanilloid receptor 1 antagonist with analgesic properties: II in vivo characterization in rat models of inflammatory and neuropathic pain. J Pharmacol Exp Ther. 2003; 306(1):387-393.

195. Premkumar LS. Targeting TRPV1 as an alternative approach to narcotic analgesics to treat chronic pain conditions. AAPS J. 2010; 12(3):361-370.

196. Price DD, Dubner R. Neurons that subserve the sensory-discriminative aspects of pain. 1977. Pain 3:307–338.

197. Price DD. Psychological and NeuralMechansims of Pain. 1988. New York: Raven. 241.

198. Priestley JV, Michael GJ, Averill S, Liu M, Willmott N. Regulation of nociceptive neurons by nerve growth factor and glial cell line derived neurotrophic factor. Can J Physiol Pharmacol. 2002; 80(5):495-505.

199. Quasthoff S, Hartung HP. Chemotherapy-induced peripheral neuropathy. JNeurol.2002; 249(1):9-17.

200. Ralston HJ 3rd. The fine structure of laminae I, II and III of the macaque spinal cord. J Comp Neurol. 1979; 184(4):619-642.
201. Ravaglia S, Corso A, Piccolo G, Lozza A, Alfonsi E, Mangiacavalli S, Varettoni M, Zappasodi P, Moglia A, Lazzarino M, Costa A. Immune-mediated neuropathies in myeloma patients treated with bortezomib. Clin Neurophysiol. 2008; 119(11):2507-2512.
202. Reagan-Shaw S, Nihal M, Ahmad N. Dose translation from animal to human studies revisited. FASEB J. 2008; 22(3):659-661.
203. Ren K. Primary afferents and inflammatory hyperexcitability. Pain. 1996; 67(1):1-2.
204. Rexed B. The cytoarchitectonic organization of the spinal cord in the cat. JComp Neurol. 1952; 96(3):414-495.
205. Richardson PG, Barlogie B, Berenson J, Singhal S, Jagannath S, Irwin D, Rajkumar SV, Srkalovic G, Alsina M, Alexanian R, Siegel D, Orlowski RZ, Kuter D, Limentani SA, Lee S, Hideshima T, Esseltine DL, Kauffman M, Adams J, Schenkein DP, Anderson KC. A phase 2 study of bortezomib in relapsed, refractory myeloma. N Engl J Med. 2003; 348(26):2609-2617.
206. Richardson PG, Briemberg H, Jagannath S, Wen PY, Barlogie B, Berenson J, et al. et al.,Frequency, characteristics, and reversibility of peripheral neuropathy during treatment of advanced multiple myeloma with bortezomib. J Clin Oncol. 2006; 24(19):3113-3120.
207. Richardson PG, Xie W, Jagannath S, Jakubowiak A, Lonial S, Raje NS, Alsina M, Ghobrial IM, Schlossman RL, Munshi NC, Mazumder A, Vesole DH, Kaufman JL, Colson K, McKenney M, Lunde LE, Feather J, Maglio ME, Warren D, Francis D, Hideshima T, Knight R, Esseltine DL, Mitsiades CS, Weller E, Anderson KC. A phase II trial of lenalidomide, bortezomib and dexamethasone in patients with relapsed and relapsed/refractory myeloma. Blood. 2014.
208. Ripamonti CI. Pain management. Ann Oncol. 2012; 23 Suppl 10:x294-301.
209. Ripellino P, Fleetwood T, Cantello R, Comi C. Treatment of chronic inflammatory demyelinating polyneuropathy: from molecular bases to practical considerations. Autoimmune Dis. 2014; 2014:201657.
210. Sah DW, Ossipo MH, Porreca F. Neurotrophic factors as novel therapeutics for

neuropathic pain. Nat Rev Drug Discov. 2003; 2(6):460-472.

211. Saif MW, Reardon J. Management of oxaliplatin-induced peripheral neuropathy. Ther Clin Risk Manag. 2005; 1(4):249-258.

212. Sakamoto H, Spike RC, Todd AJ. Neurons in laminae III and IV of the rat spinal cord with the neurokinin-1 receptor receive few contacts from unmyelinated primary afferents which do not contain substance P. Neuroscience. 1999; 94(3):903-908.

213. San Miguel JF, Schlag R, Khuageva NK, Dimopoulos MA, Shpilberg O, Kropff M, Spicka I, Petrucci MT, Palumbo A, Samoilova OS, Dmoszynska A, Abdulkadyrov KM, Schots R, Jiang B, Mateos MV, Anderson KC, Esseltine DL, Liu K, Cakana A, van de Velde H, Richardson PG; VISTA Trial Investigators. Bortezomib plus melphalan and prednisone for initial treatment of multiple myeloma. N Engl J Med. 2008; 359(9):906-917.

214. Sanchez JF, Krause JE, Cortright DN. The distribution and regulation of vanilloid receptor VR1 and VR1 5' splice variant RNA expression in rat. Neuroscience. 2001;107 (3):373-381.

215. Sauer SK, Bove GM, Averbeck B, Reeh PW. Rat peripheral nerve components release calcitonin gene-related peptide and prostaglandin E2 in response to noxious stimuli: evidence that nervi nervorum are nociceptors. Neuroscience. 1999; 92(1):319-325.

216. Schaible HG. Peripheral and central mechanisms of pain generation. Handb Exp Pharmacol. 2007;(177):3-28.

217. Scholz J, Woolf CJ. Can we conquer pain? Nat Neurosci. 2002; 5 Suppl: 1062-7.

218. Schwartz R, Davidson T. Pharmacology, pharmacokinetics, and practical applications of bortezomib. Oncology (Williston Park). 2004;18(14 Suppl 11):14-21.

219. Scott K, Kothari MJ. Evaluating the patient with peripheral nervous system complaints. J Am Osteopath Assoc. 2005; 105(2):71-83.

220. Shah SA, Potter MW, McDade TP, Ricciardi R, Perugini RA, Elliott PJ, Adams J, Callery MP. 26S proteasome inhibition induces apoptosis and limits growth of human pancreatic cancer. J Cell Biochem. 2001; 82(1):110-122.

221. Shin CY, Shin J, Kim BM, Wang MH, Jang JH, Surh YJ, Oh U. Essential role of

mitochondrial permeability transition in vanilloid receptor 1-dependent cell death of sensory neurons. Mol Cell Neurosci. 2003; 24(1):57-68.

222. Silverman JD, Kruger L. Acid phosphatase as a selective marker for a class of small sensory ganglion cells in several mammals: spinal cord distribution, histochemical properties, and relation to fluoride-resistant acid phosphatase (FRAP) of rodents. Somatosens Res. 1988;5 (3):219-246.

223. Silverman JD, Kruger L. Selective neuronal glycoconjugate expression in sensory and autonomic ganglia: relation of lectin reactivity to peptide and enzyme markers. J Neurocytol. 1990; 19(5):789-801.

224. Smith BH, Torrance N. Epidemiology of neuropathic pain and its impact on quality of life. Curr Pain Headache Rep. 2012; 16(3):191-198.

225. Snider WD, McMahon SB. Tackling pain at the source: new ideas about nociceptors. Neuron. 1998; 20(4):629-32.

226. Sommer C. Painful neuropathies. Curr Opin Neurol. 2003; 16 (5):623-628.

227. Sommer EW, Kazimierczak J, Droz B. Neuronal subpopulations in the dorsal root ganglion of the mouse as characterized by combination of ultrastructural and cytochemical features. Brain Res. 1985; 346(2):310-326.

228. Stengel M, Baron R. Oxaliplatin-induced painful neuropathy-flicker of hope or hopeless pain? Pain. 2009; 144(3):225-256.

229. Stillman M, Cata JP. Management of chemotherapy-induced peripheral neuropathy. Curr Pain Headache Rep. 2006; 10(4):279-287.

230. Story GM, Peier AM, Reeve AJ, Eid SR, Mosbacher J, Hricik TR, Earley TJ, Hergarden AC, Andersson DA, Hwang SW, McIntyre P, Jegla T, Bevan S, Patapoutian A. ANKTM1, a TRP-like channel expressed in nociceptive neurons, is activated by cold temperatures. Cell 2003; 112:819–829.

231. Streit WJ, Schulte BA, Balentine JD, Spicer SS. Evidence for glycoconjugate in nociceptive primary sensory neurons and its origin from the Golgi complex. Brain Res. 1986; 377(1):1-17.

232. Stucky CL, Dubin AE, Jeske NA, Malin SA, McKemy DD, Story GM. Roles of transient receptor potential channels in pain. Brain Res Rev. 2009; 60(1):2-23.

233. Sunwoo JB, Chen Z, Dong G, Yeh N, Crowl Bancroft C, Sausville E, Adams J, Elliott P, Van Waes C. Novel proteasome inhibitor PS-341 inhibits activation of

nuclear factor-kappa B, cell survival, tumor growth, and angiogenesis in squamous cell carcinoma. Clin Cancer Res. 2001; 7(5):1419-1428.

234. Szolcsányi J. A pharmacological approach to elucidation of the role of different nerve fibres and receptor endings in mediation of pain. J Physiol (Paris). 1977; 73(3):251-259.

235. Ta LE, Bieber AJ, Carlton SM, Loprinzi CL, Low PA, Windebank AJ. Transient Receptor Potential Vanilloid 1 is essential for cisplatin-induced heat hyperalgesia in mice. Mol Pain. 2010; 6:15.

236. Tatsushima Y, Egashira N, Kawashiri T, Mihara Y, Yano T, Mishima K, Oishi R.Involvement of substance P in peripheral neuropathy induced by paclitaxel but not oxaliplatin. J Pharmacol Exp Ther. 2011; 337(1):226-235.

237. Tavee J, Zhou L. Small fiber neuropathy: A burning problem. Cleve Clin J Med. 2009; 76(5):297-305.

238. Todd AJ. Anatomy of primary afferents and projection neurones in the rat spinal dorsal horn with particular emphasis on substance P and the neurokinin 1 receptor. Exp Physiol. 2002; 87(2):245-249.

239. Todd AJ. Neuronal circuitry for pain processing in the dorsal horn. Nat Rev Neurosci. 2010; 11(12):823-836.

240. Tominaga M, Caterina MJ, Malmberg AB, Rosen TA, Gilbert H, Skinner K, Raumann BE, Basbaum AI, Julius D. The cloned capsaicin receptor integrates multiple pain-producing stimuli. Neuron. 1998; 21(3):531-543.

241. Trafton JA, Basbaum AI. The contribution of spinal cord neurokinin-1 receptor signaling to pain. J Pain. 2000; 1 (3 Suppl):57-65.

242. Trevisan G, Materazzi S, Fusi C, Altomare A, Aldini G, Lodovici M, Patacchini R, Geppetti P, Nassini R. Novel therapeutic strategy to prevent chemotherapy-induced persistent sensory neuropathy by TRPA1 blockade. Cancer Res.2013; 73(10):3120-3131.

243. Truong H, McGinnis L, Dindo L, Honda CN, Giesler GJ Jr. Identification of dorsal root ganglion neurons that innervate the common bile duct of rats. Exp Brain Res. 2004; 155(4):477-484.

244. Ueda H, Rashid MH. Molecular mechanism of neuropathic pain. Drug News Perspect. 2003; 16(9):605-613.

245. Ueda H. Peripheral mechanisms of neuropathic pain - involvement of lysophosphatidic acid receptor-mediated demyelination. Mol Pain. 2008; 4:11.
246. Urban MO, Gebhart GF. Supraspinal contributions to hyperalgesia. Proc Natl Acad Sci U S A. 1999 Jul 6;96(14):7687-92.
247. Usunoff KG, Popratiloff A, Schmitt O, Wree A. Functional neuroanatomy of pain. Adv Anat Embryol Cell Biol. 2006; 184:1-115.
248. Valtschanoff JG, Rustioni A, Guo A, Hwang SJ. Vanilloid receptor VR1 is both presynaptic and postsynaptic in the superficial laminae of the rat dorsal horn. J Comp Neurol. 2001; 436(2):225-235.
249. Van Dongen AM, editor. Biology of the NMDA Receptor. Boca Raton (FL): CRC Press; 2009.
250. Verdú E, Vilches JJ, Rodríguez FJ, Ceballos D, Valero A, Navarro X.Physiological and immunohistochemical characterization of cisplatin-induced neuropathy in mice. Muscle Nerve. 1999; 22(3):329-340.
251. Vetter I, Wyse BD, Roberts-Thomson SJ, Monteith GR, Cabot PJ. Mechanisms involved in potentiation of transient receptor potential vanilloid 1 responses by ethanol. Eur J Pain. 2008; 12(4):441-454.
252. Visovsky C, Daly BJ. Clinical evaluation and patterns of chemotherapy-induced peripheral neuropathy. J Am Acad Nurse Pract. 2004; 16(8):353-359.
253. Visovsky C. Chemotherapy-induced peripheral neuropathy. Cancer Invest. 2003; 21(3):439-451.
254. Voets T, Talavera K, Owsianik G, Nilius B. Sensing with TRP channels. Nat Chem Biol. 2005; 1(2):85-92.
255. Voorhees PM, Dees EC, O'Neil B, Orlowski RZ. The proteasome as a target for cancer therapy. Clin Cancer Res. 2003 Dec 15;9(17):6316-6325.
256. Wall PD. Dorsal horn electrophysiology. In Handbook of Sensory Physiology—Somatosensory System, ed. A Iggo, pp. 253–70. 1973 Berlin: Springer-Verlag.
257. Wall PD. The laminar organization of dorsal horn and effects of descending impulses. J Physiol. 1967; 188(3):403-423.
258. Willis WD. The Pain System. 1985. Basel, Switz.: Karger.
259. WillisWD, Westlund KN. Neuroanatomy of the pain system and of the pathways that modulate pain. 1997, J. Clin. Neurophysiol. 14:2–31.

260. Wolf SL, Barton DL, Qin R, Wos EJ, Sloan JA, Liu H, Aaronson NK, Satele DV,Mattar BI, Green NB, Loprinzi CL. The relationship between numbness, tingling, and shooting/burning pain in patients with chemotherapy-induced peripheral neuropathy (CIPN) as measured by the EORTC QLQ-CIPN20 instrument, N06CA. Support Care Cancer. 2012; 20(3):625-632.
261. Woolf C, Wiesenfeld-Hallin Z. Substance P and calcitonin gene-related peptide synergistically modulate the gain of the nociceptive flexor withdrawal reflex in the rat. Neurosci Lett. 1986; 66(2):226-230.
262. Woolf CJ, Mannion RJ. Neuropathic pain: aetiology, symptoms, mechanisms, and management. Lancet. 1999; 353(9168):1959-1964.
263. Woolf CJ, Salter MW. Neuronal plasticity: increasing the gain in pain. Science. 2000; 288(5472):1765-1769.
264. Wu ZH, Shi Y. When ubiquitin meets NF-κB: a trove for anti-cancer drug development. Curr Pharm Des. 2013; 19(18):3263-3275.
265. Xiao WH, Zheng H, Bennett GJ. Characterization of oxaliplatin-induced chronic painful peripheral neuropathy in the rat and comparison with the neuropathy induced by paclitaxel. Neuroscience. 2012 Feb 17;203:194-206.
266. Xiao WH, Zheng H, Bennett GJ. Characterization of oxaliplatin-induced chronic painful peripheral neuropathy in the rat and comparison with the neuropathy induced by paclitaxel. Neuroscience. 2012, 17;203:194-206.
267. Yu L, Yang F, Luo H, Liu FY, Han JS, Xing GG, Wan Y. The role of TRPV1 in different subtypes of dorsal root ganglion neurons in rat chronic inflammatory nociception induced by complete Freund's adjuvant. Mol Pain. 2008;4:61.
268. Zhang X, Li L, McNaughton PA. Proinflammatory mediators modulate the heat-activated ion channel TRPV1 via the scaffolding protein AKAP79/150. Neuron. 2008, 14;59(3):450-461.
269. Zhao M, Isami K, Nakamura S, Shirakawa H, Nakagawa T, Kaneko S. Acute cold hypersensitivity characteristically induced by oxaliplatin is caused by the enhanced responsiveness of TRPA1 in mice. Mol Pain. 2012 vol.8; pp 55.
270. Zheng H, Xiao WH, Bennett GJ. Mitotoxicity and bortezomib-induced chronic painful peripheral neuropathy. Exp Neurol. 2012; 238(2):225-34.

271. Zheng LF, Wang R, Xu YZ, Yi XN, Zhang JW, Zeng ZC. Calcitonin gene-related peptide dynamics in rat dorsal root ganglia and spinal cord following different sciatic nerve injuries. Brain Res. 2008; 1187:20-32.
272. Zhou XF, Rush RA. Endogenous brain-derived neurotrophic factor is anterogradely transported in primary sensory neurons.Neuroscience. 1996; 74(4):945-953.
273. Zygmunt PM, Petersson J, Andersson DA, Chuang H, Sørgård M, Di Marzo V, Julius D, Högestätt ED. Vanilloid receptors on sensory nerves mediate the vasodilatoraction of anandamide. Nature. 1999, 29;4.